TrpA1 activation dampens neuroinflammation via MHC class II modulation on astrocytes

Dissertation zur Erlangung des Grades

Doktor der Naturwissenschaften

Im Promotionsfach Biologie

Am Fachbereich Biologie der Johannes Gutenberg-Universität Mainz

Samantha Schmaul

Geboren am 27.05.1992 in Marburg

Dekan

1. Betreuer

2. Betreuer

Tag der mündlichen Prüfung

Hiermit versichere ich gemäß §12 Abs. 2 Nr.7 der Promotionsordnung vom 27.03.2018, dass ich die als Dissertation vorgelegte Arbeit selbst angefertigt und alle benutzten Hilfsmittel (Literatur, Geräte, Materialien) in der Arbeit angegeben habe. Ich habe oder hatte die jetzt als Dissertation vorgelegte Arbeit nicht als Prüfungsarbeit für eine staatliche oder andere wissenschaftliche Prüfung eingereicht. Ich hatte weder die jetzt als Dissertation vorgelegte Arbeit noch Teile einer Abhandlung bei einer anderen Fakultät bzw. einem anderen Fachbereich als Dissertation eingereicht.
Die als Dissertation vorgelegte Arbeit wurde in der Zeit von Oktober 2016 bis November 2020 am Institut für Neurologie an der Universitätsmedizin der Johannes Gutenberg Universität Mainz in der Arbeitsgruppe für Neuroimmunologie durchgeführt.

Table of Contents

Publication list

(1) Julia Loos, **Samantha Schmaul**, Theresa Noll, Miriam Schillner, Julian T Löffel, Frauke Zipp, and Stefan Bittner. 2020. Functional characteristics of Th1, Th17 and ex-Th17 cells in EAE revealed by intravital two-photon microscopy.

(Loos, Schmaul *et al.*, 2020)

---

(2) Birkner, Katharina, Beatrice Wasser, Tobias Ruck, Carine Thalman, Dirk Luchtman, Katrin Pape, **Samantha Schmaul**, Lynn Bitar, Eva-Maria Krämer-Albers, Albrecht Stroh, Sven G. Meuth, Frauke Zipp, and Stefan Bittner. 2020. "B1-Integrin– and KV1.3 Channel–Dependent Signaling Stimulates Glutamate Release from Th17 Cells." Journal of Clinical Investigation.

(Birkner *et al.*, 2020)

---

(3) Erik Ellwardt, Christina Francisca Vogelaar, Carlos Maldet, **Samantha Schmaul**, Stefan Bittner, and Dirk Luchtman. 2020. "Targeting CD52 Does Not Affect Murine Neuron and Microglia Function." European Journal of Pharmacology.

(Ellwardt *et al.*, 2020)

---

(4) Schmitt, Kerstin, Nadine Smolinski, Piotr Neumann, **Samantha Schmaul**, Verena Hofer-Pretz, Gerhard H. Braus, and Oliver Valerius. 2016. Asc1p/RACK1 Connects Ribosomes to Eukaryotic Phospho-Signaling.

(Schmitt *et al.*, 2017)

Abstract

TrpA1 Activation Dampens Neuroinflammation via MHC Class II Modulation on Astrocytes

Samantha Schmaul, Master of Science

Multiple sclerosis (MS) and its animal model experimental autoimmune encephalomyelitis (EAE) are autoimmune diseases characterised by chronic autoimmune inflammation, demyelination and axonal loss. Disease progression in MS is driven both by adaptive and innate immune responses within the central nervous system (CNS) compartment, as well as by bi-directional communication of immune cells with endogenous CNS cells. This thesis focused on the interplay between astrocytes and CNS-infiltrating Th17 cells, especially during neuroinflammatory conditions. Using two-photon imaging of organotypic hippocampal slice cultures (OHSC), we were able to identify a subset of Th17 cells that contact astrocytes and interact with them for an extended period of time. This astrocyte-contacting subpopulation showed characteristics that differ from the overall population of Th17 cells. They were slower than the average Th17 cells, they display a lower displacement rate and their meandering index is decreased. We could show by blocking of MHC class II in the OHSCs as well by the addition of CNS-autoantigen-unspecific Th17 cells that this process was antigen-dependent and that blockade of this process changed the properties of the astrocyte-contacting TH17 subset. In a next step, we showed that astrocytic antigen presentation was not restricted to the *in vitro* situation but could be observed *in vivo* as well. Additionally, the expression was regulated in a disease-state dependent manner during EAE. An astrocytic-specific deletion of MHC class II significantly weakened EAE disease progression and led to a milder course. The cation channel TrpA1 has been recently implicated as astrocytic sensor of the local microenvironment. Specifically, TrpA1 was described to be involved in neurogenic inflammation and demyelination, both prototypical conditions in MS and EAE. Indeed, TrpA1 was present on astrocytes and was regulated by distinct autoimmune-inflammatory stimuli on the mRNA level. Importantly, absence of TrpA1 led to an upregulation of astrocytic MHC class II expression, underlining the important role of this ion channel for perpetuating CNS-specific immune responses. In line with this, deletion of TrpA1 during EAE exacerbated the disease course significantly. Overall, it could be shown that TrpA1 expression on astrocytes regulated MHC class II expression, thereby modulating T cell responses and disease symptoms in an animal model of neuroinflammation.

Zusammenfassung

TrpA1-Aktivierung unterdrückt die Neuroinflammation durch eine Modulation von MHC II auf Astrozyten

Samantha Schmaul, Master of Science

Multiple Sklerose (MS) und sein Tiermodel experimentelle autoimmune Enzephalomyelitis (EAE) sind Autoimmunerkrankungen die durch chronische Entzündung, Demyelinisierung und axonalen Verlust charakterisiert sind. Der Krankheitsverlauf wird durch das adaptive und angeborene Immunsystem im zentralen Nervensystem, so wie bidirektionale Kommunikation mit endogenen nervösen Zellen angetrieben. Diese Arbeit konzentriert sich auf die Interaktion zwischen Astrozyten und infiltrierenden Th17 Zellen, besonders unter neuroinflammatorischen Bedingungen. Durch Zwei-Photonen-Mikroskopie von organotypischen Hippocampus-Schnittkulturmodellen (OHSC) war es uns möglich eine Th17 Subpopulation zu identifizieren, die Astrozyten kontaktieren und mit ihnen über längere Zeit interagieren. Diese astrozytenkontaktierende Subpopulation zeigt Charakteristika die sie von der Gesamtpopulation unterscheiden. Sie sind langsamer als die durchschnittliche Th17 Zelle, sie zeigen eine verlangsamte Verschiebungsrate und ihr Mäandrierungsindex ist verringert. Wir konnten durch die Blockade von MHC II in den OHSC sowie die Gabe von ZNS-Antigenunspezifischen Th17 zeigen, dass dieser Prozess Antigenabhängig ist und die Blockade die Eigenschaften der astrozytenkontaktierenden Th17 Population verändert. In einem nächsten Schritt konnten wir zeigen, dass dieser Prozess nicht nur *in vitro*, sondern auch *in vivo* gültig ist. Darüber hinaus war die Expression von MHC II in der Maus abhängig vom Krankheitsstadium. Eine astrozytenspezifische Deletion von MHC II führte zu einem signifikant schwächeren Verlauf der EAE. Der Kationenkanal TrpA1 wurde kürzlich als ein astrozytärer Sensor des extrazellulären Milieus identifiziert. TrpA1 ist laut Literatur beteiligt an neurogener Inflammation und Demyelinisierung, beides prototypische Anteile der MS und EAE. Tatsächlich konnten wir zeigen, dass TrpA1 auf Astrozyten exprimiert wird und dass seine Transkriptionslevels von definierten autoimmuninflammatorischen Stimuli abhängig sind. Wichtig dabei, die Abwesenheit von TrpA1 führt zu einer Hochregulation von astrozytärer MHC II Expression, was die wichtige Rolle dieses Ionenkanals in der Aufrechterhaltung von ZNS-spezifischen Immunantworten unterstreicht. In Einklang damit steht, dass die Deletion des Kanals die Symptome der EAE verschlimmert. Zusammenfassend konnten wir zeigen, dass TrpA1 Expression astrozytäre MHC II Expression reguliert, wodurch T Zell Antworten und Krankheitssymptome in einem Tiermodell der Neuroinflammation reguliert werden.

Acknowledgements

My first thanks are addressed to my first supervisor who allowed me to perform my PhD thesis under his supervision. Moreover, I would like to thank my second supervisor for readily taking over my co-supervision.

At last, I would like to thank my family. Their warm and supportive attitude towards everything I did and want to do is the reason why I am where I am now. I can always rely on a welcoming home and a never-ending stream of productive and open discussions. Thank you so much for always being there for me.

I Introduction

A Multiple Sclerosis and Experimental Autoimmune Encephalomyelitis

One of the key characteristics of many autoimmune diseases is recurring and widespread inflammation of the central nervous system (CNS) (Kim *et al.*, 2014). Multiple sclerosis (MS), as a prototypical autoimmune disease of the CNS, is characterised by prolonged inflammation and demyelination as well as axonal loss. Disease onset usually occurs between the age of 20 and 40 in more than 2.5 million people worldwide (Ellwardt and Zipp, 2014; Glatigny and Bettelli, 2018). It is proposed to be initiated and sustained by a dysregulated adaptive as well as innate immune system in conjunction with genetic susceptibility and environmental influences (Brambilla, 2019). As there are no designated lesion sites, initial clinical symptoms range from visual disturbances, sensory misperceptions, ataxia and muscle weakness (Lublin and Reingold, 1996) to bladder dysfunction and cognitive deficits (Herz, Zipp and Siffrin, 2010). Pathologically, manifestation begins with local inflammation as well as demyelination, gliosis and axon degeneration, transiently at first. Over time, these pathological hallmarks become dominant, although their severity varies individually (Compston & Coles, 2008; Kim *et al.*, 2014; Figure 1)

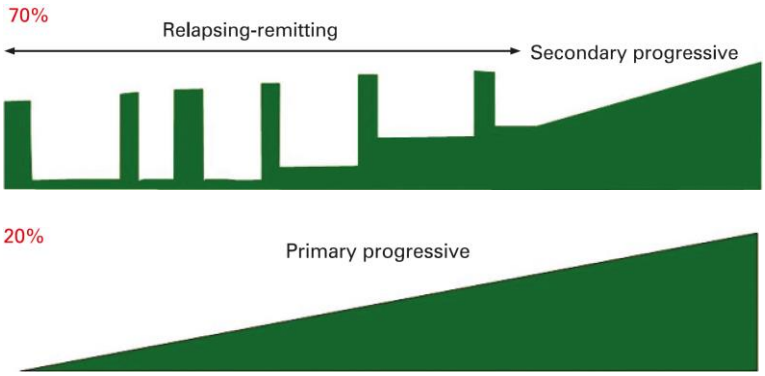

***Figure 1**: Prevalent MS types. The horizontal axis depicts time whereas the vertical axis depicts disability severity* (modified from Coles, 2009).

The main disease course is relapsing-remitting multiple sclerosis (RRMS; Figure 1 top) which is characterised by multiple episodes of inflammatory demyelination and immune infiltration, interspersed with periods of recovery (remission). Over time, remission becomes incomplete and RRMS slowly transforms into a secondary progressive disease course (SPMS), characterised by gradual worsening (Coles, 2009; Figure 1 top).

Alternatively, approximately 20 % of MS cases exhibit a primary progressive disease course (PPMS; Figure 1 bottom) and, as with the secondary progressive disease course, usually starts around the age of 40. Symptoms are similar to the SPMS course, with continued worsening without periods of remission (Compston and Coles, 2008).

Underlying the different disease courses, especially the RRMS-SPMS disease course, is continuous, debilitating white matter atrophy. Grey matter atrophy, although present from onset, increases dramatically during the progressive disease phase of MS (Larochelle *et al.*, 2016). While the aetiology is still unclear, some factors have been identified (Luessi, Siffrin and Zipp, 2012). For example, many patients show autoimmune reactions against myelin sheath proteins (Sofroniew, 2015). Additionally, genetic predisposition and environmental influences as well as immune system dysfunctions are correlated with onset of disease (Bittner *et al.*, 2014).

To better understand these disease mechanisms, murine models like experimental autoimmune encephalomyelitis (EAE), or using demyelinating agents like cuprizone feeding as well as viral models like Theiler's murine encephalomyelitis (TMEV) virus are used (Bittner *et al.*, 2014). Each model focuses on some specific aspect of the underlying meshwork of potential causes and supporting factors. EAE is the most common MS-mimic in many species, although mice are used most prevalently (Krishnamoorthy and Wekerle, 2009). The basic underlying mechanism of EAE is an autoimmune reaction of the immune system against brain-specific antigens (most commonly myelin sheath associated) which in turn leads to neuroinflammation and antigen-dependent destruction in the CNS (Bittner *et al.*, 2014). Three main proteins of the myelin sheath that are used for the induction of EAE are proteolipid protein (PLP), myelin basic protein (MBP) and myelin oligodendrocyte glycoprotein (MOG). All three are used for active immunisation; their efficiency varies in different mouse strains and lead to different disease courses.

MBP as well as PLP induce a relapsing-remitting disease course in SJL/J mice, whereas MOG application can induce a variety of disease courses depending on the dosage and mouse strain. These include the development of a chronic disease course in C57BL/6 (B6), while in NOD mice one acute relapse is induced followed by chronic progression (Figure 2, Glatigny and Bettelli, 2018). The application of MOG_{35-55}, the reactive MOG peptide, is one of only a few ways to induce EAE in B6, which are otherwise mostly resistant to the application of other peptides like other H-2^b mice (Amor *et al.*, 1994). MOG_{35-55} application is the most common model, as most transgenic mouse lines are based upon the B6 background. This active form of EAE induction leads to ascending symptoms starting with paralysis of the tail and leading to massive inflammation of the spinal cord (Figure 2, Stromnes and Goverman, 2006).

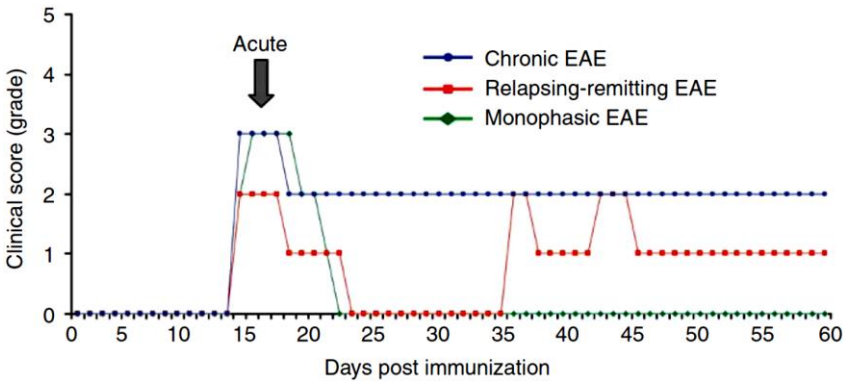

***Figure 2**: Typical EAE disease courses in mice* (Stromnes and Goverman, 2006). *A chronic EAE course can usually be found upon MOG-EAE in NOD or B6 mice, relapsing-remitting upon PLP-EAE in SJL mice and monophasic EAE upon MOG-EAE in B6.*

Different disease models are only able to mimic partial aspects of the complex pathogenesis of MS in humans. However, EAE and MS both show immune cell infiltration in the CNS and available MS therapeutics are able to modulate EAE disease course as well (Compston and Coles, 2008; Bjelobaba *et al.*, 2018; Glatigny and Bettelli, 2018).

B Disease Pathogenesis

In homeostasis, the ability to maintain self-tolerance against tissue-specific antigens eliminates autoreactive T and B cells in the thymus or bone marrow. During MS, as well as EAE, these cells can be found more abundantly in the periphery and especially in the CNS. Most commonly, myelin-associated proteins can be found as epitopes for auto reactivity (Glatigny and Bettelli, 2018). In the absence of

myelin, it has been shown that the same autoreactive cells attack structurally or sequentially similar neuronal epitopes, leading to neuronal destruction in the absence of myelin destruction (Krishnamoorthy *et al.*, 2009).

The common pathological hallmarks, irrespective of clinical manifestation, are formed by a tetrad of inflammation, demyelination, axonal damage and gliosis (Trapp *et al.*, 1998). Early on, immune infiltrates can be found in CNS plaques of MS patients. These mostly consist of lymphocytes and myeloid cells. During EAE, especially in SJL mice, T cells and macrophages dominate inflammation, demyelination and neuronal damage (Herz, Zipp and Siffrin, 2010). Regardless of the course of EAE (Figure 2), its disease pathology includes perivascular accumulation of immune cells, followed by infiltration into the parenchyma. Within the CNS, activation of microglia (and potentially subsequently astrocytes), is followed by demyelination and axonal death (Brambilla, 2019). Temporal occurrence, severity and localisation, however, vary significantly between strains and induction protocols of EAE.

Comparable to the grey (and white) matter atrophy that underlie MS disease progression, neuronal loss in EAE could be shown from an early time point in the spinal cord (Vogt *et al.*, 2009). Thus, EAE models are able to mimic many aspects of the human disease (Figure 3).

The pathology has been linked to different pathways involved in dysbalancing axonal energy supply by the redistribution of ion channels (Kornek *et al.*, 2000). These channels include members of the transient receptor potential (TRP) family like TRPM4 (Schattling *et al.*, 2012) and TRPV1 (Tsuji *et al.*, 2010) whose modulations lead to an attenuated EAE disease course, and potassium channels like TASK-1 (Bittner *et al.*, 2009) and ASIC-1 (Friese *et al.*, 2007; Vergo *et al.*, 2011). In addition, glutamate excitotoxicity (Birkner *et al.*, 2020) as well as mitochondrial dysfunction caused by extrinsic reactive

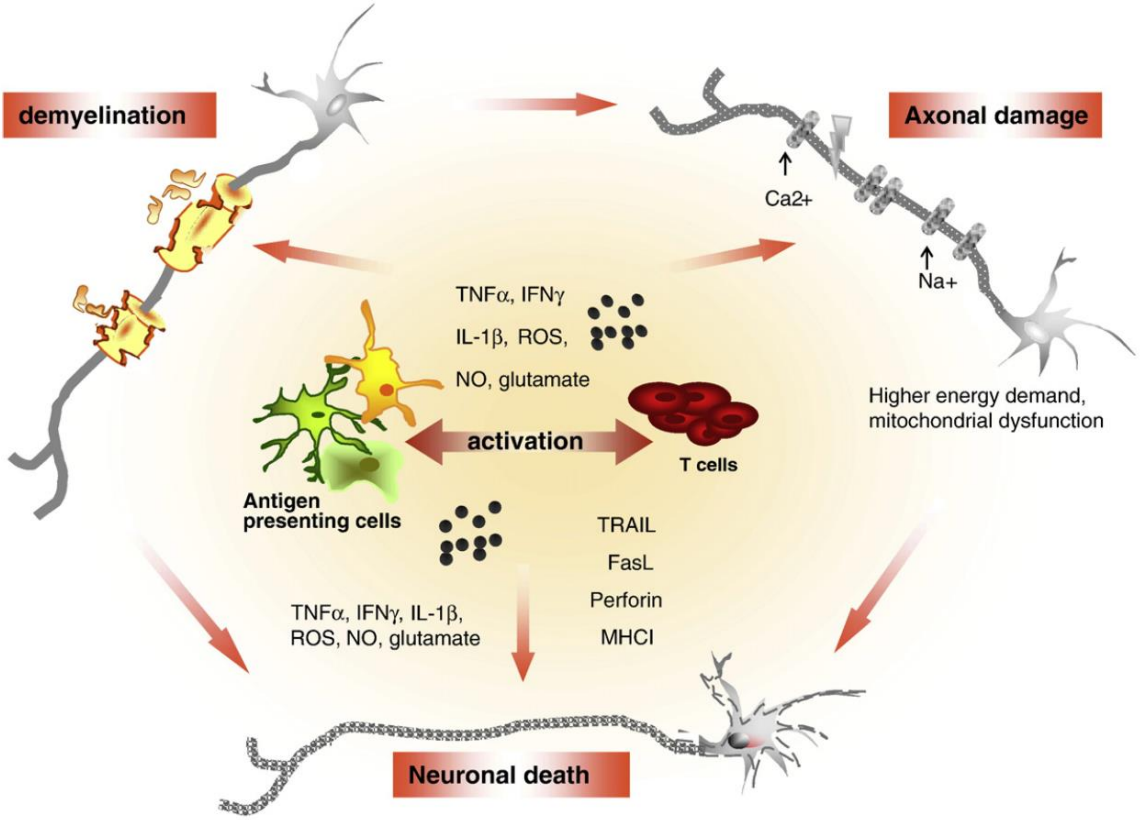

Figure 3: *Key aspects in disease pathology of MS/EAE* (Herz, Zipp and Siffrin, 2010). *Based on the current knowledge, (proinflammatory) T cells are (re)activated by antigen-presenting cells in the CNS leading to the release of inflammatory as well as cytotoxic substances (middle). Furthermore, contact-dependent mechanisms are described for neuronal damage and destruction by T cells (top), ultimately leading to demyelination and neuronal loss (top and bottom).*

nitrogen (RNS) and oxygen (ROS) species (Nikić *et al.*, 2011) results in neuronal degeneration, independent of remyelination.

C The Mystery and Magic of Astrocytes

I The light Side - In Health

Once considered to be a homogenous population, it has become apparent that astrocytes are diverse from the moment they develop (Sofroniew and Vinters, 2010; Zhang and Barres, 2010). Protoplasmic astrocytes are prevalent within the grey matter and exhibit a highly arborized and branched morphology, mostly ensheathing synapses (Andriezen, 1893). Whereas fibrous astrocytes are mainly found in the white matter and are characterised by fewer and more fibrillary processes contacting nodes of Ranvier. Both ensheath blood vessels and connect via gap junctions (Barres, 2008; Sofroniew and Vinters, 2010). They derive from at least two, if not three, origins; originating from precursor cells that are either astrocyte-specific, shared with neurons or even with oligodendrocytes or directly derived from neuroepithelial cells (Wang and Bordey, 2009; Hu *et al.*, 2016). This developmental diversity may provide an explanation for functional differences in the same region as well as similarities in different brain regions, potentially deriving from the same source (Kriegstein and Götz, 2003; Volterra and Meldolesi, 2005). They differ morphologically, in their expression patterns of receptors, transporters and ion channels as well as in their functional specialisation (Verkhratsky and Nedergaard, 2016). Although astrocytes *in vitro* are able to express most receptors present in the brain, *in vivo* the expression seems largely to correlate with the predominant neurotransmitters present locally (Verkhratsky, 2010).

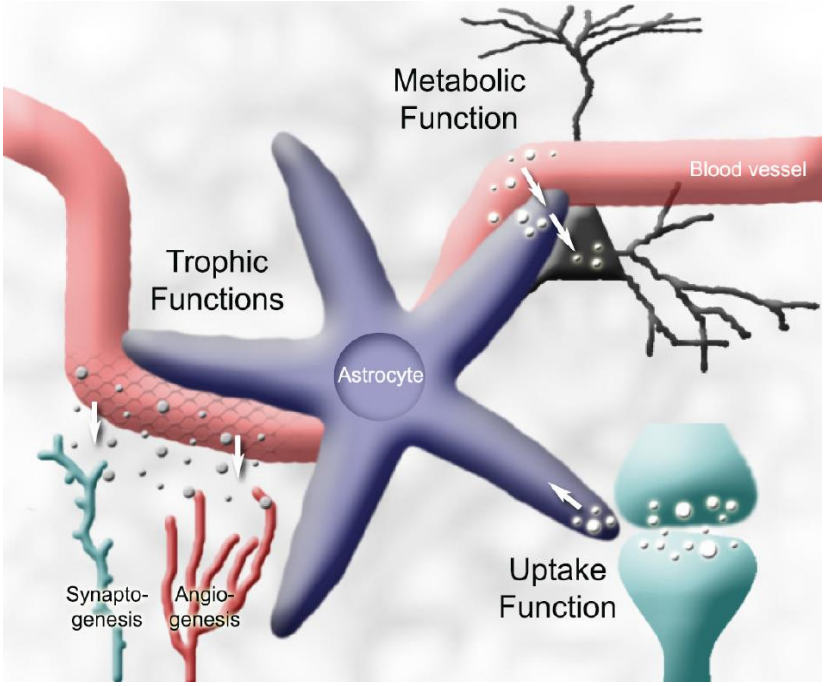

Figure 4: *The established astrocytic functions in homeostasis* (Wang and Bordey, 2009). *Examples include trophic support by taking up ions, reactive oxygen species and neurotransmitters, neuronal metabolic support, regulation of extracellular volume including synaptic clearance, as well as synaptogenesis and angiogenesis* (Verkhratsky and Nedergaard, 2016).

Astrocytic functions can be divided into three major groups: housekeeping for neuronal functionality, synaptic sculpture and neurogenic functions. The latter will not be examined here. One of the best established functional characteristics of astrocytes are their neuronal support abilities. They maintain a stable CNS especially for neuronal survival. This maintenance function goes far beyond the initially proposed function of stability, or 'Nervenkitt' propagated by Rudolf Virchow in 1858 (Somjen, 1988; Kettenmann and Verkhratsky, 2008). It includes lactate for neuronal

energy consumption (Sofroniew and Vinters, 2010) as well as for neutralising ROS providing anti-oxidant defences both for themselves and surrounding cells (Kimelberg, 2010; Magistretti, 2011; Fernandez-Fernandez, Almeida and Bolaños, 2012)

Astroglia are the major source of extracellular matrix as well as adhesion molecules in the CNS (Wang and Bordey, 2009), both stimulating as well as inhibiting neuronal growth. These factors include N-CAM, I-CAM1 and V-CAM1 (Liddelow and Hoyer, 2016), as well as laminin, fibronectin or proteoglycans, providing a complex network of stimulation and glial boundaries for neurite path finding and stability (Liesi, Dahl and Vaheri, 1983; Liesi, Kirkwood and Vaheri, 1986; Liesi and Silver, 1988; Matthiessen, Schmalenbach and Müller, 1989; Snow *et al.*, 1990).

Additionally, it is well known that astrocytes are able to buffer excess potassium, glucose and neurotransmitters, including brain-derived neurotrophic factor (BDNF) or fibroblast growth factor (FGF, Rudge *et al.*, 1992; Vaca and Wendt, 1992). Moreover, they release S100β, a calcium-binding protein, to buffer neuronal glutamate release and prevent excitotoxicity via reuptake (Emsley, Arlotta and Macklis, 2004; Donato R., 2003). These and many known and unknown factors influence neuronal maturation and survival in the developing and adult brain (Ojeda *et al.*, 2003).

Furthermore, astrocytes, although not able to conduct action potentials, are excitable on an ionic level (Sofroniew and Vinters, 2010), usually through a cationic influx of calcium, potassium or sodium into the cytosol. These commonly function either by selective binding (usually Ca^{2+}) or through electrochemical gradients across membranes (commonly for Na^{+}), often influencing only small domains within the cell by active limitation (Verkhratsky, Reyes and Parpura, 2013). Especially the calcium changes come from different sources and induce differential gene expression, as well as e.g., the release of secretory vesicles. Sodium, on the other hand, usually varies upon neuronal activity changes and acts more like a homeostatic sensor (Verkhratsky and Nedergaard, 2016). Both influxes can be conducted by a special family of channels, namely the TRP channel superfamily (Bosson *et al.*, 2017). They are involved in storage release of both Na^{+} and Ca^{2+}, which in turn activate solute carrier transporters for extracellular transmitter clearance (e.g., glutamate, GABA or glycine transporters; Kimelberg, 2010; Verkhratsky, Reyes and Parpura, 2013). These are highly concentrated on perisynaptic astrocytic processes for efficient clearance of neuronal synaptic releases (Verkhratsky and Nedergaard, 2016), especially glutamate and GABA. Glutamine, the basis for those neurotransmitters, is provided by astrocytes and shuttled back to the presynaptic neuron, making the astrocytes indispensable for efficient and continuous neurotransmission (Hertz *et al.*, 1999). Uniquely, astrocytes are able to synthesize glutamate *de novo* from a modified pyruvate cycle, providing a close source for essential neuronal transmission (Hertz and Zielke, 2004).

Apart from the tripartite synapse, astrocytes form tight connections with vascular structures (Abbott, Rönnbäck and Hansson, 2006). They are able to secrete both vasodilators and vasoconstrictors; the specific identities of which are still unknown (Barres, 2008). The blood-brain barrier (BBB), being a specialised border, was initially associated with astrocytic orchestration (Abbott, Rönnbäck and Hansson, 2006). However, it has now been shown that astrocytes are non-essential for the generation of the BBB, but necessary for its maintenance, especially under challenge (Cahoy *et al.*, 2008; Daneman and Prat, 2015). Aquaporin 4 (AQP-4), expressed on astrocytic end-feet, is essential for the brain's water homeostasis (Ludwin *et al.*, 2016). The astrocytic link between neuronal signalling and the BBB allows the regulation of blood flow upon neuronal activity (Attwell *et al.*, 2010).

II The dark side - In Neuroinflammation

Although astrocytes do not primarily belong to the immune system, they gain important immunological functions when challenged during neuroinflammation. Müller provided the earliest mechanistic link between MS and astrocytes in 1904 and claimed that the observed demyelination in MS is rooted in astrocytic dysfunction (Kıray et al., 2016). Over the years, a clear correlation between EAE disease severity and astrocytic inflammatory state could be shown (Brosnan and Raine, 2013; Brambilla, 2019), whether this is a pathologic gain of function or a homeostatic loss of function remains unknown.

As early as day 3 post EAE induction, long before the first clinical symptoms, reactive astrocytes may already be observed in both white and grey matter (D'Amelio, Smith and Eng, 1990; Luo *et al.*, 2008). After onset of disease symptoms, astrocytes in close proximity to infiltrating T lymphocytes react distinctively and become hypertrophic. These hypertrophic astrocytes can be seen as one of the earliest histological sign at the border of active MS lesions. Within active lesions, reactive astrocytes can be observed that display swollen cell bodies and damaged end-feet, which in homeostasis would be a part of the glia limitans. This BBB disruption by swelling allows for more immune cell infiltration (Figure 5, Brosnan and Raine, 2013).

Astrocytes are also a major source of destructive ROS and RNS species (Brosnan and Raine, 2013). Recently, this induction was shown to be BDNF-dependent (Brambilla *et al.*, 2014), turning a neuroprotective mechanism into a potentially damaging one. Astrocytic BDNF ablation exacerbates clinical symptoms, underscoring the dual role as both neuroprotective and damaging at the same time

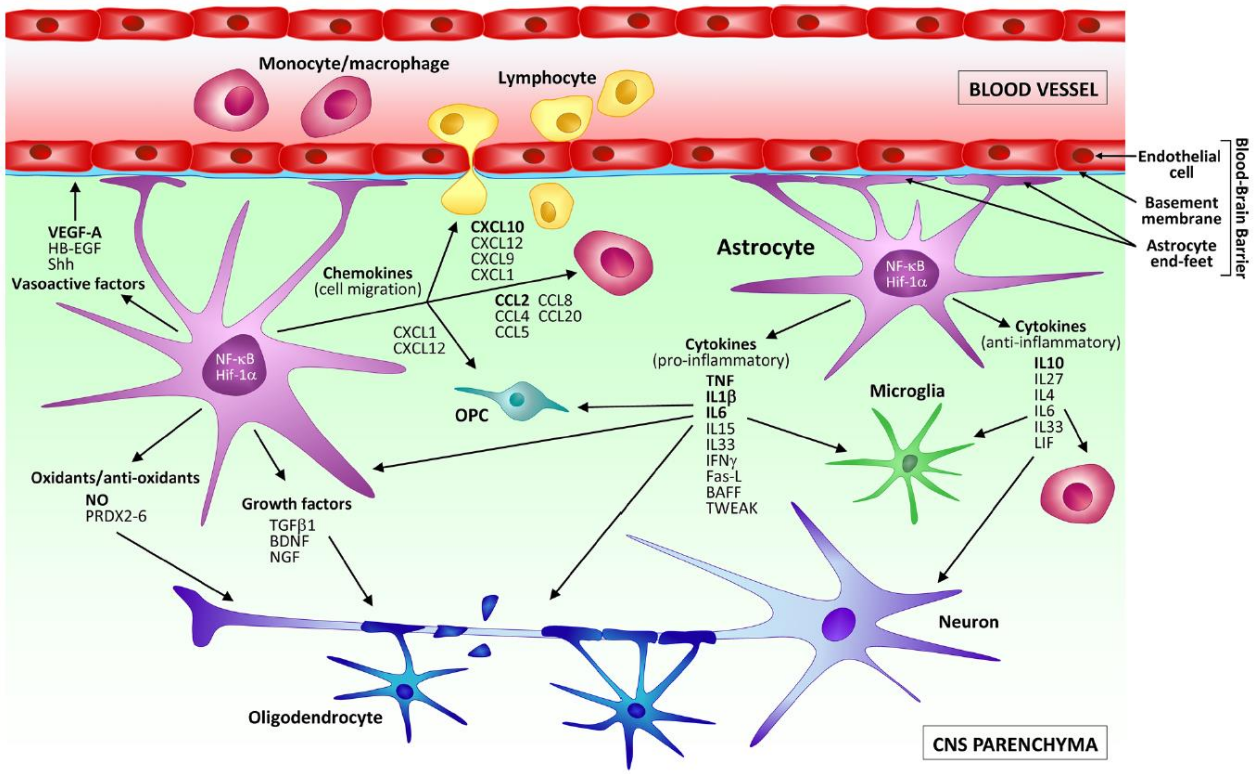

Figure 5: *Soluble astrocytic molecules in MS and EAE. These factors include proinflammatory as well as anti-inflammatory cytokines, chemokines as well as oxidative agents and growth factors. This potpourri allows for the interaction with the infiltrating as well as the resident immune system in addition to neuronal and glial resident cells to either cause or prevent damage* (Brambilla, 2019).

(Linker *et al.*, 2010). These hypertrophic astrocytes re-enter the cell cycle and upregulate immunoreactive proteins like vimentin and glial fibrillary acidic protein (GFAP), among others (Moreno *et al.*, 2013), even beyond the active lesion into the normal-appearing white and grey matter (Brosnan and Raine, 2013; Ludwin *et al.*, 2016). This persists even after the retraction of T cells.

Two major pathways of astrocytic influence on disease progression are the secretion of chemokines and cytokines for further recruitment of immune cells and the maintenance of the BBB in conjunction with endothelial cells and pericytes (Zlokovic, 2008). Depletion studies have shown that the lack of some of these chemokines such as CCL2, which normally is responsible for peripheral immune cell recruitment, diminishes EAE disease progression (Figure 5, Moreno et al., 2013). NF-κB is often referred to as the master transcription regulator of inflammation (Meares *et al.*, 2012), regulating cytokines like TNFα or IL-6 as well as BAFF or TWEAK production in astrocytes during EAE development and progression (Brambilla *et al.*, 2009, 2014). The lack of astrocytic NF-κB leads to a diminished recruitment of immune cells from the spleen especially during the chronic stages of disease, potentially because CCL2, responsible for recruitment of immune cells, is down-regulated (Figure 5, Kim et al., 2014; Mayo et al., 2014a; b; Rothhammer and Quintana, 2015). Additionally, inhibition of NF-κB increases remyelination after lesioning correlating with functional recovery (Brambilla *et al.*, 2014). These depletion studies all point towards a major involvement of astrocytes in the pathomechanisms of MS.

Acute depletion of astrocytes themselves during EAE has shown a shift in astrocytic contribution to the course of disease. Initially, the maintenance of the BBB functionality (as well as other protective astrocytic functions) prevents a more detrimental disease course, indicating a protective astrocytic influence. Their functional presence during the chronic phase worsens the course, showing a shift towards a detrimental astrocytic phenotype (Figure 5, D'Amelio et al., 1990; Mayo et al., 2014a).

Although there are no astrocyte-specific disease-modifying drugs, some therapeutic effects are not provided by the immune system alone. Fingolimod (FTY720) for instance acts on the sphingosine 1-phosphate receptor (S1P-R) pathway. In the immune system, this drug sequesters T and B cells inside the lymph nodes, preventing their infiltration. Dendritic cells and monocytes are less proinflammatory upon FTY720 treatment (Luessi *et al.*, 2015). In another study, it was shown that the loss of S1P-R on astrocytes, but not on neurons, diminishes the drug's efficacy (Choi *et al.*, 2011) pointing towards a more systemic effect of fingolimod. Astrocytes, upon treatment with fingolimod, are shifted to an anti-inflammatory phenotype and downregulate proinflammatory cytokine production (Rothhammer *et al.*, 2017).

In neuromyelitis optica (NMO), astrocytic destruction was shown to be causative to myelin destruction (Brosnan and Raine, 2013) posing the question, whether this mechanism may be relevant for MS. NMO is also associated with astrocyte-specific antibodies, usually against AQP-4, leading to the destruction of the end-feet and increased permeability of the BBB (Ludwin *et al.*, 2016). Some argue that a similar mechanism may be involved in MS as well.

D Astrocytic Interaction with T Lymphocytes

The immune system with its two main brain branches, adaptive and innate, is a complex and systemic network. The diversity of cells involved would be too much to cover in this context, therefore, the main focus will be on $CD4^+$ αβ T lymphocytes (Clambey *et al.*, 2014). These can differentiate into different subtypes including T helper (Th) cells such as Th1, Th2, Th9 and Th17; regulatory T (Treg) cells and T follicular helper (T_{FH}) cells; depending on the cytokine milieu (Figure 6, Luckheeram et al., 2012). For possible interactions of astrocytes and T helper cells, the latter have to pass several cellular and molecular borders for direct contact (Ransohoff and Engelhardt, 2012). This process was long thought to be only possible when the BBB is not intact, but it could be shown that activated T cells are capable of passage even under homeostatic conditions (Hickey, Hsu and Kimura, 1991). Once adhered to the endothelium, the entry through the endothelial cell layer connected by tight junctions is tightly controlled by numerous molecules (Sofroniew, 2015). Before entering the CNS, T cells accumulate within the perivascular space where they are primed and potentially held back. These molecular instructions can be soluble or via cell-cell interactions and may be provided by different cell types including astrocytic end-feet that limit the perivascular space on the CNS side (Quintana, 2017). *In vivo* imaging of the BBB recognised continuous coverage of vasculature by astrocytic end-feet including arterioles and veins allowing for long-distance relay of T cell-derived signals via gap junctions (McCaslin *et al.*, 2011).

Most homeostatic interaction studies so far have been performed *in vitro* using neonatal astrocytes. These were able to polarise $CD4^+$ T cells towards Th1 as well as Treg, although the latter could only be partially reproduced (Beurel *et al.*, 2014; Xie *et al.*, 2015). Th1 polarisation may be regulated via the astrocytic glutamate control. Increased glutamate induces more Tbet expression inducing a Th1 phenotype (Beurel *et al.*, 2014; Xie and Yang, 2015).

As Figure 5 nicely depicts, astrocytes express a variety of cytokines during inflammation, many of which have been associated with T cell proliferation and differentiation *in vitro*. Interleukin-6 (IL-6) for example is implicated in Th17 as well as Treg differentiation in the periphery, whereas IL-15 largely effects $CD8^+$ T cell lytic enzyme content or Ag-specific cytotoxicity. IL-33 in EAE was shown to reduce IL-17 and interferon gamma (IFNγ) load, limit Th1 and Th17 cells, induce anti-inflammatory macrophages peripherally and ameliorate the disease course (Jiang *et al.*, 2012). However, none of these effects has been linked to astrocytes in particular, providing only circumstantial evidence for astrocytic involvement.

Exposure of astrocytes to Th17-specific cytokine IL-17 *in vitro* stimulates proinflammatory cytokine production including iNOS, IL-6, TNFα or chemokines like CCL2, CCL3 and CCL20 (Figure 5 Rothhammer and Quintana, 2015; Meares et al., 2012). Whether these in turn are responsible for T cell recruitment into the CNS in MS and EAE is still under debate (Xie and Yang, 2015). CCL20 expression in astrocytes can be induced via a different route as well. T cell-derived, most probably Th2- or Th17-derived, IL-9 induces its expression in astrocytes and thereby favours Th17 migration towards the source (Harrington *et al.*, 2005). Neutralising IL-9 in EAE reverses the recruitment and ameliorates the disease course (Zhou *et al.*, 2011; Xie and Yang, 2015).

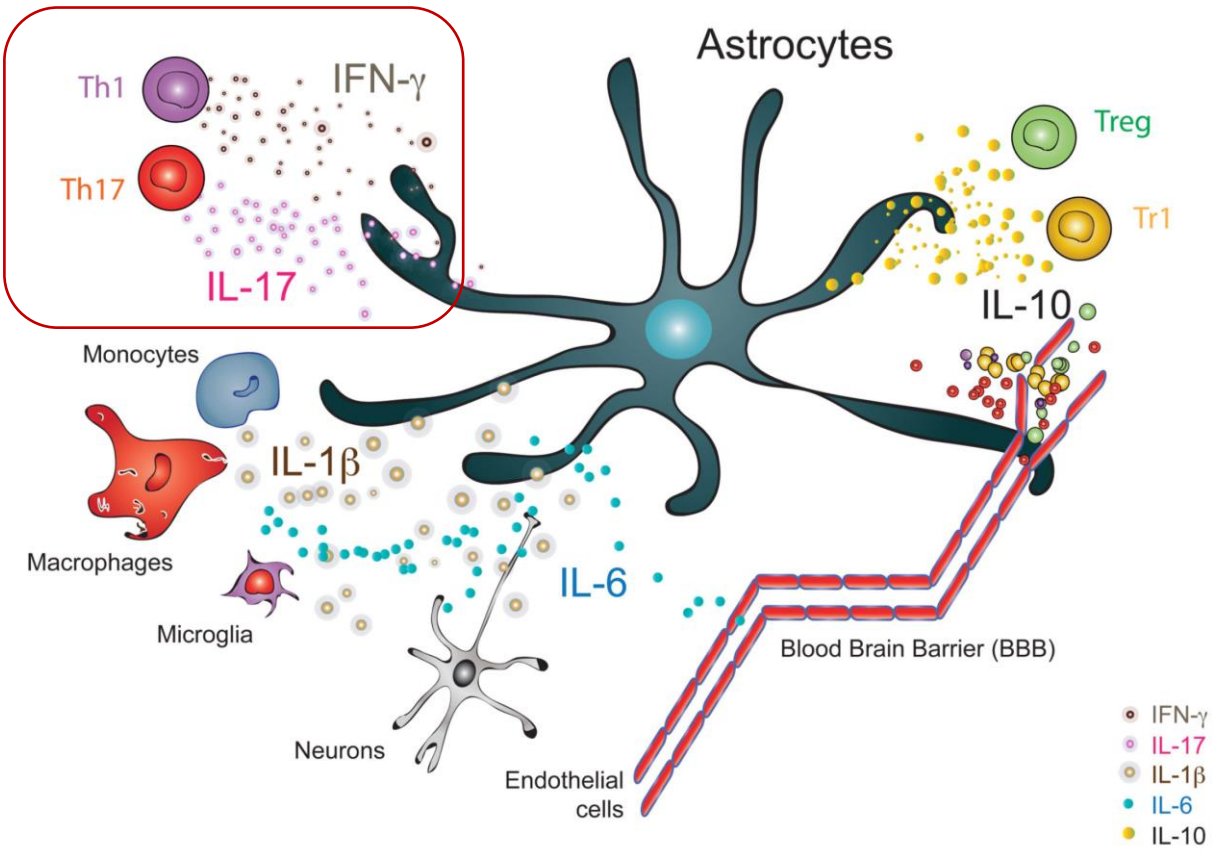

***Figure 6**: Inflammatory cytokines influencing astrocytes during inflammation and their cellular origins. Signature cytokines from inflammation-associated T lymphocyte subsets including regulatory (Treg, Tr1) as well as helper subsets (Th1, Th17) influencing astrocytic reactivity. Monocytes and macrophages as well as microglia secrete their own cytokine subset. Modified from Rothhammer and Quintana, 2015.*

Depleting IL-17-dependent responses in astrocytes ameliorates the EAE disease course as well (Kang *et al.*, 2010). Essentially, IL-17 lifts the inhibition on NF-κB in inflammation which in turns allows for the recruitment of T and B cells into the CNS (Figure 6, Liu et al., 2014). The influence of IFNγ, the major Th1 cytokine, on the other hand is not as straightforward (Figure 6). Lentiviral receptor silencing in astrocytes ameliorated the EAE course whereas a receptor binding mutant did the opposite (Hindinger *et al.*, 2012; Ding *et al.*, 2015).

What has not been debated in this context so far, is that *in vitro* exposure of astrocytes to IFNγ induces major histocompatibility complex (MHC) class II expression, as it does *in vivo* for other antigen-presenting cells (APC, Muhlethaler-Mottet et al., 1998). This exposure activates astrocytes and their secretion of IL-12 and IL-23 and impairs their IL-27 production resulting in increased MOG-specific T cell (2d2) proliferation, differentiation and survival (Constantinescu *et al.*, 2005; Yang *et al.*, 2012). If IL-27 production is not downregulated, it will in turn suppress Th17 cells and induce Tr1 cells instead (Mascanfroni *et al.*, 2013, 2015). IL-27 expression is increased after initial exposure of astrocytes with EAE-derived lymphocytes (Yang *et al.*, 2012). This effect can be silenced by pre-treatment with IFNγ, pointing towards a very fragile balance between protective and detrimental IFNγ-dependent astrocytic effects.

A completely different mode of interaction between astrocytes and Th cells is adhesion molecules. They are involved in virtually all cell-cell interactions including activation, antigen priming and recognition or recirculation (Etzioni, 1996). Interesting candidates for further consideration in this context would be VCAM1 (CD106), ICAM1 (CD54) and NCAM1 (CD56, Liddelow and Hoyer, 2016). VCAM1 is traditionally heightened in cancer and well characterised in this context (Ruco *et al.*, 1996; Ding *et al.*, 2003; Chen, Zhang and Massagué, 2011). It is associated with tumour progression and a potential target for therapy (Liddelow and Hoyer, 2016). VCAM1 interacts with VLA4 and integrin α4β7 expressed on circulating immune cells. In the homeostatic brain, VCAM1 is almost exclusively expressed by astrocytes in the CNS, although its transcription levels do not change upon astrocytic activation (Cahoy *et al.*, 2008; Foo *et al.*, 2011) or do so in a region-dependent manner (Williams *et al.*, 2020). The latter study considered this effect to be Th17 dependent. NCAM1, with up to 27 different splice variants depending on the organ, is responsible for cell-cell adhesion and widely expressed on CNS cell types ranging from neurons, to endothelial cells, as well as micro- and macroglia (Zhang *et al.*, 2014). In addition to the splice variants, NCAM1 is also posttranslationally modified with polysialic acid (PSA). PSA-NCAM is associated with plasticity, especially in stem cell niches (Kiss and Muller, 2001). Both isoforms are associated with CNS repair and plasticity upon upregulation (Stork *et al.*, 2000; Bonfanti, 2006). Both immune and central nervous systems express ICAM1. It usually interacts with CD11a/CD18 (LFA1) or CD11b/CD18 (MAC1) on the immune side. Astrocytes express ICAM1 at a low level under homeostatic conditions and upregulate at least the transcription upon injury and activation (Carpentier *et al.*, 2005; Zamanian *et al.*, 2012).This increase especially on astrocytic end-feet is a potential protective mechanism against increased immune infiltration, basically a mechanism to keep immune cells within the perivascular space (Liddelow and Hoyer, 2016).

E TRP-Channels

TRP-channels can be found in many eukaryotes, ranging from *C. elegans* to humans. Even yeast display a TRP channel precursor (Montell, 2005). This superfamily constitutes of seven families, six of which are expressed in mammals, and 27 human members (Montell, 2005; Vennekens, Menigoz and Nilius, 2012). They cover all fundamental types of sensory perception, thermal perception, nociception, chemoception and many more. All channels are cationic plasma membrane channels, permeable to many cations with many different affinities and modalities of permeation (Nilius and Owsianik, 2011). The common feature for all members are their six transmembrane domains (Montell, 2005). The CNS families are TRPV, TRPC and TRPM, which are constitutively expressed on many central cell types; whereas TRPA, TRPP and TRP-ML are more restricted in their expression pattern (Vennekens, Menigoz and Nilius, 2012). Their functional implications range from store-operated calcium entry in non-excitable cells like astrocytes, to T cell activation and apoptosis, as well as cellular migration and proliferation (Montell, 2005).

TrpA1, being the only mammalian representative of the TRPA nociceptive TRP-family, is a multimodal cation channel (Nilius and Owsianik, 2011). The name derives from the protein's repetitive Ankyrin repeats and was initially identified in an oncogenic screen (Jaquemar, Schenker and Trueb, 1999). It is preferentially permeable for Ca^{2+}, although sodium is able to pass through to a lesser extent as well (Nilius and Owsianik, 2011). Activation is equally diverse including noxious cold (debated in mammals), pungent stimuli like mustard oil or cinnamaldehyde, growth factors (via metabotropic receptors) or proinflammatory factors like H^+ or pH-changes (Nilius, Appendino and Owsianik, 2012), as well as marijuana and bradykinin, and initiates a PLC-coupled pathway (Bandell *et al.*, 2004).

The TrpA1 channel is mostly expressed in association with nociception and pain. It was described on sensory neurons (Kádková *et al.*, 2017), oligodendrocytes (Hamilton *et al.*, 2016), as well as astrocytes (Shigetomi *et al.*, 2013). It has been functionally implicated in cuprizone-induced demyelination (Kriszta *et al.*, 2019), as well as in Alzheimer's disease (Lee *et al.*, 2016) and neurogenic inflammation and pain (Meseguer *et al.*, 2014), linking the channel functionally to degeneration and demyelination as well as to inflammation. All of these intertwine in MS, putting TrpA1 as a prime target for potential functional involvement in MS.

F Aims and Strategies

This thesis aims to answer the question to which extent and by which means astrocytes and proinflammatory T lymphocytes interact and functionally influence one another during inflammation. Little is known in a time-resolved manner about these interactions, especially *in vivo*. Astrocytes as part of the first defence line during proinflammatory T cell infiltration have long been neglected during analysis of central inflammatory processes.

The first major question we aim to answer is whether astrocytes and T lymphocytes locally interact in inflammatory lesions and how that interaction influences T cell behaviour, both in cell culture and in the living animal. For that purpose, we studied astrocytic interactions with Th17 cells in an antigen dependent manner. We utilised organotypic hippocampal slice cultures and analysed the potential changes in Th17 behaviour when contacting astrocytes in an antigen-dependent manner using two-photon microscopy.

In a next step, we transferred these findings to an *in vivo* situation. The question whether and under which conditions astrocytes may or may not express MHC class II has long been debated yielding contradicting results. We designed *in vivo* experiments to answer that question for EAE, the most established animal MS model finally. Firstly, the expression dynamics during the EAE course were characterised and analysed using flow cytometry and in a next step, MHC class II protein was deleted on all astrocytes. We could observe distinct changes in the disease course, especially during the chronic phase of disease progression leading to the conclusion that astrocytes functionally express MHC class II and thereby influence the inflammatory disease course of EAE in mice.

How astrocytes detect this inflammation in the first place led us to the TrpA1-channel. It was been functionally linked to demyelination and neurogenic inflammation, thereby posing as a prime target. We could show that TrpA1 expression is downregulated in conditions mimicking the EAE lesion milieu (including pH-changes and Th17 presence and many more). Additionally, the deletion of TrpA1 dysregulates MHC class II expression in conditions that have beforehand been identified to selectively induce its expression on astrocytes. The astrocytic deletion of MHC class II partially protects from EAE symptoms whereas the deletion of TrpA1 leads to the opposite effect on the symptoms.

II Material and Methods

A Instruments

Table 1: Instruments

Instrument	Company
Analog Vortex Mixer	VWR International GmbH, Darmstadt (Germany)
Autoclave Heraeus	Thermo Fisher Scientific, Waltham (USA)
BD FACS Aria I	BD Bioscience, Franklin Lakes (USA)
BD FACS Canto II	BD Bioscience, Franklin Lakes (USA)
Cell Counting Chamber Neubauer improved	Brand , Wertheim (Germany)
Cell Culture Incubator	Binder GmbH, Tuttlingen (Germany)
Cell Culture Microscope, bright field	Hund, Wetzlar (Germany)
Centrifuge Heraeus Fresco 21	Thermo Fisher Scientific, Waltham (USA)
Centrifuge Multifuge Heraeus XIR	Thermo Fisher Scientific, Waltham (USA)
CFX Connect™ Real Time Detection System	Bio-Rad Laboratories, München (Germany)
Confocal Laser Scanning System SP8	Leica GmbH, Wetzlar (Germany)
Eppendorf Research Adjustable-volume Pipettes	Eppendorf GmbH, Wesseling-Berzdorf (Germany)
Fridges and Freezers	Liebherr, Bulle (Switzerland)
Gamma irradiator Gammacell 2000	Mølsgaard Medical, Risø (Denmark)
Greiner pipettes	Greiner, Kremsmünster (Germany)
Horizontal Laminar Flow Hood Heraguard	Thermo Fisher Scientific, Waltham (USA)
LUNA	Logos biosystems, Berlin (Germany)
Magnetic Stand Ambion	Thermo Fisher Scientific, Waltham (USA)
McILWAIN tissue chopper	Campden Instruments LTD, Loughborough (England)
MidiMACS and QuadroMACS Separators	Miltenyi Biotec GmbH, Bergisch Gladbach (Germany)
NanoDrop 2000c	Thermo Fisher Scientific, Waltham (USA)
Pipetus	Hirschmann Laborgeräte GmbH & Co.KG, Eberstadt (Germany)
Platform Shaker	Edmund Bühler GmbH, Hechingen (Germany)
Semi-sterile bench	Thermo Scientific™ Heraguard™ ECO
Surgery Instruments	Fine Science Tools Inc., Heidelberg (Germany)
Thermal Cycler	Peqlab GmbH, Erlangen (Germany)
Vertical Laminar Flow Hood SAFE 2020	Thermo Fisher Scientific, Waltham (USA)
Water bath Aqualine AL18	Lauda GmbH & CO. KG, Lauda-Königshofen (Germany)

B Two-photon Laser Scanning Microscopy System

Table 2: Two photon microscopy set-up components

Instrument	Company
Bold-Line series of stage top incubators	Okolab, Pozzuoli (Italy)
Chameleon Ultra-II	Coherent
GaAsP High Sensitivity PMTs, H7422-40	Hamamatsu
Mai Tai laser	Spectra-Physics
motorized stage SM-5	Luigs & Neumann
OKO Stage Top Chamber	Okolab

Olympus BX51 WI upright microscope fitted with an Olympus XLUMPlanFI 20x/0.95 W objective	Olympus Soft Imaging Solutions GmbH, Münster (Germany)
Optical Parametric Oscillator (OPO)	APE, Berlin (Germany)
TriMScope I 2-photon microscope	La Vision BioTec GmbH, Bielefeld (Germany)

C Laboratory supplies, plastics and glassware

Table 3: Necessary laboratory supply

Product	Company
Cell Culture Dish, polystyrene, Ø 60 mm	Greiner Bio-One GmbH, Frickenhausen (Germany)
Cell scraper	Corning, Corning (USA)
Cell strainer, nylon mesh, 70 and 100 µm	BD Bioscience, Franklin Lakes (USA)
Centrifuge Tubes, polypropylene (PP), 15 mL + 50 mL	Greiner Bio-One GmbH, Frickenhausen (Germany)
Cling film	Carl Roth GmbH, Karlsruhe (Germany)
Eppendorf Tubes 1.5 mL + 2 mL	Eppendorf GmbH, Wesseling-Berzdorf (Germany)
Filter pipette tips 10 µL,100 µL 200 µL, 1000 µL	Starlab, Hamburg (Germany)
Gloves size M	Starlab, Hamburg (Germany)
Hypodermic Needle 20G - 27G	BD Microlance, Gateshead (UK)
LUNA counting chambers	Logos biosystems, Berlin (Germany)
MACS LS Columns	Miltenyi Biotec GmbH, Bergisch Gladbach (Germany)
Microscope glass slides	Thermo Fisher Scientific Inc., Waltham (USA)
Millicell cell culture insert, 30 mm, 0,4 µm	Merck Millipore, Darmstadt (Germany)
Multiplate PCR Plates, 96 Wells, clear	Bio-Rad Laboratories GmbH, München (Germany)
Multiwell Plate, tissue-culture treated polystyrene, 6-well, 24-well, 48-well, 96-well	BD Bioscience, Franklin Lakes (USA)
Netwell insert, 15 mm, mesh size 74 µm	Sigma-Aldrich Corp., St Louis (USA)
Pipette tips 10 µL, 200 µL, 1000 µL	VWR International GmbH, Darmstadt (Germany)
Polystyrene Round Bottom Test Tubes 5 mL (FACS tubes)	BD Bioscience, Franklin Lakes (USA)
Scalpels	B. Braun AG, Melsungen (Germany)
Serological Pipettes, polystyrene, 5 mL + 10 mL + 25 mL	Greiner Bio-One GmbH, Frickenhausen (Germany)
Syringe, 1 mL + 2 mL + 30 mL	B. Braun AG, Melsungen (Germany)

D Chemicals and reagents

Table 4: Used chemicals and reagents

Compound	Company
4,6-diamidino-2phenylindole, dihydrochloride (DAPI)	Thermo Fisher Scientific, Waltham (USA)
Acridine Orange/Propidium Iodide LUNA cell counter	Logos Biosystems, Berlin (Germany)
Albumin bovine, cell culture grade (BSA)	Serva Electrophoresis, Heidelberg (Germany)

Ammonium chloride (NH_4Cl)	Sigma-Aldrich Corp., St Louis (USA)
Aqua bi. dest. Sterile	B. Braun AG, Melsungen (Germany)
Brefeldin A	Sigma-Aldrich Corp., St Louis (USA)
Collagenase	R&D Systems, Inc., Minneapolis (USA)
D-Glucose	Carl Roth GmbH, Karlsruhe (Germany)
Dispase	R&D Systems, Inc., Minneapolis (USA)
DNase I	F. Hoffmann-La Roche AG, Basel (Switzerland)
dNTP mix (10 mM each)	Thermo Fisher Scientific, Waltham (USA)
Dulbecco's PBS with and without Ca^{2+} & Mg^{2+}	Gentaur, Kampenhout (Belgium)
EDTA disodium salt dehydrate (Na_2EDTA) solution (0.5 M)	Sigma-Aldrich Corp., St Louis (USA)
Ethanol 100 % (v/v) (EtOH)	AppliChem GmbH, Darmstadt (Germany)
Ethanol 70 % (v/v) (EtOH)	AppliChem GmbH, Darmstadt (Germany)
Ethylenediaminetetraacetic acid (EDTA)	Carl Roth GmbH, Karlsruhe (Germany)
Foetal Bovine Serum, heat inactivated (FBS)	Biochrom AG, Berlin (Germany)
HEPES	Life Technologies Corp., Grand Island (USA)
Horse Serum, heat inactivated	Thermo Fisher Scientific, Waltham (USA)
IMDM	Life Technologies Corp., Grand Island (USA)
iQ™ SYBR® Green Supermix	Bio-Rad Laboratories, München (Germany)
Ketamine	Hameln Pharma Plus GmbH, Hameln (Germany)
L-Glutamine (200 mM)	Sigma-Aldrich Corp., St Louis (USA)
Lipopolysaccharide (LPS)	Enzo Life Sciences GmbH, Lörrach (Germany)
Magnesium chloride ($MgCl_2$)	Sigma-Aldrich Corp., St Louis (USA)
NaCl solution 0.9 %	B. Braun AG, Melsungen (Germany)
Normal goat serum (NGS)	Vector Laboratories, Burlingame (USA)
Paraformaldehyde (PFA)	Carl Roth GmbH, Karlsruhe (Germany)
Penicillin / Streptomycin (P/S) (10,000 units penicillin and 10 mg streptomycin per mL)	Sigma-Aldrich Corp., St Louis (USA)
Percoll	Sigma-Aldrich Corp., St Louis (USA)
Potassium bicarbonate	Sigma-Aldrich Corp., St Louis (USA)
ProLong Gold Antifade Mountant	Thermo Fisher Scientific, Waltham (USA)
RNase inhibitor	Clontech, Mountain View (USA)
Rompun 2% injection solution (Xylazin)	Bayer Health Care, Leverkusen (Germany)
Saponine	Carl Roth GmbH & Co. KG, Karlsruhe (Germany)
Triton X-100	Sigma-Aldrich Corp., St Louis (USA)
ß-Mercaptoethanol	Sigma-Aldrich Corp., St Louis (USA)

E Kits

Table 5: Used kits

Kit	Company
CD4 T Cell Isolation Kit	Miltenyi Biotec GmbH, Bergisch Gladbach (Germany)
DNase I recombinant, RNase free with 10x Incubation buffer	F. Hoffmann-La Roche AG, Basel (Switzerland)
eBioscience™ Foxp3 / Transcription Factor Fixation/Permeabilisation Concentrate and Diluent	Invitrogen, Carlsbad (USA)
RNeasy® Micro Kit	Qiagen, Hilden (Germany)
Superscript III First Strand Synthesis System	Thermo Fisher Scientific, Waltham (USA)

F Microbeads

Table 6: Used microbeads

Kit	Isotype	Company
CD62L MicroBeads	rat-α-mouse monoclonal IgG2a	Miltenyi Biotec GmbH, Bergisch Gladbach (Germany)
CD90.2 MicroBeads	rat-α-mouse monoclonal IgG2b	Miltenyi Biotec GmbH, Bergisch Gladbach (Germany)

G Cytokines

Table 7: Used cytokines for cell culture and treatment

Cytokines	Company
huTGF-β	R&D Systems, Inc., Minneapolis (USA)
IL-2	R&D Systems, Inc., Minneapolis (USA)
IL-23	R&D Systems, Inc., Minneapolis (USA)
IL-17	Peprotech
IFNγ	Peprotech
αIFNγ	BioXcell
LPS	Alexis Biochemicals
TNFα	Peprotech
αCD3	BD Biosciences
IL-12	BioXcell
IL-18	MBL

H Custom buffers, solutions and media

Table 8: Recipes for custom buffers and media used

Buffer/Solution	Ingredients
Ammonium chloride	**For 400 ml** **PBS 0,1M (Use tablets) 400ml** **NH4Cl 1,06g**
Anaesthesia solution	**20 mL 50 mg/mL Ketamine** **2.5 mL 2% Rompun** **in 77.5 mL 0.9 % NaCl solution**
Astrocyte medium	**DMEM (500 mL)** **+50 ml FBS** **+ 5 ml Penicillin-Streptavidin (P/S)** **+ 5 ml L-Glutamine (L-Glu)**
FACS Buffer	**0.5 % BSA** **in PBS**
Lysis Buffer	**8.29 g/L NH4Cl** **1 g/L KHCO3** **37.2 mg/L NA2EDTA** **in dH2O**
MACS Buffer	**0.5 % BSA** **0.5 M EDTA** **in PBS**

MEM (2x)	**160.93 g MEM** **+ 0.35 g NaHCO3** **+ 5 L Aqua dest.**
Saponine Buffer	**0.5 % Saponine** **0.5 % BSA** **in PBS**
Mouse Medium (MM)	**10 % FCS** **1 % P/S** **1 % L-Glutamine** **0.1 % β-mercaptoethanol** **1 % HEPES** **in RPMI**
Wash Medium (WM)	**5 % FCS** **1 % P/S** **1 % HEPES** **in RPMI**
Slice culture Medium	**50 mL 2x MEM** **+ 41.8 mL Aqua dest. sterile** **+ 50 mL BME** **+ 50 mL heat inactivated horse serum** **+ 2 mL 200 mM L-Glutamine** **+ 6.25 mL 20 % Glucose** **pH 7.2**
Slice preparation medium	**100 mL 2x MEM** **+ 98 mL Aqua dest. sterile** **+ 1 mL 200 mM L-Glutamine** **pH 7.35**

I Antibodies

i FACS

Table 9: Flow cytometry antibodies

Antibody	Clone	Isotype	Concentration	Company
Life/dead-V450			1 mg/mL	BD Horizon
αCD16/ αCD32 (FC-block)	2.4G2	rat-α-mouse monoclonal IgG2b, κ	0.5 mg/mL	BD Bioscience, Franklin Lakes (USA)
αCD4-AF647	RM4-5	rat-α-mouse monoclonal IgG2a	0.1 mg/mL	Life Technologies Corp., Grand Island (USA)
αCD4-Horizon (V450)	RM4-5	rat-α-mouse monoclonal IgG2a, κ	0.2 mg/mL	BD Bioscience, Franklin Lakes (USA)
αCD4-PECy7	RM4-5	rat-α-mouse polyclonal IgG	0.2 mg/mL	BD Bioscience, Franklin Lakes (USA)
αCD62L-APC	MEL-14	rat-α-mouse monoclonal IgG2a, κ	0.2 mg/mL	BD Bioscience, Franklin Lakes (USA)

αCD80-FITC	16-10A1	Armenian hamster / IgG	0.5 mg/mL	Invitrogen
αCD86-PE	GL1	rat-α-mouse	0.2 mg/mL	BD Bioscience, Franklin Lakes (USA)
αGLAST-APC	ACSA-1	mouse IgG2aκ	For 100 test	Miltenyi Biotec
αIFN-γ-Horizon (V450)	XMG1.2	rat-α-mouse monoclonal IgG1, κ	0.2 mg/mL	BD Bioscience, Franklin Lakes (USA)
αIL-17A-APC	eBio17B7	rat-α-mouse monoclonal IgG2a, κ	0.2 mg/mL	Thermo Fisher Scientific, Waltham (USA)
αMHC II-BV605	M5/114.15.2	rat-α-mouse monoclonal IgG2b, κ	0.5 mg/mL	Biolegend
αTNF-α-AF700	MP6-XT22	rat-α-mouse monoclonal IgG1, κ	0.2 mg/mL	BD Bioscience, Franklin Lakes (USA)

ii Histology

Table 10: Histology antibodies

Antibody	Species	Dilution	Company
αCD4-647	Rat	1:200	BD Biosciences
αGFAP	Mouse	1:1000	Synaptic Systems
αGFAP	Rabbit	1:1000	Millipore
αGFP	Mouse	1:1000	Synaptic Systems
αGFP	Rabbit	1:1000	abcam
αMHC II	Rat	1:100	abcam
αMouse 488	Goat	1:1000	Invitrogen
αMouse 568	Goat	1:1000	Invitrogen
αMouse 647	Goat	1:1000	Invitrogen
αNeuN	Mouse	1:1000	Millipore
αRabbit 488	Goat	1:1000	Invitrogen
αRabbit 647	Goat	1:1000	Invitrogen
αRabbit568	Goat	1:1000	Invitrogen
αRat 568	Goat	1:1000	Invitrogen
αRFP	Rabbit	1:500	Rockland
αTrpA1	Rabbit	1:100	Novus Biologicals

J qRT-PCR primers

Gene	Fw Sequence	Rev Sequence	Concentration [nm]	Tm [°C]
GFAP	TCAACTAACAGGATACTC	ATAACAACAAGGATGAAG	200 nM	52 °C
Rps29	CAAATACGGGCTGAACAT	GTCGCTTAGTCCAACTTAA	200 nm	58 °C
Trpa1	CAACATAACCGCATAGAACT	AATCCATAGGCACACCAT	400 nM	60 °C

K Mice

i Wildtype mice

Table 11: Wildtype mouse strains

Strain	Laboratory
C57BL/6 (B6)	Envigo

ii Genetically modified mice

Table 12: Genetically modified mouse strains

Strain	Target properties	Reference/In house breeding
B6.Tg(Aldh1l1-EGFP,-DTA)D8Rth/J (Aldh1l1-eGFP)	Astrocytes expressing GFP	(Tsai *et al.*, 2012)
B6.129X1-H2-Ab1tm1konj/J x GFAP-Cre (GFAP-Cre)	Astrocyte-specific MHC II ko	In house breeding
B6.OT2.RFP	$CD4^+$ T cells are OVA specific and labelled in red	B6.OT2 x B6.acRFP
B6;129P-Trpa1tm1Kykw/J (TrpA1 ko)	Complete TrpA1 channel knockout	(Kwan KY *et al.*, 2006)
B6.2D2.CFP	$CD4^+$ T cells are MOG35–55 specific and labelled in cyan	B6.2D2 x B6.CFP
B6.2D2.RFP	$CD4^+$ T cells are MOG35–55 specific and labelled in red	B6.2D2 x B6.acRFP

L Software

Table 13: Software used for acquisition and analysis of data

Software	Application	Company
Adobe Photoshop	Image analysis	Adobe
Beacon Designer 8 Software	Primer design	Premier Biosoft International, Palo Alto (USA)
Beamsplitter	Two-photon image acquisition	LaVision
Bio-Rad CFX Manager	Assessment of qRT-PCR data	Bio-Rad Laboratories, Munich (Germany)
FACSDiva	FACS Analysis	BD Bioscience, Franklin Lakes (USA)
FlowJo	FACS Analysis	Tree Star, Ashland (USA)
GraphPad Prism 6, 7, 8	Statistical Analysis	GraphPad Software, Inc., La Jolla (USA)
ImageJ	Analysis of histological stainings	National Institutes of Health, Bethesda (USA)

Imaris (v. 8.1.2)	Analysis and Video preparation of two-photon images	Bitplane AG, Zurich (Switzerland)
ImSpector Pro	Two-photon image acquisition	LaVision
NanoDrop 2000 Operating Software	Determination of RNA concentrations	Thermo Fisher Scientific, Waltham (USA)

M T-cell isolation and culture

For Th17 and Th1 cultures, naïve T cells were co-cultured with APC in the presence of αCD3e and polarizing cytokines as described below.

i Isolation of APC

For the isolation of APC, spleens from cervically dislocated C57BL/6 mice (6 to 12 weeks old) were dissected and transferred into a 15 mL tube containing 5 mL Wash medium (WM). Cells were put through a nylon mesh (100 µm) and resuspended in 50 mL WM. After centrifugation (550 g, 5 min, 4 °C), erythrocytes were lysed by resuspending the cell pellet in 10 mL Lysis buffer. To stop the lysis, 5 mL WM were added. The cells were centrifuged again (550 g, 5 min, 4 °C) and taken up in 50 mL MACS buffer. Cells were counted to determine the most appropriate reagent volume for the magnetic bead-based cell sort of CD90.2 negative cells. For MACS sorting, the cell pellet was resuspended in 95 µL of MACS buffer and 5 µL of CD90.2 beads for every $1x10^7$ cells. The incubation occurred for 15 min at 4 °C. CD90.2-directed microbeads were used to label splenic lymphocytes without the capacity of antigen presentation. Throughout the magnetic cell sort, all CD90.2 positive cells were removed from the APC fraction, due to fixation in the magnetic field created between the magnet and the column. The flow-through containing the unlabelled APC was centrifuged and the APC were resuspended in 10 mL of sterile filtered mouse medium (MM). In order to avoid proliferation of APC in the co-culture with T cells and to limit APC lifetime during culturing, APC were irradiated in a gamma irradiator, applying 3000 rad. Cells were then centrifuged (550 g, 5 min, 4 °C), taken up in 20-50 mL depending on the pellet size and counted manually.

ii Isolation of naïve $CD4^+$ T cells

For the isolation of naïve $CD4^+$ T cells, spleens from cervically dislocated B6.2D2.CFP mice or B6.2D2.RFP mice (6 to 9 weeks old) were dissected and transferred into a 15 mL tube, containing 5 mL WM. Cells were put through a nylon mesh (100 µm) and resuspended in 50 mL WM. After centrifugation (550 g, 5 min, 4 °C), erythrocytes were lysed by resuspending the cell pellet in 10 mL lysis buffer. To stop the lysis, 5 mL WM were added. The cells were centrifuged (550 g, 5 min, 4 °C) and taken up in 20-50 mL MACS buffer, depending on the pellet size. Cells were counted to determine the most appropriate reagent volume for the magnetic bead-based cells sort of naïve $CD4^+CD62L^{hi}$ cells. The magnetic bead-based sort of murine $CD4^+CD62L^{hi}$ T cells was performed using a Miltenyi CD4 isolation kit followed by a CD62L positive sort according to the manufacturer's instructions. Thereby 40 µL MACS buffer and 10 µL of the CD4 T cell biotin antibody cocktail were applied for every 10^7 cells. The pellet was resuspended in the corresponding volume and incubated for 10 min at 4 °C in the dark. According to the manufacturer`s instructions, 30 µL MACS buffer and 20 µL anti-biotin microbeads

were added after this incubation. An additional incubation time of 5 min followed. At this step, 5 µL CD8 microbeads were also added to the anti-biotin microbeads to reduce the amount of contaminating $CD8^+$ cells in the target fraction, which are hard to remove by purely applying the CD4 isolation kit. After this untouched sort of $CD4^+$ cells, the efficiency was evaluated via flow cytometry. Therefore, αCD4-Horizon was used to stain for surface molecule stainings. Usually, $CD4^+$ purity reached around 90 % of the lymphocytes. The CD62L positive sort was performed subsequently. For this, 960 µL of MACS buffer and 40 µL of CD62L microbeads were added to the cell pellet of enriched CD4-expressing cells. The incubation occurred for 10 min at 4 °C in the dark. The efficiency of the cell sort was routinely analysed via flow cytometry using αCD4-PeCy7 (1:1000) and αCD62L-APC (1:200) antibodies. Only naïve T cells with purity better than 96 % were used for further experiments.

iii T cell culture and differentiation

To differentiate the naïve T cells into Th17 cells or Th1 cells, cells were cultured on a 24-well plate in 2 mL MM in the presence of 2 µg/mL αCD3e and with the irradiated $CD90.2^+$-depleted C57BL/6 splenic APC (II .M .i in a one-to-five or a one-to-ten ratio. For the initial stimulation into Th17 or Th1 differentiation, the following cytokines were added: Th17 received 3 ng/mL huTGF-β, 20 ng/mL IL-23, 20 ng/mL IL-6, 10 µg/mL α-IL-4, 10 µg/mL α-IFNγ and 2µg/mL α-CD3. Th1 cells received 25 µg/mL IL-18, 2 µg/mL α-CD3, 10 µg/mL IL-12 and 10µg/mL α-IL-4.

After 3 and 5 days of culture, T cells were split and fed with the individually necessary cytokines. Th17 cells were fed with 50 U/mL (d3) or 25 U/mL IL-2 (d5) and 10 ng/mL IL-23 (d3 and d5). Th1 cells were fed with 100 U/mL IL-2 on d3 and d5.

Th17 cells were either used for co-cultures after 5 days of culture or restimulated after one week. For the restimulation, Th17 were harvested, counted and seeded on 24-well plates with freshly isolated, irradiated $CD90.2^+$-depleted C57BL/6 splenic APC, at a one-to-five ratio and in the presence of 2 µg/mL αCD3e. The following cytokines where added for restimulation: 0.75 ng/mL TGFβ, 20 ng/mL IL-23 and 10 ng/mL IL-6.

Restimulated cells were used three days after the restimulation for further experiments (co-culture with organotypic hippocampal slices or induction of passive transfer EAE).

iv Cytokine check in T cell cultures

Cytokine expression was routinely checked on day 5 and day 10 of culture using flow cytometry to detect successful T cell polarization. 24 h prior to the cytokine check, one well per culture was coated on a 48-well plate with αCD3e and αCD28 antibodies. For this, 120 µL PBS, containing 3 µg/mL αCD3e and 2.5 µg/mL αCD28 were applied per well. The 48-well plate was covered with a cling film pre-sprinkled with 70 % ethanol and incubated at 4 °C overnight. For stimulation, the coating solution was removed. 2 mL of the T cell culture were resuspended and divided into two 1 mL cell suspensions, which was transferred to either the coated or to the uncoated control well of the 48-well plate. Brefeldin A was added with a final concentration of 5 µg/mL into each well to block the cytokine secretion of the cells. After 4 h of stimulation, cells were harvested for the FACS staining which was performed according to using CD4-PECy7 for extracellular staining, Fc-blocking solution in combination with IFNγ-Horizon, IL-17-APC and TNFa-AF700 for intracellular staining analysing Th17 and Th1 cells. Th17 cells usually yielded 30-40 % IL-17 and no IFNγ expression, while Th1 cells showed the opposite expression pattern.

N FACS staining and analysis

To stain the surface of cell populations, cell suspensions were centrifuged (550 g, 5 min, 4 °C), supernatants were removed and the cell pellets were washed twice with 1 mL of FACS buffer. After these washing steps, the cell pellets were taken up in a staining solution, prepared with fluorescently labelled antibodies directed to the target antigens diluted in PBS. If not otherwise mentioned, 100 µL of staining solution was used for up to $10x10^6$ cells. Cells were incubated with the staining solution for 10 min at 4 °C in the dark. After incubation, 1 mL of PBS was added to the cell suspension to wash the cells. Cell suspensions were centrifuged (550 g, 5 min, 4 °C) and cell pellets were taken up in 1000 µL FACS buffer. The cell suspensions were then transferred to FACS tubes. Staining was performed in PBS to avoid unspecific binding in FACS buffer.

The surface stained cell suspension could be either directly analysed in the flow cytometer or used for further intracellular staining. For intracellular staining, cells had to be fixed and permeabilised. In this case, cell suspensions were centrifuged (550 g, 5 min, 4 °C) and washed with PBS.

For fixation and subsequent intracellular staining, cells were incubated in 1 mL of 2 % PFA for 20 min at 4 °C in the dark. For intranuclear stainings, cells were incubated with eBioscience Fixation/ Permeabilisation Concentrate and Diluent for at least 30 minutes. After fixation, all subsequent centrifugation steps were performed at 1000 g for 5 minutes at 4 °C. Following fixation, cells were washed with PBS. For membrane permeabilisation, 2 mL Saponine buffer or perm buffer were added to the cells and cell suspensions were centrifuged. The cell pellets were then washed with another 2 mL Saponine buffer or perm buffer to complete permeabilisation. Cells were centrifuged and the supernatants were removed. For FC-blocking, 70 µL Fc-blocking solution (αCD16/αCD32, 1:70 in Saponine buffer/ perm buffer) was added and incubated for 10 min at 4 °C in the dark. For the intracellular staining, 20 µL of staining solution, prepared with fluorescently labelled antibodies directed to the intracellular target antigens diluted in Saponine buffer or perm buffer were added. The dilutions of the target antibodies were calculated for 100 µL of total staining volume (70 µL + 20 µL + cell pellet and Saponine residues). Incubation occurred for 20 min at 4 °C in the dark. After the intracellular staining, cells were washed with 2 mL Saponine buffer or perm buffer and in a second washing step with 2 mL FACS buffer. The washed cells were then resuspended in 200-300 µL FACS buffer, depending on the cell number. The cell suspensions were transferred to FACS tubes and acquired at the flow cytometer.

O Murine organ dissections

Prior to dissection of the target organs, surgery instruments were wiped with ethanol (70 %). Mice were either sacrificed via cervical dislocation or lethally anesthetized by the application of 1 mL/mouse anaesthesia solution, containing Ketamine and Rompun in sterile NaCl solution (0.9 %). Surgery began as soon as no reflexes were detectable. The abdominal skin was opened and detached from the abdominal cavity.

i Spleen preparation

To dissect the spleen, the abdominal cavity was opened with sterile scissors at the side. Sterile forceps were used to take out the spleen and to remove the attached pancreas as well as fatty tissue. The separated spleen was used for T cell cultures.

ii CNS preparation

Prior to CNS dissection, mice were perfused with PBS to remove the whole blood from the mouse in order to avoid the presence of blood cells in the dissected CNS. To this end, the thorax of the mice was opened. The diaphragm was removed to enable access to the heart and a small incision was made into the right atrium. A syringe of PBS was used to inject 20-30 mL PBS into the left ventricle. After perfusion, the CNS and spinal cord were removed and transferred to a 15 mL tube containing 5 mL of IMDM if used for further work-up and subsequent FACS analysis.

The CNS was homogenised using a scalpel and digested with 50 µL collagenase (5 mg/µL), 50 µL collagenase/dispase (1000 U/µL) and 50 µL DNase (1 mg/mL) for 30 min at 37 °C. The solution was filtered through a 100 µm mesh and washed with 50 mL IMDM. After centrifugation (550 g, 5 min, 4 °C), the pellet was resuspended in either 30 % percoll for T cell isolation or 20 % percoll for astrocyte isolation. The upper phase was carefully layered on top of either 70 % percoll (T cells) or 40 % percoll (astrocytes). After continuous centrifugation (750 g, 30 min, room temperature (RT), no break), the interphase was isolated and washed once with PBS.

For histological stainings, mice were additionally perfused with PFA for fixation purposes. Fixed organs were dehydrated in sucrose for freezing.

P Experimental autoimmune encephalomyelitis

At least one week prior to the EAE induction, mice were transported from the animal facility into the laboratory for acclimatisation. Induction was performed according to Bittner, Afzali, Wiendl, & Meuth, 2014. In brief, on the day of induction, 250 µg/mouse MOG_{35-55} peptide and 800 µg/mouse H37Ra were injected subcutaneously in complete freund adjuvant (CFA). 4 h after the application, 400 ng/mouse pertussis toxin (PTX) were applied intraperitoneally. Two days after induction, PTX was applied again. Each day, the animals' weight was recorded and the disease course was evaluated accessing the murine symptoms, starting with tail paresis and plegia, followed by weakening of the righting reflex and continuing with hind paw paresis and plegia.

Q Isolation of astrocytes for cell culture

For astrocyte cultures, p0-p1 B6 pups were beheaded and brains were removed from the skull. The brains were prepared in ice-cold HBSS. The olfactory bulbi and the meninges were removed from the cortex. The hippocampus was stripped from the cortex and all cortices were collected in ice-cold HBSS. Cortices from up to three animals were pooled. The tissue was washed once with ice-cold HBSS and digested in HBSS with 1 % DNase and 0.5 % trypsin for 10 min at 37 °C. For homogenisation, tissue was sucked through two small glass pipettes and finally poured over a 70 µm mesh. 75,000 – 150,000 cells/well were seeded in DMEMC (DMEM with 1 % Pen/Strep, 10 % foetal bovine serum, 2 mM L-Glutamine) on a 24-well plate with glass cover slips or a 6-well plate for qPCR. The next day, cells were washed with DMEMC. The cultures were washed vigorously every two to three days with DMEMC. Astrocytic cultures were treated at day eight. Cultures were either fixed 24 h later with 5 min 2 % paraformaldehyde (PFA) and 20 min 4 % PFA, or scraped in PBS for qPCR. Fixed cells were used for histological stainings.

R RNA Isolation and cDNA synthesis

i RNA isolation using RNeasy© Micro Kit

For RNA extraction, astrocytes were harvested by scraping from a six-well plate. RNA was isolated using the RNeasy® Micro Kit (Qiagen). The first resuspension steps were performed by up and down pipetting (at least ten times) in RLT buffer using a syringe (20 G) in order to allow complete lysis of the cells.

The RNA isolation was performed according to the manufacturer's instructions. Consequently, cells were resuspended and homogenized in 350 µL RLT buffer with a blunt 20-gauge needle. 350 µL of 70 % ethanol (freshly prepared from 100 % ethanol and RNAse-free water) were added to the lysate and the sample was mixed by pipetting. The sample was then transferred to an RNeasy MinElute spin column in a 2 mL collection tube and centrifuged (8000 g, 15-60 s, at RT). The flow-through was discarded before the column was washed with 350 µL RW1 buffer. The sample was centrifuged (8000 g, 15-60 s, RT) and the flow-through was again discarded. 10 µL DNase I stock solution was diluted in 70 µL RDD buffer to freshly prepare 80 µL of a DNase I incubation mix, which was transferred to the column membrane. Incubation occurred at RT for 15 min to allow DNA digestion. 350 µL RW1 buffer were then used to wash to the column. After centrifugation (8000 g, 15-60 s, RT), the collection tube was discarded. The column was placed in a new 2 mL collection tube and washed with 500 µL RPE buffer. After centrifugation (8000 g, 15-60 s, RT), the flow-through was discarded. An additional washing step was performed with 500 µL of 80 % ethanol (freshly prepared from 100 % ethanol and RNAse-free water) (8000 g, 15-60 s, RT). The column was again placed in a new 2 mL collection tube. To dry the membrane, the lid of the column was opened before the next centrifugation step (21000 g, 5 min, RT). To elute the RNA, the column was placed in a 1.5 mL collection tube, 20 µL RNase-free water were added directly to the centre of the column membrane and the column was centrifuged (21000 g, 1 min, RT). The RNA was either directly used for further experiments or stored at -80 °C.

ii cDNA synthesis

For qRT-PCR, RNA was transcribed into cDNA using the SuperScript® III First Strand Synthesis System following the manufacturer's instructions. Per reaction, 1 µg RNA was used in a reaction volume of 50 µL. If less material was available, all RNA was used. 5 µL of random hexamer primers (50 ng/µL) were added to 18 µL of the diluted RNA sample. To allow primer hybridization, samples were incubated for 5 min at 65 °C. The tubes were then placed on ice and 27 µL of the following reaction mix was added to each sample:

Table 14: cDNA synthesis master mix

Component	Volume [µL]
MgCl2	10
10x RT buffer	5
0.1 M DTT	5
dNTP mix (10 mM each)	5
RNaseOUT	1
Superscript III reverse transcriptase	1

The samples were then transferred into a thermal cycler and the following program was started:

Table 15: PCR cycler program for cDNA synthesis

Cycle step	Temperature (°C)	Time
1	25	10 min
2	50	50 min
3	85	5 min
4	4	hold

If 1 µg RNA was used for cDNA syntheses, the resulting cDNA was diluted with 150 µL nuclease-free water. If less RNA was applied, the volume was adjusted for qRT-PCR.

S qRT-PCR

For qRT-PCR, 4 µL of cDNA was amplified using iQ SYBR® Green supermix in a CFX Connect™ Real Time Detection System. Therefore, 100-400 nM of the respective forward and reverse primers (II .J designed using Beacon Designer 8 Software and subsequently tested for amplification efficiency and specificity) were added to 10 µL of the iQ SYBR® Green supermix. Nuclease-free water was used to fill each reaction mix up to 16 µL. The reaction mix was then pipetted into 4 µL of the diluted RNA sample on a clear 96-well plate. The plate was placed in the CFX Connect™ Real Time Detection System and the following thermal cycle was performed:

Table 16: qRT-PCR cycler program

cycle	Temperature (°C)	Time
1	95	3 min
2-41	95	10 s
melting temperature	45 s	
Plate read		
42	95	1 min
43	55	1 min

Technical triplicates of gene expressions were applied to ensure accuracy of the quantity determination. Data were analysed using Bio-Rad CFX Manager Software. Only triplicates with an SD < 0.5 were used for the analysis. As described above, amplification was performed for 40 cycles. Samples which were not detectable were included in the analysis with a C_q value of 40. Gene expression was normalized to RPS29 expression.

T Organotypic hippocampal slice cultures

For organotypic hippocampal slice cultures (OHSC), p3-5 pups from either B6, Aldh1l1-eGFP or TrpA1 knockout (ko) mice were used. The scissors, forceps and spatula were disinfected in ethanol and transferred to PBS for sterile isolation.

The pups were decapitated and the skull was opened to isolate the brain, which was transferred to 6 cm petri dishes filled with 5 mL of SPM. The brain was split in half at the midline and the two cortices were placed on the interior side. The meninges were taken away from the cortex and the halves were turned so that the hippocampus was visible. To separate the hippocampus from the cortex, two incisions were made on the shorter sides of the hippocampus. It was flipped to the side and the last connection was cut. The hippocampi were coronally cut into 300 µm-thick slices using a McILWAIN

tissue chopper. Intact hippocampal slices were then transferred onto Millicell cell culture inserts and cultivated for 3 to 4 days in slice culture medium. The medium was changed 24 h after the isolation of the hippocampus and then every other day. After 3 to 4 days of culture, hippocampal slices were used for experiments. For co-cultures, either 1 x 10^5 Th17 or 1 x 10^5 Th1 cells were added in a volume of 10 µL on top of the hippocampal slices and cultured for 24 h before histology or two-photon imaging. For some experiments, an MHC class II blocking antibody was added to the slice culture medium in addition to the added T cells.

U Two-photon *ex vivo* imaging and analysis

Co-cultures of T cells and hippocampal slices (with or without blocking MHC class antibody) were used after 24 h of co-culture for two-photon imaging. For imaging, the cell culture inserts with the organotypic hippocampal slices were transferred to 60 mm cell culture dishes with pre-warmed medium. The dish was transferred to the TriMScope I from LaVision Biotec with the multi-photon system with a heated and gas perfused (95 % O2/5 % CO2) Bold-Line series of stage top incubators. Volumes of 300 µm x 300 µm at 70 µm were acquired for at least 20 min at 850 nm. B6 and TrpA1 ko slices were counterstained with SR101; Aldh1l1-eGFP pups were already fluorescently-labelled.

All image analysis was performed using Imaris software. Cell tracks were created using the tracking tool and manually corrected. Contact types and durations were determined manually with 3D rotation and surface analysis to verify contacts. Short contacts were defined as less than 5 min, temporary contacts were defined as contacts lasting more than 5 min and less than 10 min, stable contacts consisted of contacts lasting longer than 10 min.

V Immunohistochemistry

i Tissue preparation

For histological stainings, mice were additionally perfused with PFA for fixation purposes. Fixed organs were dehydrated in sucrose for freezing. The organs were cut using a cryostat at 10 µm thickness in 10er series.

Slices were first fixated by transferring the slice culture inserts to a 6-well plate containing 1 mL PFA (4 %). 1 mL additional PFA (4 %) was added on top of the slice. Incubation occurred for 20 min at RT. PFA was removed and the fixation step was repeated two times using fresh PFA (4 %) to complete fixation. The slices were then washed with phosphate buffer (PB) three times (each time 5 min at RT), before the membrane was cut out using a scalpel. The cut culture insert was glued with HistoFix onto a block of agarose to enable re-slicing of the slices with a vibratome. The agarose block was glued to a metal plate which was submerged in the PB-water (1:1) bath of the vibratome cooled to 4 °C. Using the vibratome, the original slices were re-sliced into 50-µm-thick slices. These slices were transferred to Netwell inserts (74 µm mesh size) for free-floating immunohistochemistry and either stored in PB at 4 °C or directly used for the immunostaining.

ii Staining procedures

Before immunostaining was started, all samples were incubated with ammoniochloride for 10 min at RT. In addition, non-specific binding sites were blocked using a serum blocking buffer containing NGS or NDS (5 %) and Triton X-100 (0. 2 %) diluted in PB. Therefore, the slices were incubated in 1.5 mL of blocking buffer for 1 h. This incubation step and all subsequent incubation steps were performed in the dark on a platform shaker. For stainings, the primary rat antibody was stained overnight at 4 °C. The staining solution was then removed and the slices were washed 3 times with PB (5 min each). The fluorophore-conjugated anti-rat secondary antibody was then added in blocking solution at RT for 3 h. The staining solution was removed and the slices were washed 3 times with PB (5 min each). The same procedure was repeated for the other antibodies of the staining mix. To stain the nucleus, DAPI was used at a concentration of 500 ng/mL in PB and incubated for 20 min at RT. Following incubation, slices were washed five times with PB for 7 min at RT. The slices were then mounted on microscope glass slides using ProLong Gold Antifade Mountant. The confocal laser scanning system SP8 from Leica was used to acquire images, which were then exported as TIFFs for analysis in ImageJ or Imaris software.

W Legendplex (Biolegend)

Astrocytic supernatants were collected after the cultivation period described above. The Legendplex was performed after the manufacturer's instructions. In brief, the standard was diluted in 250µL assay buffer for the top S7 and diluted serially 1:4 for standard S6 to S1. Samples were not diluted beforehand. All conditions were run in duplicates. The assay was performed at RT. All wells were diluted 1:2 with assay buffer. One more portion of beads was added to the mix. The sealed plate was shaken for 2h at 800 rpm protected from light. The plate was centrifuged at 250g for 5min and the supernatant discarded. Wash once with washing buffer and centrifuge again. One portion of detection antibodies was added to the beads and shaken for one hour at 800 rpm protected from light. One portion of SA-PE was added directly and shaken for 30 min at 800 rpm protected from light. The plate was centrifuged at 250 g for 5 min. The supernatant was discarded. Two portions of wash buffer were added to the beads and the samples were analysed using a FACS Canto II and the data was analysed using the Biolegend Legendplex Data Analysis Software.

X Statistical analysis

If not otherwise mentioned, all data were analysed using GraphPad Prism 6 or 8. Mean group differences were investigated by one-way ANOVA followed by Tukey's multiple comparison test, Mann-Whitney test or independent-sample t-tests. Significance levels were set to 0.05. The ROUT method implemented in GraphPad was used to identify and exclude outliers.

III Results

A MHC Class II Induction is Selectively Induced by 2d2.Th17 Cells on Astrocytes *In Vitro*

In order to study astrocytic interactions with T cells in a tissue-specific context, we chose the organotypic hippocampal slice culture (OHSC) model. This approach allowed us to study astrocytes in their cellular context integrated into a network rather than completely isolated in single cell cultures providing a closer resemblance to the *in vivo* cellular context. OHSC are an established model to study longer-term *ex vivo* cellular functions, including neuroprotection from stroke or cancer during its development (Yoshikawa *et al.*, 1998; Hölsken *et al.*, 2006) as well as astrocyte-neuron interactions in the context of Parkinson's disease (Loria *et al.*, 2017) and the astrocytic ability to protect neurons during challenge (Greenwood and Bushell, 2010). This culture system remains viable for weeks in culture but we chose to examine an early time point when microglial response after the initial preparation has calmed down and astrocytic scar formation has not been triggered to its full extent (Gerlach *et al.*, 2016).

OHSC were isolated from p3-p6 Aldh1l1.eGFP mice and cultured for four to five days. The Aldh1l1.eGFP strain has green eGFP-fluorescent astrocytes. Naïve $CD4^+$ brain-specific antigen recognising T cells (2d2) were isolated from the spleen and shifted towards a Th17 phenotype. We used 2d2.RFP animals, which show a red fluorescence in all cells, also in the isolated naïve $CD4^+$ T cells. 2d2.Th17 cells were cocultured with the OHSC for at least 24h to allow migration into the tissue and the interactions with astrocytes were analysed using two-photon imaging in the living slice (Figure 7a). The green fluorescent astrocytes are easily distinguishable by size and fluorescence from the 2d2.Th17 cells. During recording time, the temperature as well as the gas levels were kept constant in a specialised coculture chamber to maintain stable experimental conditions.

A variety of contact behaviours, including short as well as stable contacts were observed; exemplary time lapses can be seen in Figure 7a (right panel). Typically, astrocytes were static cells under these conditions. Only the 2d2.Th17 cells were dynamic and displayed movement. During a short contact, the 2d2.Th17 cells would usually approach the astrocyte, probe one or two sides on the astrocytic surface and leave again. This interaction often lasted only two to three minutes. During a stable contact, most 2d2.Th17 cells would already be sitting at the side of the astrocyte. They might have display some moving protrusions, but usually the cells remained in place where it was initially observed (compare Figure 7a right, lower panel).

About one third of the analysed 2d2.Th17 cells interacted with astrocytes (Figure 7b). The rest may have interacted with other brain resident cells present in the OHSC such as microglia or neurons or may not have interacted for long with cells at all. These other potential interactions will not be analysed in this work. Generally, the astrocyte-contacting 2d2.Th17 cells were significantly slower than the non-contacting ones (Figure 7b). They also differed in other major characteristics including displacement rate and meandering index (data not shown); they exhibited a lower displacement rate and less meandering. Overall, the astrocyte-contacting 2d2.Th17 cells showed a more stationary phenotype than the average tissue invading 2d2.Th17 cells.

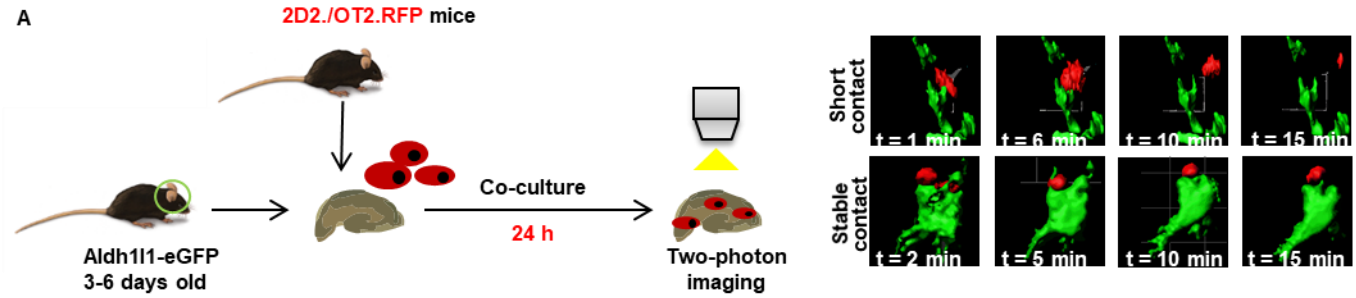
A
2D2./OT2.RFP mice
Co-culture
24 h
Aldh1l1-eGFP
3-6 days old
Two-photon
imaging
Short contact
Stable contact
t = 1 min
t = 6 min
t = 10 min
t = 15 min
t = 2 min
t = 5 min
t = 10 min
t = 15 min

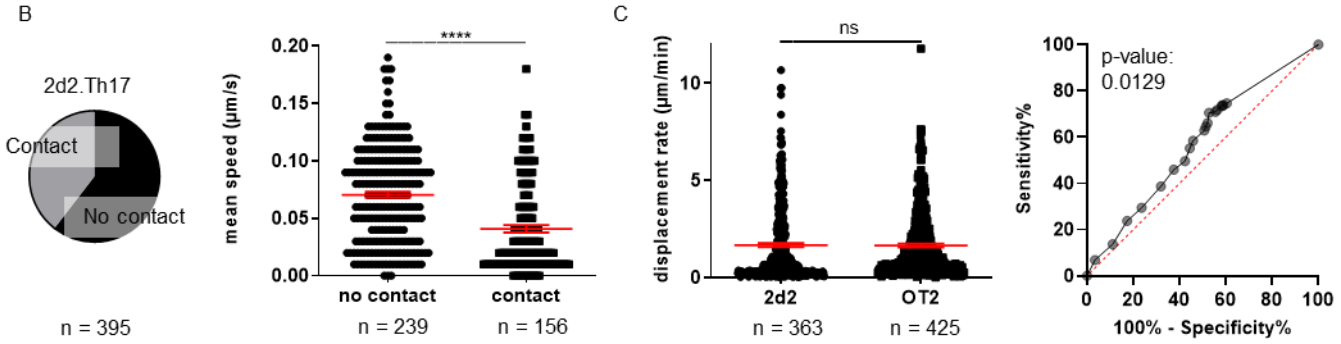
B
2d2.Th17
Contact
No contact
n = 395
mean speed (µm/s)
****
no contact
contact
n = 239
n = 156
C
displacement rate (µm/min)
ns
2d2
OT2
n = 363
n = 425
Sensitivity%
p-value:
0.0129
100% - Specificity%

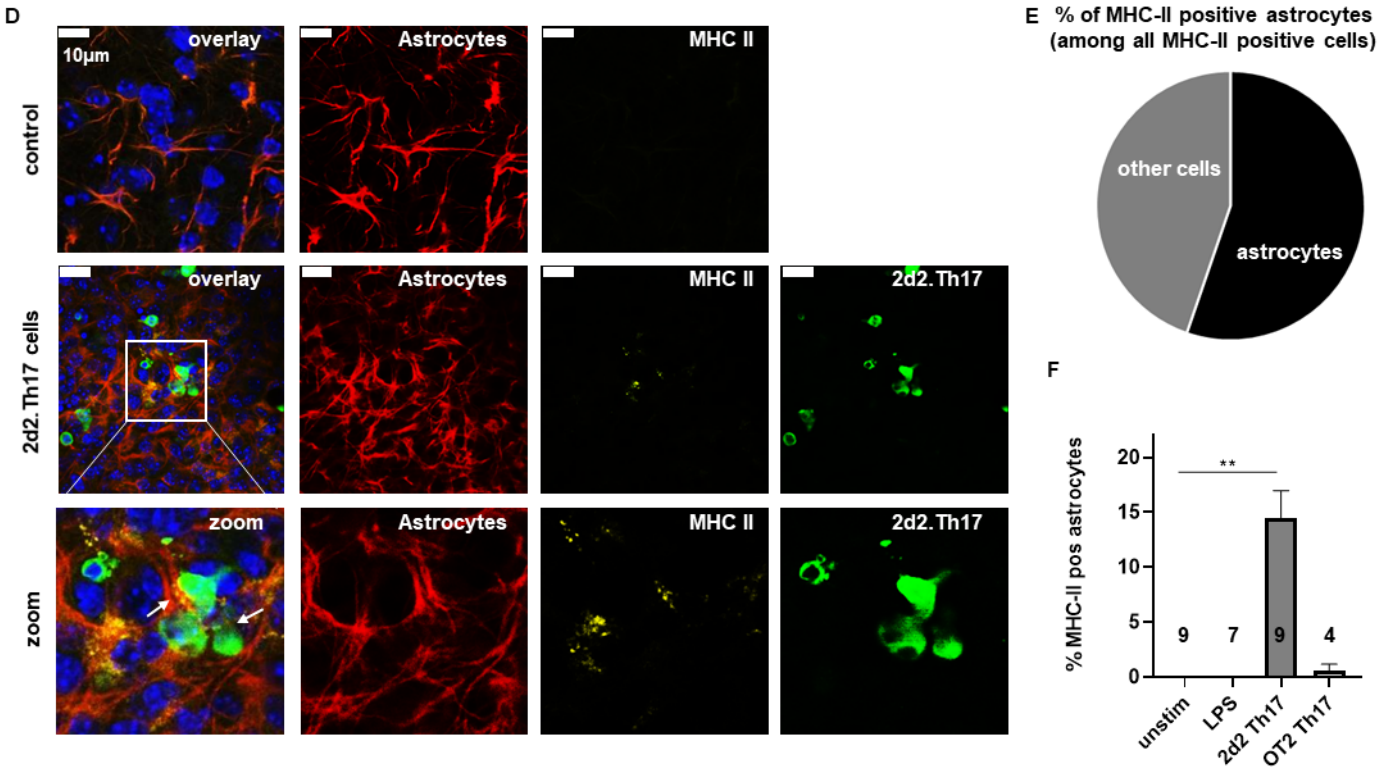
D
control
2d2.Th17 cells
zoom
10µm
overlay
Astrocytes
MHC II
2d2.Th17
zoom
E % of MHC-II positive astrocytes
(among all MHC-II positive cells)
other cells
astrocytes
F
% MHC-II pos astrocytes
**
9
7
9
4
unstim
LPS
2d2 Th17
OT2 Th17

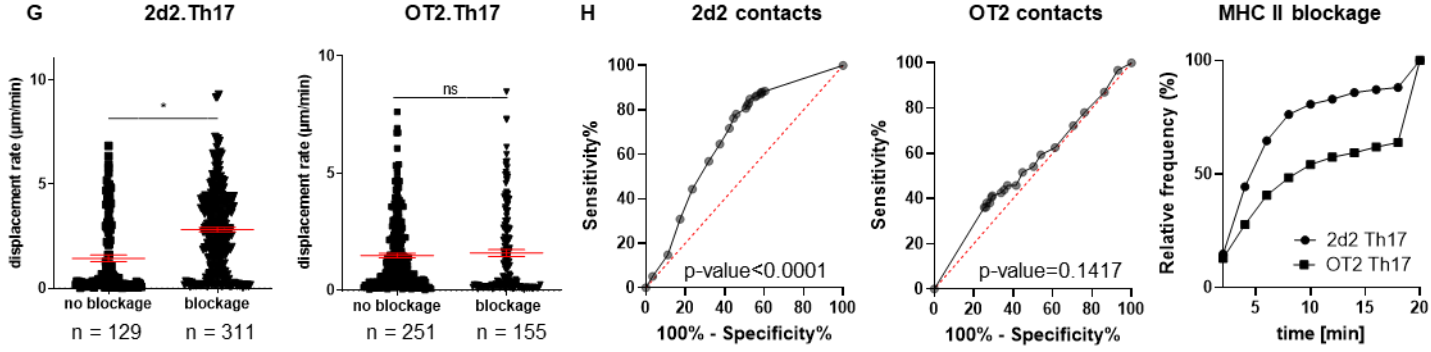
G
2d2.Th17
OT2.Th17
displacement rate (µm/min)
*
ns
no blockage
blockage
n = 129
n = 311
n = 251
n = 155
H
2d2 contacts
OT2 contacts
MHC II blockage
Sensitivity%
p-value<0.0001
p-value=0.1417
100% - Specificity%
Relative frequency (%)
2d2 Th17
OT2 Th17
time [min]

***Figure 7**: Astrocytes interact with Th17 cells in an antigen dependent manner. **A left**) Schematic experiment layout. Naïve T cells were isolated from either 2d2.RFP or OT2.RFP mice, and shifted towards Th17 cells. For coculture, OHSC were isolated from Aldh1l1.eGFP neonates and cultured for four to five days beforehand. Coculture was performed for 24h, and analysed via two-photon imaging. **A right**) Visualisation of exemplary contacts, both short and stable, between Th17 cells and astrocytes. **B left**) Subsets of 2d2.Th17 contacting or not-contacting eGFP-astrocytes. n = 395 from eight independent experiments. **B right**) Comparison of the mean speed of astrocyte-contacting and non-contacting 2d2.Th17 cells. n = 239 and 156 from 8 independent experiments, ****p < 0.0001. **C left**) Both 2d2.Th17 and OT2.Th17 show similar displacement rates when in the OHSC. n = 363 and 425 from eight and seven independent experiments. **C right**) When comparing the interaction time with astrocytes of both 2d2.Th17 as well as OT2.TH17, there is a significant difference between 2d2 and OT2.Th17 cells p = 0.0129. **D**) Under basal conditions, astrocytes do not express MHC class II. Upon exposure of OHSC to 2d2.Th17, a subset of astrocytes express MHC class II. Expression can be observed at interaction sites (white arrows) between astrocytes and 2d2.Th17 cells. DAPI is shown in blue, Astrocytes in red, MHC class II in yellow and 2d2.Th17 cells in green. Scale bar 10µM. **E**) Upon 2d2.Th17 exposure, astrocytes are the major MHC class II expressing cell type. n = 9. **F**) Quantification of histological stainings for MHC class II expression on astrocytes. Only 2d2.Th17 cells are able to induce a significant amount of MHC class II expression on astrocytes. n = 4-9 (numbers in the figure) from at least two independent experiments. **G**) Quantification of T cell behaviour after blockage of MHC class II in OHSC. Only 2d2.Th17 change their behaviour when MHC class II functionality is blocked. The displacement rate is significantly increased in comparison to both no blockage as well as OT2.Th17 cells. *p < 0.05; n = 129-311 from seven or eight independent experiments. **H**) ROC analysis of contacting behaviour towards astrocytes. The 2d2.Th17 contacting behaviour towards astrocytes is significantly different if MHC class II is blocked or not. p < 0.0001. The OT2.Th17 contacting behaviour towards astrocytes is similar whether MHC class II is blocked or not. p > 0.05. The relative frequency of contacting behaviour towards astrocytes between 2d2.Th17 and OT2.Th17 is significantly different upon MHC class II blockage.*

In a next step, the brain-specific antigen recognising T cells were compared to brain non-specific antigen recognising T cells (OT2) with otherwise identical properties. They were both isolated as naïve T cells from the spleen and shifted into Th17 cells using an identical protocol. The OT2.Th17 cells are also RFP positive. When comparing 2d2.Th17 and OT2.Th17 on a population basis (no distinction between subsets contacting or not contacting astrocytes), they shared similar displacement rates (Figure 7c) as well as a similar mean speeds and meandering indexes (data not shown). When analysing the astrocyte-contacting populations, 2d2.Th17 and OT2.Th17 were significantly different in the time they interacted with astrocytes. OT2.Th17 cells spent less time with the astrocytes when interacting (Figure 7c right). Apart from that, these population shared similar properties. Their displacement rates, meandering index and mean speed were not significantly different (data not shown).

These distinct, potentially antigen recognition-dependent behaviours raised questions regarding how astrocytes and T cells interact and which information may be exchanged. Seeing the potential for antigen-specific effects, we identified MHC class II as a possible interaction partner for especially 2d2.Th17 cells to study in depth (Figure 7d). Under basal as well as broad inflammatory conditions (LPS), astrocytes did not express MHC class II *ex vivo* (Figure 7d). Only when 2d2.Th17 were present, we observed MHC class II expression on astrocytes, in direct proximity to 2d2.Th17 cells (Figure 7d, white arrows). Other cells expressed MHC class II as well, but will not be characterised here (Figure 7e). This observation led us to question of the specificity of this behaviour, namely whether the induction of MHC class II is antigen-dependent or if all Th17 cells are able to induce MHC class II expression on astrocytes. In fact, we could show that not all Th17 cells are able to induce MHC class II expression, as OT2.Th17 cells induced little if any expression (quantified in Figure 7f). Quantification showed that about 15 % of the astrocytes analysed displayed MHC class II expression in the presence of 2d2.Th17, whereas no expression could be quantified for basal or general inflammatory conditions (LPS). OT2.Th17 marginally induced MHC class II, in about 1 % of astrocytes. Overall, only 2d2.Th17 cells significantly induced MHC class II expression on astrocytes.

In order to characterise the role of MHC class II, we blocked MHC class II function in slice cultures under 2d2.Th17 as well as OT2.Th17 conditions. If MHC class II is involved in the interaction between astrocytes and Th17 cells, its blocking should change the characteristics of the T cells that interact with astrocytes. Indeed, upon MHC class II blockage with an MHC class II blocking antibody, the 2d2.Th17 cells interacting with astrocytes displayed a higher displacement rate (Figure 7g), both in comparison to the non-blocked 2d2 condition as well as to the OT2.Th17 cells. Among OT2.Th17 cells, the blockage did not influence the displacement rate in comparison to either unblocked OT2.Th17 or unblocked 2d2.Th17 cells. Analysing the contact duration of 2d2.Th17 cells with or without blockage of MHC class II in the OHSC, contacts were significantly shorter when MHC class II was blocked (Figure 7h). The blockage of MHC class II did not change the contact duration of OT2.Th17 cells with astrocytes. Therefore, it can be concluded that the presence of 2d2.Th17 induces MHC class II expression on astrocytes in a tissue context. Whether this effect is direct or indirect, potentially via microglia, remains to be elucidated. This MHC class II induction on astrocytes is involved in functional interactions between the two cell types that are disrupted upon blocking of MHC class II.

B MHC Class II Expression is Functionally Relevant *In Vivo*

After establishing selective MHC class II expression and function on astrocytes *in vitro* and *ex vivo*, the question remained whether astrocytes *in vivo* are able to express MHC class II as well and whether and at what stage of disease it may become functionally relevant. Because we did not see any expression *ex vivo* in non-challenged OHSC, we hypothesised that the same would be true for healthy brain tissue. In healthy brain tissue, we could occasionally detect an astrocyte expressing MHC class II (histology not shown), but the vast majority did not express any MHC class II. These expression patterns were comparable to the MHC class II levels induced by OT2.Th17 *in vitro* (Figure 7f). Therefore, we decided to look at EAE, a disease driven by proinflammatory T cells, largely including Th17 cells, which we showed could induce MHC class II expression on astrocytes *in vitro* and *ex vivo*. In a first step, we stained EAE spinal cord tissue for MHC class II expression (Figure 8a). Microglia and macrophages as well as monocytes are the major population expressing MHC class II upon challenge in the brain. Therefore, we used microglia as a positive control for MHC class II expression (Figure 8a, upper panel). Additionally, we observed astrocytes expressing MHC class II during the chronic phase of EAE (Figure 8a both panels). We could thereby show that astrocytes indeed are able to express MHC class II *in vivo* upon chronic immune infiltration and stimulation.

To understand the dynamics of MHC class II expression on astrocytes better, we analysed different phases of the EAE disease (healthy, peak, chronic phase; Figure 8b left). The peak of disease was defined as the maximum disease severity in each individual animal, whereas a constant score for at least three consecutive days defined the chronic phase of disease. As control, healthy animals were age- and gender-matched to the diseased animals. Indeed, we could confirm, using flow cytometry that under baseline conditions MHC class II expression was only present on a few astrocytes (comparable to the histology). More than half of the astrocytes expressed MHC class II during the peak of the disease, when the symptoms of EAE were most severe. Expression levels dropped again to about a third of astrocytes during the chronic phase, where the histology was taken (Figure 8a and b). The increase in MHC class II expression during the peak phase was significantly different to the healthy baseline condition pointing towards an acute astrocytic reaction to the inflammatory milieu during the peak phase of disease.

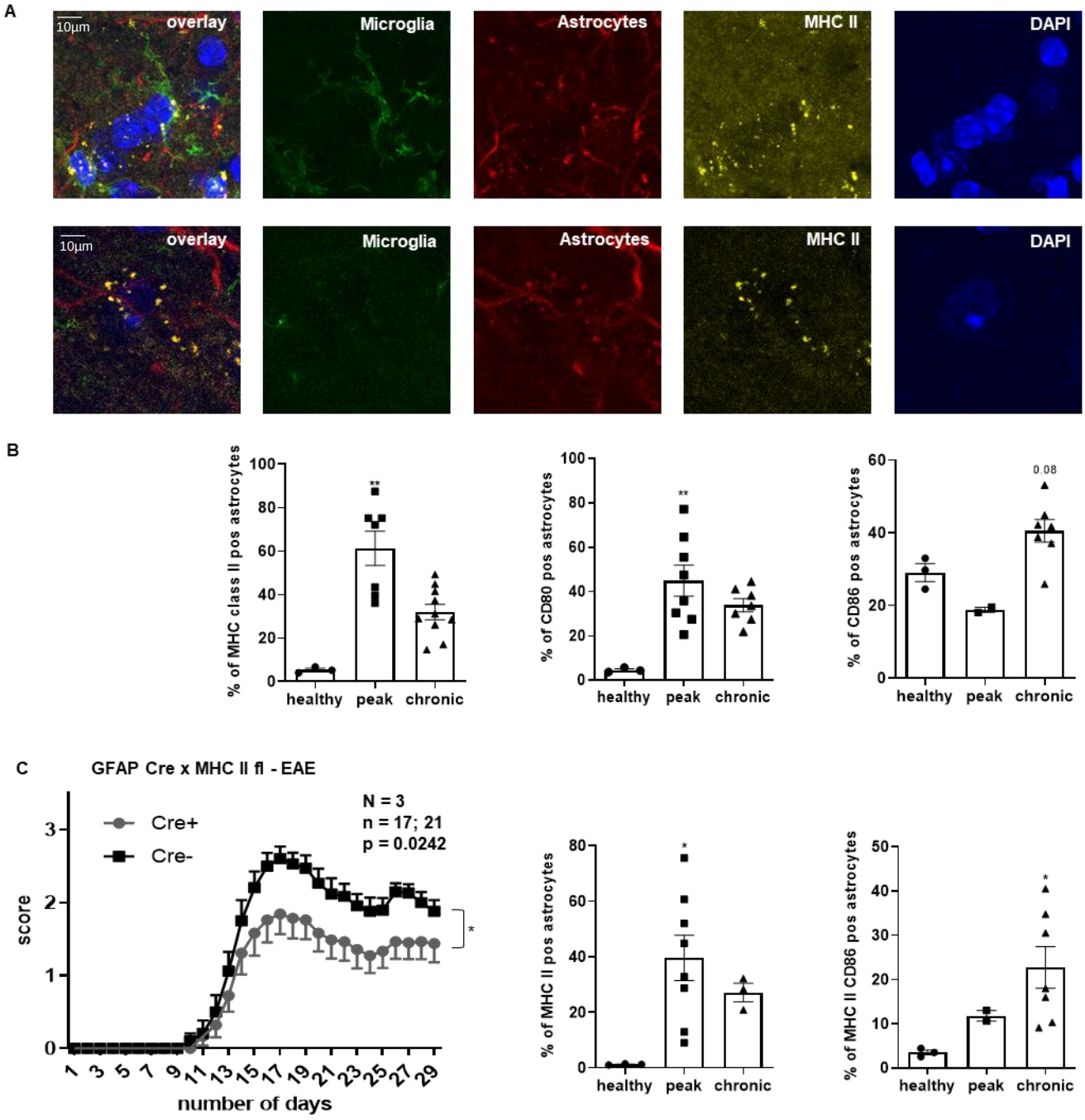

Figure 8: *Astrocytes differentially and functionally express MHC class II* in vivo ***A****) Exemplary histological spinal cord staining of MHC class II expressing cells during the chronic phase of EAE. Within a spinal cord EAE lesion (animal score 2.5), microglia as well as astrocytes are able to express MHC class II. Microglia are stained in green, astrocytes in red, MHC class II in yellow and nuclei in blue* ***B****)* In vivo *analysis of MHC class II , CD80 and CD86 expression at different time points during the EAE disease course. Astrocytes were isolated from healthy, peak and chronic EAE animals and analysed for the expression of MHC class II, CD80 and CD86 using flow cytometry. The lower panel shows CD80 and CD86 expression on MHC class II positive astrocytes. Three or more independent experiments *p < 0.05, **p < 0.01.* ***C****) Astrocyte-specific deletion of MHC II leads to a change in EAE course. MHC class II was deleted in GFAP-Cre positive littermates. Upon deletion, the disease course is less severe and animals remain less impacted by symptoms chronically. *p = 0.0242, n = 17 and 21 animals from 3 independent EAE immunisations.*

MHC class II *in vivo* is functionally expressed in tandem with either a stimulatory or an inhibitory cofactor. Therefore, we aimed to identify the astrocytic cofactor(s), and if possible, their evolution over the disease course. We focused on CD80 (B7-1) and CD86 (B7-2; Figure 8b middle and right), which are the most common and well-defined cofactors. In our model, CD80 expression was very low at baseline and significantly upregulated during the peak, although the standard deviation is relatively high. The levels during the chronic phase of disease decreased again slightly (Figure 8b). CD86 expression on astrocytes was only upregulated during the chronic phase ($p = 0.08$) of disease, whereas during the peak of disease it remained unchanged, or even reduced, compared to the healthy baseline expression level. We also investigated MHC class II co-inhibitory B7 molecules CD274 (B7H1, PDL1) and CD273 (B7DC, PDL2) (Isomura *et al.*, 2008; Jang *et al.*, 2014), neither of which could be detected on astrocytes during EAE (data not shown).

Overall, both CD80 and CD86 display differential expression during the course of EAE. Both are cofactors of MHC class II and their expression in tandem with the latter is of most interest in this context. When looking at the MHC class II expressing astrocytic subset that also expresses CD80, no coexpression was observed in the healthy animal. During the peak phase of the disease, changed dramatically; up to 75 % of cells coexpressed both markers. These levels dropped down again in the chronic phase of the disease, with up to 35 % of astrocytes showing coexpression of MHC class II and CD80 (Figure 8b lower panel). This potentially points towards a change in cofactor at this point in the disease course and may explain the different functionalities associated with astrocytes during acute and chronic neuroinflammation observed in EAE. In line with this, CD86 showed a different pattern of expression in correlation with MHC class II. Although the coexpression with MHC class II was also very low in healthy animals, unlike for CD80, the coexpression only slightly increased during the peak phase to values around 15 %. However, the coexpression increased significantly during the chronic phase of disease to up to 40 % of MHC class II positive astrocytes. Thus, CD80 appears to be the relevant cofactor during the peak phase of EAE whereas the influence of CD86 increases during the chronic phase of disease, suggesting a possible explanation why astrocytes can be both protective as well as detrimental apparently at the same time when both subsets coexist.

Next, in order to more fully characterise the role MHC class II plays in disease, we created a GFAP Cre-driven MHC class II knockout (ko) mouse. In this mouse model, MHC class II was deleted in all GFAP-expressing cells, thereby deleting MHC class II on astrocytes. The healthy mice displayed no detectable phenotype; they bred normally and the sexes of the resulting offspring were equally distributed. They showed no gross growth abnormalities and responded normally to external stimuli like noise or handling. By subjecting these mice to EAE, we were able to investigate the cell-specific role of MHC class II in CNS inflammation. In general, the Cre+ littermates (which lack MHC class II on astrocytes) showed a milder disease course. Initially, both littermate groups showed a similar day of onset and a comparable slope to the peak of disease, underlining that their immune system is not impacted by the transgene. These similarities are also not surprising, as the initial immune responses are driven by peripheral factors and should therefore not be impacted by a CNS-specific deletion of MHC class II. However, the astrocytic Cre+ MHC class II-lacking mice simply did not get as sick as their Cre- littermate counterparts did. In our hands, a typical EAE course induced as described above has a peak score between 2.5 and 3.5, comparable to our observations in the Cre- mice, whereas the Cre+ mice only reached an average score around two during peak (Figure 8c). The chronic progression itself was comparable; the Cre+ disease levels were simply lower due to the lower peak levels. The area under the curve was significantly smaller for the GFAP Cre x MHC class II knockout group compared to their wild type littermates. This functionally links MHC class II expression on astrocytes with the progression

of EAE. Taken together with the coexpression data from Figure 8b (lower panel), it may be proposed that astrocytes expressing both MHC class II and CD80 at the same time are involved in the worsening of disease symptoms, especially during the peak phase of the disease.

C TrpA1 – an Astrocytic Sensor for Inflammation?

MHC class II is involved in antigen presentation and antigen-presenting cell interaction with T cells, but it is not described as a sensor for extracellular stimuli. MHC class II provides internal information about the status of the cell and what it came in contact with (Rock, Reits and Neefjes, 2016). The observed modulation of the EAE course by MHC class II deletion on astrocytes led us to the hypothesis that astrocytes may use a non-common system of inflammation-sensing and recognition of T cell infiltration that induces MHC class II expression astrocyte-specifically. The cation channel TrpA1 has been recently implicated as an astrocytic sensor of the local microenvironment. Specifically, TrpA1 was described to be involved in neurogenic inflammation and demyelination, both prototypical conditions in MS and EAE. We hypothesized that TrpA1 may be involved in the pathomechanisms of MHC class II induction on astrocytes. Additionally, TrpA1 was recently described on astrocytes involved in Alzheimer's disease (Shigetomi *et al.*, 2013; Bosson *et al.*, 2017), another neurodegenerative disease.

As a first step, we assessed TrpA1 expression on cortical astrocyte cultures. To this end, we stained primary cortical astrocyte cultures and detected TrpA1-expressing astrocytes (Figure 9a). Next, we established that TrpA1 expression on these astrocytes could be modulated. The expression levels were responsive to CNS-relevant inflammatory stimuli like LPS or TNFα. Using qRT-PCR, we could show that the mRNA levels of TrpA1 in astrocytes decreased upon 24h exposure to these general inflammatory stimuli. After establishing general modulation by inflammatory stimuli, we took a closer look at specific EAE-relevant stimuli. Both Th17 as well as Th1 cells are involved in the induction and progression of EAE in mice. With that in mind, we designed associated stimuli to analyse whether the potential regulation is cell-contact dependent or may be soluble. It is known that the pH in EAE lesions drops to values around pH 6.6 (Friese *et al.*, 2007). TrpA1 protein is functionally activated by low pH values, so a pH-dependent expression regulation appeared both probable and potentially functionally relevant for TrpA1-dependent responses in EAE. Indeed, pH values comparable to *in vivo* EAE lesions (pH 6.6) as well as to ischemic stroke tissue (pH 6.2, Nemoto and Frinak, 1981) showed a comparable significant reduction of TrpA1 mRNA.

TrpA1 activation is known to be protective in ischemic stroke (Hamilton *et al.*, 2016; Pires and Earley, 2018); it may have similar effects in EAE. To investigate this, we analysed 2d2.Th1 and 2d2.Th17 cells and their supernatants, as well as their signature cytokines. T cells were isolated from the spleen as naïve CD4+ T cells and shifted for five days into either 2d2.Th1 or 2d2.Th17 cells. Astrocytes mildly downregulated their TrpA1 mRNA expression in the presence of Th17 cells (Figure 9b middle). Th17 supernatant on the other hand significantly downregulated TrpA1 mRNA expression on astrocytes, to very close to the detection limit of the method. IL-17, one of the major Th17-associated cytokines, showed comparable results to the Th17 cells alone. This implies that a soluble factor cocktail, which may include IL-17, can induce TrpA1 mRNA expression downregulation during inflammation. A very similar picture was observed for Th1 cells, their supernatants and their signature cytokine IFNγ. Th1 cells may slightly downregulate TrpA1 mRNA levels, although this trend was not statistically significant (Figure 9b right). Their supernatant on the other hand, clearly includes soluble factors that drastically and significantly downregulated TrpA1 mRNA expression to the point of non-detection, or close to the detection limit of the individual sample. IFNγ is very likely one of the factors involved, but not the only one, as the TrpA1 mRNA expression in the presence of IFNγ alone remained detectable at a slightly higher level than the complete supernatant ($p = 0.1$).

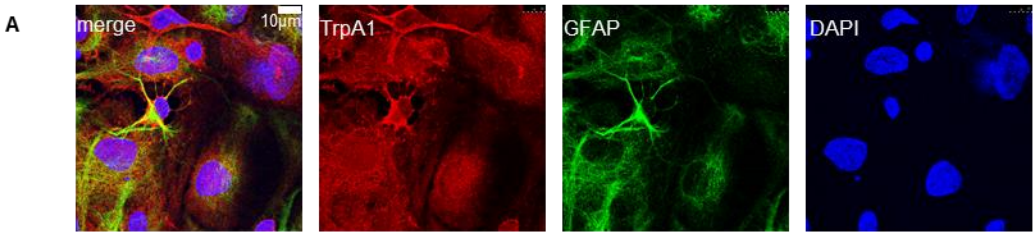
A
merge
10µm
TrpA1
GFAP
DAPI

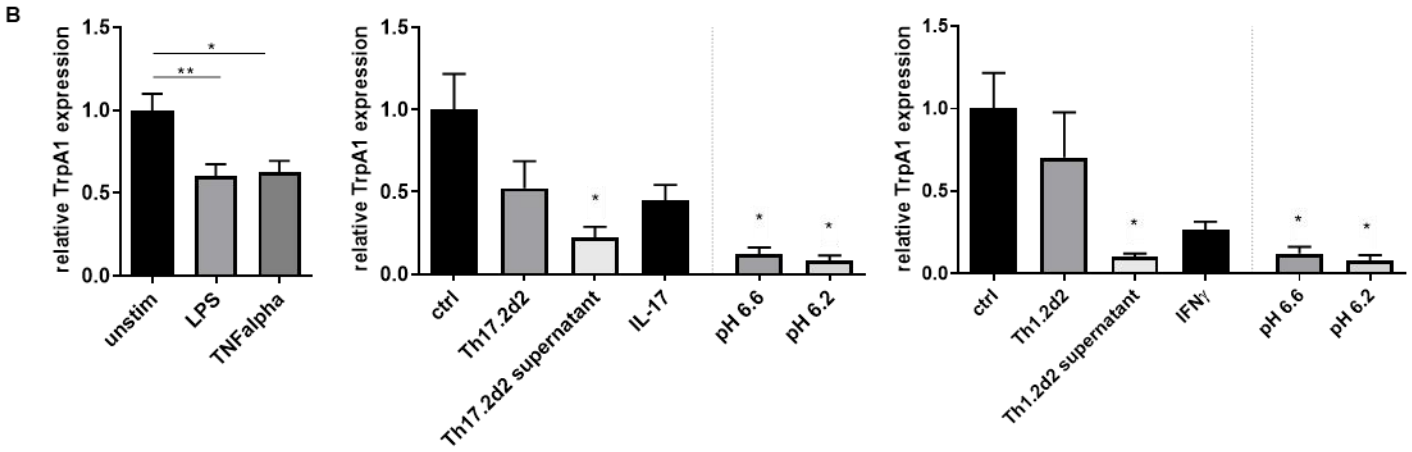
B
relative TrpA1 expression
1.5
1.0
0.5
0.0
*
**
unstim
LPS
TNFalpha
ctrl
Th17.2d2
Th17.2d2 supernatant
IL-17
pH 6.6
pH 6.2
Th1.2d2
Th1.2d2 supernatant
IFNγ

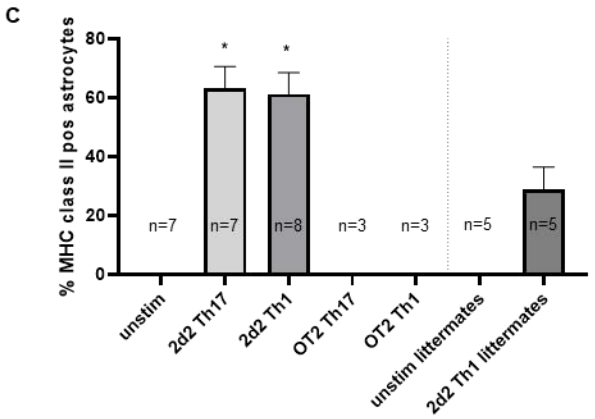
C
% MHC class II pos astrocytes
80
60
40
20
0
n=7
n=7
n=8
n=3
n=3
n=5
n=5
unstim
2d2 Th17
2d2 Th1
OT2 Th17
OT2 Th1
unstim littermates
2d2 Th1 littermates

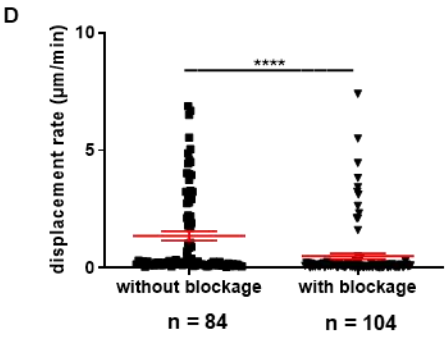
D
displacement rate (µm/min)
10
5
0
****
without blockage
with blockage
n = 84
n = 104

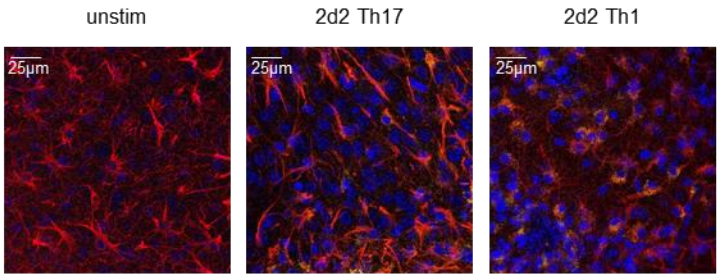
unstim
2d2 Th17
2d2 Th1
25µm
25µm
25µm

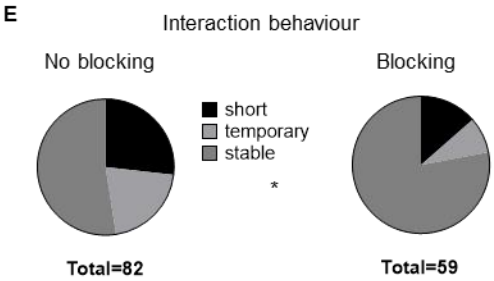
E
Interaction behaviour
No blocking
Blocking
short
temporary
stable
*
Total=82
Total=59

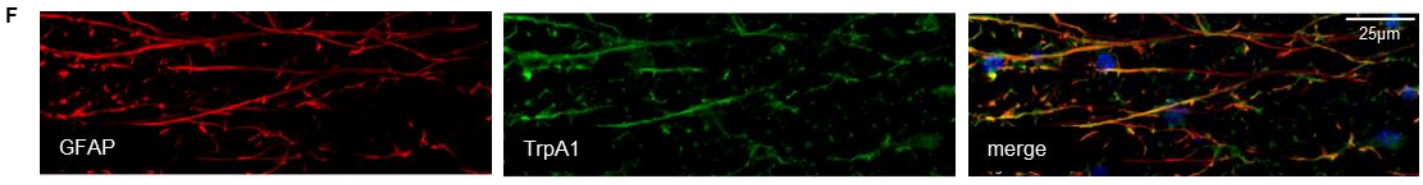
F
GFAP
TrpA1
merge
25µm

Figure 9: *Astrocytic TrpA1 downregulation is induced by inflammation and pH changes.* ***A****) Primary cortical astrocyte culture with TrpA1 staining on astrocytes. TrpA1 is stained in red, astrocytes in green and nuclei in blue* ***B left****) TrpA1 mRNA expression in cortical astrocyte cultures is downregulated by different systemic inflammatory stimuli: LPS and TNFα. p < 0.05, n = 14 - 15* ***B middle****) Th17-dependent regulation of TrpA1 mRNA expression in cortical astrocyte cultures. Exposure of astrocytes to 2d2.Th17 cells, 2d2.Th17 supernatants, IL-17 or pH adjusted control medium.* p < 0.05, **p < 0.01, n for treatments = 5 - 9* ***B right****) Th1-dependent regulation of TrpA1 mRNA expression in cortical astrocyte cultures. Exposure of astrocytes to 2d2.Th1 cells, 2d2.Th1 supernatants, IFNy or pH adjusted control medium. p < 0.05, n for treatments = 4 - 8* ***C****) Analysis of hippocampal slices cultures shows systemic absence of TrpA1. MHC class II expression on astrocytes treated with 2d2.Th17 or 2d2.Th1 cells in these OHSC is doubled in comparison to littermate controls. OT2.Th17 as well as OT2.Th1 cells do not induce MHC class II expression. *p < 0.05, n = 3 - 8* ***C bottom****) exemplary histological stainings of MHC class II expression in TrpA1 ko OHSC for unstimulated, 2d2.Th17- and 2d2.Th1-treated OHSC. Astrocytes are shown in red, MHC class II expression in yellow and nuclei are shown in blue. Scale bar is 25 µm* ***D****) Quantification of the influence of the blockage of MHC class II in TrpA1 ko OHSC on 2d2.Th17 behaviour. The displacement rate of 2d2.Th17 cells with MHC class II blockage is significantly decreased in comparison to the condition without blockage. ****p < 0.001, n = 84, 104 from two independent experiments* ***E****) Analysis of the interactions between astrocytes and 2d2.Th17 cells without and with MHC class II blockade. Interactions are grouped as stable (> 10 min), temporary (between 5 and 10 min) and short (< 5 min). *p < 0.05, n = 82, 59 from two independent experiments.* ***F****) TrpA1 is expressed on astrocytes* in vivo *in chronic EAE. Tyramide-based histological signal amplification of B6 EAE. Staining performed in the anterior column of the spinal cord. Astrocytes are stained in red, TrpA1 in green and nuclei in blue, scale bar 25 µm. [Figure 9F courtesy of Nicholas Hanuscheck]*

TrpA1 expression downregulation may also be due to a combination of IL-17 or IFNγ in conjunction with a lower pH value, closely resembling an EAE lesion milieu. A lower pH was used as a positive control for the downregulation of TrpA1 mRNA.

To establish that MHC class II and TrpA1 are functionally linked in astrocytes during inflammation, we studied MHC class II expression in OHSC of TrpA1 knockout postnatal pups. The experiments were performed as depicted in Figure 9a. TrpA1 OHSC were prepared from day 3 to 5 pups and cultured for four to five days. The applied T cells were isolated according to the protocol described above. Naïve $CD4^+$ T cells were isolated from either 2d2 or OT2 mice and shifted towards Th1 and Th17 cells for five days. The TrpA1 deletion slices are not fluorescently labelled; therefore, an astrocytic dye (SR101) was used if visualisation *in vivo* was necessary. The dye does not induce MHC class II expression (histology not shown).

Under basal conditions, no MHC class II expression could be detected on astrocytes in OHSC from TrpA1 knockout mice, comparable to wild type littermates (Figure 9c right) as well as to control B6 mice (Figure 7). Indeed, MHC class II expression increased approximately two-fold compared to TrpA1 wild type littermates (Figure 9c right) or B6 (Figure 9) with 2d2.Th17 as well as 2d2.Th1 cells only. This data points towards an antigen-dependent induction of MHC class II as seen in wild type OHSC, with an apparent TrpA1-dependent expression level regulation. Neither OT2.Th1 nor OT2.Th17 presence induced MHC class II expression; as was also the case in B6 slices (Figure 7). The lower panels of Figure 9c show exemplary pictures of basal OHSC without MHC class II expression as well as 2d2.Th17- or 2d2.Th1-treated OHSC with astrocytic MHC class II expression in yellow. Neither OT2.Th17 nor OT2.Th1 cells were able to induce MHC class II expression (histology not shown).

To characterise whether TrpA1 is involved in the interaction between 2d2.Th17 and astrocytes we performed Trpa1 ko OHSC studies with 24h incubation of T cells on the OHSC with and without blocking MHC class II (paradigm comparable to Figure 7). Without the blocking of MHC class II, the interaction behaviour of 2d2.Th17 cells with astrocytes was comparable to 2d2.Th17 exposed to wild type B6 OHSC as well as to OT2.Th17 exposed to wild type B6 OHSC. Thus, when MHC class II was accessible, no difference was observed regardless of whether TrpA1 was present or absent. In a next step, we blocked MHC class II in the TrpA1 ko OHSC (Figure 9d). In contrast to 2d2.Th17 exposed to wild type OHSC, which increased their displacement rate, 2d2.Th17 exposed to TrpA1 ko OHSC displayed a

decreased displacement rate when in contact with astrocytes (Figure 9d vs. Figure 7). The decreased displacement rate correlated well with the overall interaction behaviour. Here, interaction behaviour was grouped into stable interactions (> 10 min), temporary interactions (between 5 and 10 min) and short interactions (< 5 min). Contacts lasting less than 5 min are commonly assumed to be too short to transfer much information. In contrast, stable contacts provide enough time for immunological synapse, or kinapse, formation (Azar *et al.*, 2010). The stably interacting population of 2d2.Th17 cells increased significantly (Figure 9e, dark grey population), whereas the shortly interacting population of 2d2.Th17 cells decreased significantly (black population) when MHC class II was blocked in the TrpA1 ko OHSC. The overall change in contact behaviour distribution was significantly different. In summary, the lack of TrpA1 induced more MHC class II expression on astrocytes and led to T cells that stayed significantly longer in contact with astrocytes when MHC class II was blocked.

Again, taking the step towards the *in vivo* situation, we started with the basic characterisation of the TrpA1 channel expression in EAE before we continued with further *in vivo* experiments. This was a challenging task, since TrpA1 is a membrane channel and therefore hard to detect as expression levels are comparatively low and scattered. To counter this problem, we used tyramide-based amplification of the signal, and focussed on the spinal cord, where most of the EAE lesions are known to exist. In this way, we were able to detect TrpA1 expression on astrocytes in the anterior column of the spinal cord during EAE as an exemplary region (Figure 9f, courtesy of Nicholas Hanuscheck).

Knowing the *in vitro* regulation of TrpA1 mRNA expression led us to question whether the ubiquitous deletion of the channel *in vivo* influences the characteristics of the EAE disease progression. This experiment was littermate controlled with animals not lacking the channel (Figure 10a). When TrpA1 was deleted, the disease started typically; the onset was not delayed and the slope to the peak of disease remained similar. During the peak phase of disease, however, the two groups started to diverge. The wild type littermates peaked around a score of 2.5 whereas their TrpA1 ko counterparts peaked on average around a score of 2.8. The TrpA1 ko littermates then remained nearly as sick as they were during the peak and did not experience as strong a decrease in symptoms as their wild type littermates did. Although the deletion of the TrpA1 channel did not influence the development or onset of the disease, these observations suggest an involvement of TrpA1 functionality in the disease progression.

To obtain a clearer picture of the astrocytic antigen presentation in TrpA1 ko mice, we performed flow cytometry during the peak and chronic phases of the disease (Figure 10b). Analysing MHC class II, CD80 and CD86 expression on astrocytes in TrpA1 ko animals showed a split picture. MHC class II expression was generally regulated like in the wild type EAE (Figure 8), independent of the lack of TrpA1. Explicitly this included a higher MHC class II expression during the peak phase and a lower expression during the chronic phase of disease. In addition, during the peak phase, a clear trend can be seen between ko and wt littermates whereas the chronic phase showed no differential expression regulation. Also *in vivo* the lack of TrpA1 appears to lead to slightly increased MHC class II on astrocytes, comparable to Figure 9 *in vitro*. CD80 and CD86 show no differential regulation between the two groups, suggesting that the presence or absence of TrpA1 has little or no influence on CD80 or CD86 expression regulation during EAE. Ultimately, this data points towards a differential MHC class II expression regulation on astrocytes, which is dependent on the presence or absence of TrpA1.

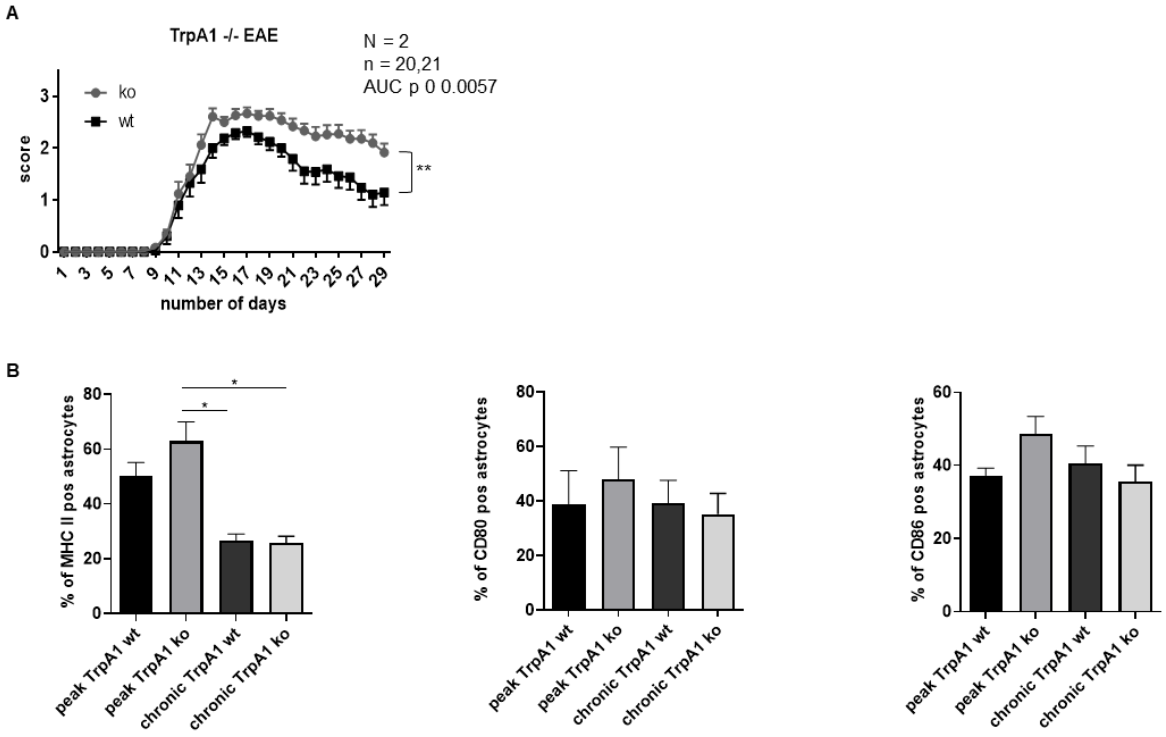

***Figure 10**: TrpA1 dependent MHC class II expression on astrocytes* in vivo. ***A**) Ubiquitous deletion of TrpA1 in mice leads to an altered EAE progression. Animals lacking TrpA1 show a more severe disease course compared to their littermate controls that express TrpA1. The experiment was performed twice; 20 vs 21 animals were analysed per group. The area under the curve was significantly different (**p = 0.0057). **B**) Analysis of MHC class II, CD80, CD86 on astrocytes during the disease course of TrpA1 ko EAE. MHC class II expression is significantly different in TrpA1 ko during the peak phase of disease in comparison to the chronic phase. CD80 and CD86 show no differential expression. *p < 0.05*

Taking a step back, the question remained how the EAE effect is potentially mediated. For that, we went back to our *in vitro* cocultures and looked at the cytokine production (Figure 11). We cocultured 2d2.Th17 and OT2.Th17 with either B6 or TrpA1 ko astrocytes for 24h. The Th17 cells were washed stringently to avoid transfer of before secreted cytokines. Using a Legendplex, it was possible to analyse multiple cytokines from the same sample. All samples were analysed in duplicates, both technical as well as biological. Whether the production of certain cytokines is astrocytic or Th17 dependent can only be assumed, but witth this experiment we aimed to answer the question of cause, not of origin of inflammation increase during EAE. Classical inflammatory markers include IL-6, GMCSF, IL-27a, IFNγ, IL-17a, and TNFα. For those we compared levels between coculture with B6 astrocytes and coculture with TrpA1 ko astrocytes. None of the data is significant due to the low n number but all show the same trend (Figure 11 top and middle row). If there is a difference in cytokine production, it is not in the expected direction. If at all, TrpA1 deficient astrocytes exposed to the same Th17 cells produce less proinflammatory agents in their cultures than more as could be expected from the EAE course.

Interestingly, IL-1β (proinflammatory) as well as IL-10 (anti-inflammatory) show the same pattern of expression regulation, although their absolute expression levels are quite different. OT2.Th17 cocultures appear to express a little less of either IL-1β or IL-10 in both cultures. What is surprising, is that the levels of 2d2.Th17 cocultured with 2d2.Th17 secrete about as much proinflammatory IL-1β and antiinflammatory IL-10 as the OT2.Th17 cells cocultured with the B6 astrocytes (Figure 11 lower row). This pattern may point towards a lower activation of the Th17 in general when trpA1 is absent, thereby leading to generally less cytokine production and secretion.

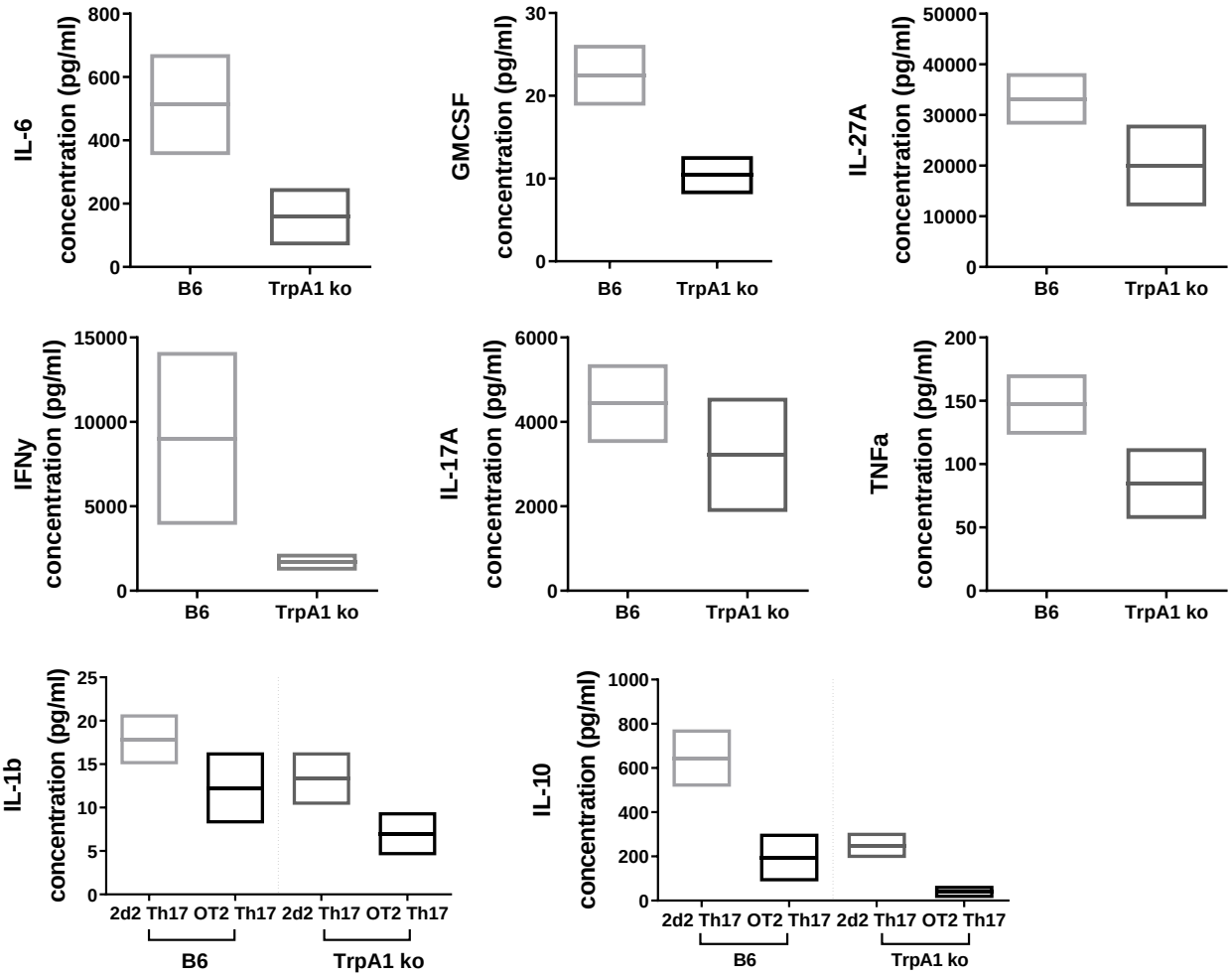

***Figure 11**: Cytokine analysis of Th17 and astrocyte cocultures. Using a Legendplex, cytokines could be analysed from the same sample. B6 and TrpA1 ko astrocyte cultures were grown until confluency and exposed to 2d2.Th17 and OT2.Th17 cells for 24h. The analysed cytokines are IL-6, GMCSF, IL-27a, IFNγ, IL-17a; TNFα, IL-1β and IL-10. All concentrations are pg/ml. Plotted are the means of the technical replicates from two biological n and their SEM. [Legendplex and analysis: courtesy of Nicholas Hanuscheck]*

IV Discussion

A Antigen Presentation

The idea that the brain is an immunologically privileged site has long been accepted to a certain extent (Xie and Yang, 2015). Traditionally it is viewed as separated from the periphery via the BBB and under homeostatic conditions neither MHC class I nor II are expressed to a noteworthy level (Cornet *et al.*, 2000). MHC class I has been identified e.g., in the foetal cat visual system as early as 1998 but only when challenged (Joly, Mucke and Oldstone, 1991; Corriveau, Huh and Shatz, 1998; Oliveira *et al.*, 2004). Due to improved technology, MHC class I has by now been functionally described in different neuronal subsets in healthy, unchallenged and pathogen-free mice (for review see Boulanger and Shatz, 2004). These MHC class I proteins belong to the non-classical family branch and have been associated with functions as diverse as synapse plasticity, learning and memory (Shatz, 2009).

Although the idea of the brain as an immunologically privileged site is still largely accepted, it was observed early on that activated T cells are able to infiltrate and survey the CNS (Wekerle *et al.*, 1986). This happens in an antigen-dependent manner where only antigen-specific T lymphocytes remain within or re-enter the CNS (Wekerle *et al.*, 1986; Hickey, Hsu and Kimura, 1991). This constant surveillance especially in the meningeal compartment is accepted although the mechanisms controlling it remain elusive until recently. One recently discovered mechanism of travel are lymphatic vessels lining sinuses in the dura and directly leading lymphocytes to the deep cervical lymph nodes (Louveau *et al.*, 2015). These vessels are distinct from the cardio vasculature and diminish pathology during EAE when ablated (Louveau *et al.*, 2018). The transported T cells were shown to be CD4 T helper cells whose absence in the homeostatic CNS impairs learning and memory (Radjavi, Smirnov and Kipnis, 2014). Generally, it can be said that the paradigm shifted from an isolated brain to an integrated one, including expressionist own immune surveillance and drainage system. However, MHC class II expression has still not been convincingly shown under steady state conditions.

For proper functionality, T cells need to be reactivated in their target organ. Therefore, they need exposure to their specific antigen via either MHC class I or II, depending on the T cell subtype. Professional peripheral antigen presenting cells (APC), like dendritic cells (DCs) or B cells, are considered to be non-existent in the steady-state CNS (Shrikant and Benveniste, 1996).Only very recently have APCs such as perivascular macrophages been studied in more depth (Yang, Guo and Zhang, 2019). These belong to the family of professional APCs that constitutively express MHC class II even in the steady state (Kambayashi and Laufer, 2014). It has long been believed that their role in the CNS is taken over by microglia, which were shown both *in vivo* and in post-mortem MS tissue to promote proliferation of CD4 T cells via the expression of MHC class II and the necessary cofactors (Matsumoto, Ohmori and Fujiwara, 1992; Windhagen *et al.*, 1995; Saijo and Glass, 2011). Additionally, CNS DCs as well as meningeal and perivascular macrophages (Greter *et al.*, 2005; Bartholomäus *et al.*, 2009; Anandasabapathy *et al.*, 2011) are considered to be involved in antigen presentation in the CNS.

During EAE, professional antigen-presenting cells are able to infiltrate the CNS milieu and are accompanied by non-professional APCs that acquire this biological function in a specific inflammatory environment. These professional DCs are the most efficient APCs that drive the reactivation of CD4 T cells (Greter *et al.*, 2005). On the other hand, it could be shown that DCs activated with MOG are insufficient on their own for EAE induction (Wu *et al.*, 2011). Additionally, their severe reduction in numbers does not influence EAE induction, suggesting that other cells are involved in antigen presentation or are able to compensate DCs potential participation (Yogev *et al.*, 2012). The severe

reduction does however worsen disease progression, pointing towards a regulatory role of DC MHC class II expression during the EAE disease course.

Microglia are the endogenous macrophage population of the CNS. Their expression of MHC class II is considered to be a sign of activation (Wolf *et al.*, 2018). Recently, it was also shown, that their MHC class II expression is non-essential for EAE disease development, progression and resolution. By the application of the CX3Cr1-Cre system, Wolf et al. potentially also targeted meningeal and perivascular macrophages that have recently been described to express this "microglia-specific" marker (Goldmann *et al.*, 2016). Overall, none of these cell types appears to be essential for EAE induction or the detrimental disease progression. This leads to the question which other CNS cell type might be involved in the reactivation of T cells in the CNS or whether compensatory effects mask the real importance of the analysed cell types.

While the involvement of microglia and macrophages in antigen-presentation has long been established, the question remained whether astrocytes as the major CNS population functionally contribute to T cell activation as well. *In vivo* they were shown to not express MHC class I or II (Matsumoto, Ohmori and Fujiwara, 1992; Bö *et al.*, 1994; Khrameeva *et al.*, 2020; Yosef, Xi and McCarty, 2020), although they do express MHC class I in cell culture. MHC class II expression is inducible by IFNγ *in vitro* and *in vivo*, although murine *in vivo* expression is patchy and at a very low expression level compared to other cell types (Fontana, Fierz and Wekerle, 1984; Vass and Lassmann, 1990). Very recently, human astrocytes have been shown to express MHC II in Parkinson's disease (Rostami *et al.*, 2020). This study also showed costimulatory factors necessary for the activation of infiltrating T cells in human cultures, similarly to murine cultures shown elsewhere. In culture, astrocytes acquired functional antigen presenting complexes allowing for the stimulation of T cell lines (Fontana, Fierz and Wekerle, 1984; Fierz *et al.*, 1985; Nikcevich *et al.*, 1997) or naïve T cells (Cornet *et al.*, 2000). The necessary co-stimulatory molecules CD80 (B7-1) and CD86 (B7-2) in mouse and man, respectively, are also inducible by IFNγ *in vitro* (Nikcevich *et al.*, 1997; Cornet *et al.*, 2000; Rostami *et al.*, 2020). *In vivo* expression in mice is debatable depending on the source (Aloisi *et al.*, 1998; Cross and Ku, 2000; Zeinstra, Wilczak and De Keyser, 2003). However, despite some earlier indications of an acquired capacity for antigen-presentation by astrocytes, in-depth investigations using current molecular biological methods are sparse.

One of the early papers studying astrocytic MHC class II expression is Matsumoto et al. (1992). Although they state otherwise, they published *in vivo mimicking* not *in vivo* data. They used mixed glial cultures exposed to IFNγ to mimic the *in vivo* situation. Under similar conditions, we obtained similar results. However, we looked more in depth and exposed both purer astrocytic cultures as well as OHSC to Th17 as well as Th1 cells, their supernatants and signature cytokines. These stimuli are much closer to the *in vivo* situation, especially in the OHSC tissue context allowing a more differential picture of MHC class II expression. *In vitro*, we found that about one third of the astrocytes expressed MHC class II only with antigen-specific proinflammatory Th1 or Th17 cells present, comparable to a recent human publication in post-mortem Parkinson's disease tissue (Rostami *et al.*, 2020).

As mentioned above, IFNγ is known to induce MHC class II expression on astrocytes, but to our knowledge, neither the direct interaction between Th1 nor Th17 cells and astrocytes in the context of MHC class II expression has been studied *in vivo*. It has been shown before that immortalised antigen-specific T cell lines induce MHC class II-associated effects on astrocytes (Sun and Wekerle, 1986) but neither the T cell subtypes nor the actual MHC class II transcription or translation in the astrocytes were investigated. Additionally, it is known that IFNγ-treated astrocytes induce T cell proliferation, also providing *in vitro* proof on MHC class II expression in the presence of an immortalised T cell line. For the first time, we could show that primary Th cells are capable of MHC class II induction and that they are functionally interacting with astrocytes, showing unique properties. To our knowledge, there is

little data on Th17 subpopulations that interact with astrocytes and their dynamic characteristics (Prajeeth *et al.*, 2017). These authors showed that Th17-derived supernatants do not significantly influence astrocytic growth factors transcription, but they were able to influence the astrocytic proinflammatory cytokine profile as well as their proinflammatory chemokine profile on a transcriptional level.

We could show that Th17 cells interact in an antigen-dependent manner and dramatically change their behaviour upon blockage of this interaction partner. The Th17 mean speed was increased; their displacement rate rose and their contacts with astrocytes became much shorter, allowing for little, if any, functional information exchange. This provides new insights into the dynamics underlying Th17 and astrocyte interaction in the context of inflamed tissue.

Vass and Lassmann (1990) took the idea of IFNγ application into the *in vivo* situation and applied the substance intrathecally to Lewis rats. They discovered patchy, discontinuous staining for MHC class II and no staining under healthy conditions. Intrathecal injections lead to a concentration gradient into the tissue, thereby possibly explaining these patchy and discontinuous stainings. On the other hand, in line with their observation we could observe only a subpopulation of astrocytes with MHC class II expression and barely any expression in the healthy animal. In our experiments, we also never observed MHC class II expression within the whole astrocytic population. Under maximal inflammatory conditions in the peak of EAE disease, only about two-thirds of the astrocytes presented MHC class II on their surface *in vivo*.

What most of these experiments lack is the direct correlation between MHC class II and a functional outcome on astrocytes. They are either descriptive or they provide functional changes that are associated with MHC class II but show no direct link. Therefore, we created an astrocyte-specific MHC class II ko mouse strain. In the healthy mice, no obvious alterations could be observed. However, when astrocytes lose the ability to express MHC class II during immune invasion and inflammation, the functional necessity therefore becomes apparent. Animals that lack the ability to respond via MHC class II expression on astrocytes are partially protected from the disease. This leads to the conclusion that astrocytic MHC class II expression might by a compensatory mechanism to the pathology triggered by proinflammatory T cell invasion and a neurodegenerative milieu during the progression of EAE disease.

For proper functionality, MHC class II requires cofactors like CD80 or CD86 (**Figure 12**). They provide potent co-stimulation through their interaction with CD28 and CTLA-4 on the T cell side (Linsley and Ledbetter, 1993; Croft, Bradley and Swain, 1994). CD80 and CD86 are functionally distinct and provide opposing effects (Kuchroo *et al.*, 1995; Racke *et al.*, 1995). CD80 is associated with Th1 differentiation, whereas CD86 is implicated in Th2 differentiation. In a more recent view, CD80 and CD86 stimulation is associated with general T cell growth and survival or the suppression of T cell responses, dependent on the cofactor provided by the T cell itself (Chen and Flies, 2014).

CD80 and CD86 have both been described to be expressed by astrocytes in active MS lesions (Zeinstra, Wilczak and De Keyser, 2003), while not being expressed either during any EAE stage (Cross and Ku, 2000) or in human foetal astrocytes (Satoh, Lee and Kim, 1995). Others have proposed a time- and development-based expression pattern in murine immortalised astrocytic cultures (Soos *et al.*, 1999; Gresser *et al.*, 2000). Additionally, some investigators have postulated IFNγ-dependent expression of both cofactors on astrocytes, with only functional implications for CD86 *in vitro* (Nikcevich *et al.*, 1997). Overall, the literary situation is complicated and confusing at best. Most studies were performed in immortalised astrocytic cell lines or in primary astrocytic cultures. It is known that astrocytes adapt their expression pattern *in vitro* and are able to express e.g., neuronal markers *in vitro,* including

potassium and GABA-gated ion channels (Barres, 1991; Lin and Matesic, 1994). However, whether they are functionally relevant *in vivo* remains elusive in these studies.

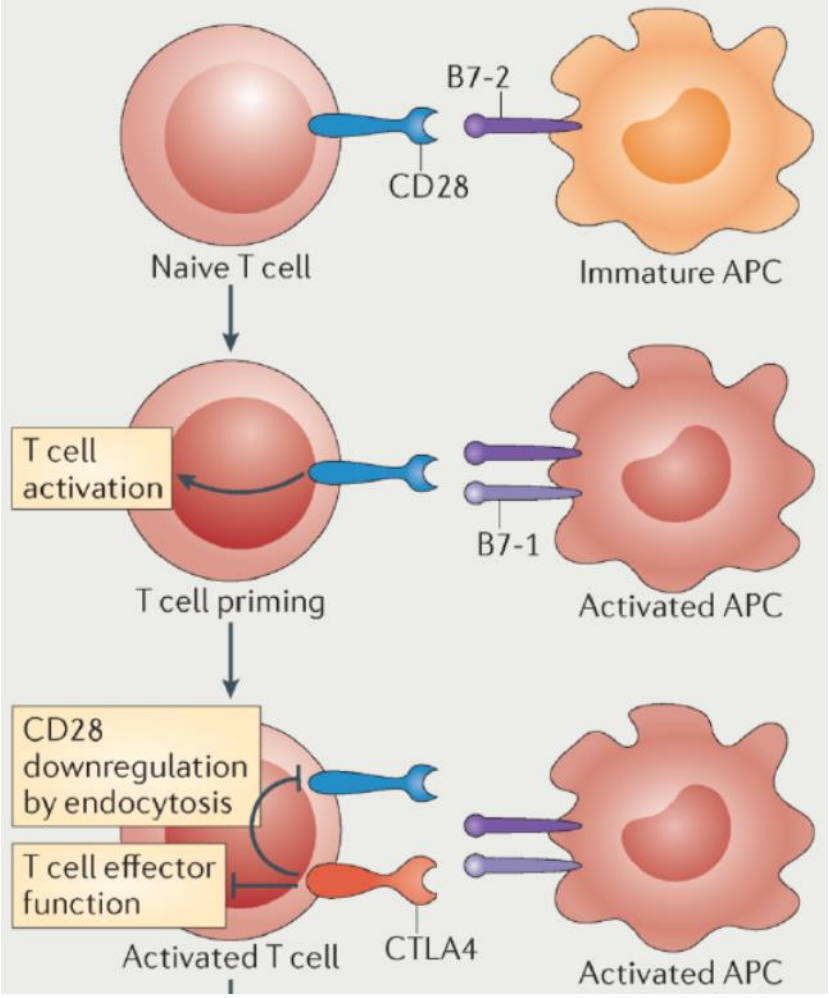

***Figure 12**: Two signal model of T cell activation. Apart from MHC on the antigen presenting cell (APC) side that binds the T cell receptor (TCR), a second signal is required for T cell activation. It can be provided by B7-1 (CD80) or B7-2 (CD86) that bind either CD28 (co-stimulatory signalling) or CTLA-4 (co-inhibitory stimulation). Modified from (Chen and Flies, 2014).*

Using an established in vivo model of autoimmune inflammation, we now provide clear evidence for CD80 and CD86 expression on MHCII-expressing astrocytes. In our hands, EAE is a potent inducer of both CD80 as well as CD86 expression on MHC class II-positive astrocytes *in vivo*. They show a specific expression pattern depending on the EAE disease stage, proposing distinct activation of pathways during the peak in comparison to the chronic phase of disease. There appears to be a shift from CD80 as the main cofactor during the peak phase towards a balanced state between both CD80 and CD86 during the chronic phase of EAE. This differential expression pattern may explain the contradictory results obtained for astrocytic involvement in EAE disease progression (Cross and Ku, 2000; Constantinescu *et al.*, 2005).

The contribution of astrocytes to the pathology of EAE and MS has been established in literature (Brambilla, 2019) in recent years. They are functioning both neuroprotective as well as neurotoxic during the disease in mouse and man. We could shed light on their antigen-presenting capacities that drive disease progression although many questions remain. In the future, we may be able to answer whether Th17 induce MHC class II expression on astrocytes or whether the observed MHC class II expression is a secondary process to e.g. microglial activation beforehand. The details on what is the driving force behind this interaction may be unveiled by future work. Apparent astrocytic involvement in late stage disease pathogenesis in EAE also poses them as potential targets for drug development in MS. Inhibiting the pathogenic switch of astrocytes during the disease may inhibit disease progression and symptomatic worsening and could provide the potential to stabilise the disease rather than slowing it.

B TrpA1 – an Astrocytic Sensor for Inflammation

TrpA1 is a multimodal cationic channel originally characterised in the peripheral nervous system where it senses diverse extra- and intracellular stimuli, both chemical and physical (Nilius and Owsianik, 2011; Nilius, Appendino and Owsianik, 2012). Functionally, the channel has been diversely linked to inflammation, pain as well as homeostasis of nociception and the immune system among many others (Bandell *et al.*, 2004; Kwan KY *et al.*, 2006; Kádková *et al.*, 2017). Many chemical stimuli including mustard oil (allyl isothiocyanate) and cinnamon oil (cinnamaldehyde) elicit painful burning and prickling that is oftentimes linked to TrpA1 activation (reviewed by Stucky et al., 2009). The channel is highly implied in inflammatory diseases like colitis, chronic monoarthritis or chronic airway inflammation (Caceres *et al.*, 2009; Engel *et al.*, 2011; Fernandes *et al.*, 2011). In peripheral organs it is important for the continuation of inflammation (Straub, 2014). Recently, TrpA1 was linked to migraine, a disease that links the peripheral to the central nervous system (Bautista *et al.*, 2005; Shibata and Tang, 2020). It has been described as a fast responder to detrimental stimuli like LPS, initiating acute excitatory neuronal responses as well as vasodilation, while the immune system is not yet activated (Meseguer *et al.*, 2014).

In the last couple of years, the channel has been identified in more diverse organs and functionalities than originally proposed. It has been implicated in functions as varied as mechanical transduction in the Organ of Corti (Nagata *et al.*, 2005; García-Añoveros and Duggan, 2007) and vasodilation in vascular endothelial cells (Earley, Gonzales and Crnich, 2009). The expression ranges from epithelial and smooth muscle cells for the secretion of IL-8 (Mukhopadhyay *et al.*, 2011; Nassini *et al.*, 2012) to keratinocytes and skin fibroblasts where it facilitates erythema (Jain *et al.*, 2011).

Centrally, little evidence has been found for TrpA1 expression (Cahoy *et al.*, 2008) or functionality until recently. About ten years ago, data started to emerge showing TrpA1 on different glial cell types in addition to neurons. The channel is expressed in astrocytic peripheral processes (Lee *et al.*, 2012) or within hippocampal astrocytes (Shigetomi *et al.*, 2011, 2013) and oligodendrocytes (Hamilton *et al.*, 2016) as well as potentially in brain endothelial cells and neurons (Lee *et al.*, 2016). No convincing evidence has been provided for microglial expression so far.

Little is known about the central functions of TrpA1. Physiologically, astrocytic TrpA1 was shown to modulate resting Ca^{2+} levels and limit GABA transport, thereby regulating inhibitory transmission and long term potentiation (Shigetomi *et al.*, 2011, 2013). Pathophysiologically, the channel has been studied in a few neurological diseases, namely cuprizone-induced demyelination, ischemia and Alzheimer's disease. One group has studied the role in cuprizone-induced demyelination in depth, both in a full-body knockout of TrpA1 as well as in a GFAP-Cre driven astrocyte-specific modality (Saghy *et al.*, 2016; Bölcskei *et al.*, 2018; Kriszta *et al.*, 2019). The full-body ko of TrpA1 leads to significantly less demyelination in the corpus callosum, the most studied area in this disease model, serving as a surrogate for overall demyelination (Praet *et al.*, 2014). The knockout does not influence oligodendrocyte precursors and was proposed to be an astrocyte-mediated phenomenon via reduced induction of apoptosis in mature oligodendrocytes due to the lack of astrocytic Ca^{2+} waves caused by the absence of TrpA1 (Saghy *et al.*, 2016). These mice additionally show mildly improved behavioural changes. The TrpA1 ko mice display reduced rearing behaviour in conjunction with attenuated accumulation of astrocytes and microglia (Bölcskei *et al.*, 2018). The astrocyte-specific knockout showed that astrocytes participate in the phenomenon but are not the only cell type involved (Kriszta *et al.*, 2019).

Hamilton et al. (2016) proposed direct TrpA1 functionality on oligodendrocytes, implicated in ischemia. Here, the lack of the channel also led to a reduction in demyelination. They dissected the ionic transient

and molecular mechanisms activating the extracellular influx of calcium. They could show that the acute blockade of TrpA1 reduces the acute myelin damage in a mouse model of ischemia up to 70 %. The chronic knockout led to a weaker reduction in calcium influx, pointing towards compensatory mechanisms potentially by TrpV1 or other related TRP channels. Knowing these compensatory effects have been shown before, one may propose a similar effect looking at our *in vivo* data. Our *in vitro* data suggest a larger MHC class II expression level effect after an acute immune-inflammatory challenge. The *in vivo* model on the other hand, is a chronic model allowing compensatory mechanisms to develop.

Moreover, TrpA1 was recently described on astrocytes (Shigetomi *et al.*, 2013) involved in Alzheimer's disease, another neurodegenerative disease (Lee *et al.*, 2016; Bosson *et al.*, 2017). Bosson et al. could show that the activation of TrpA1 by amyloid-β oligomers led to astrocytic hyperactivity and subsequent neuronal modulation. In the Alzheimer's disease model, TrpA1 channel functionality only becomes relevant under pathological conditions, comparable to our observations in EAE as well. The channel is only relevant for the pathomechanisms of Alzheimer's disease, not for the physiological calcium levels of astrocytes (Bosson *et al.*, 2017). A similar statement can be posed for EAE. Under physiological conditions, TrpA1-depleted astrocytes do not display different properties from wild type ones. Only when challenged does the lack become detrimental, suggesting a potentially protective role for TrpA1 activity in EAE.

In contrast to Alzheimer's disease, we could observe decreasing TrpA1 levels upon inflammation. Both general inflammatory stimuli LPS and TNFα mildly reduce transcription of TrpA1. EAE-specific inflammatory stimuli led to the reduction of TrpA1 transcription close to the level of non-detection, comparable to disease-associated pH reductions. Assuming also an opposing regulation to Alzheimer's disease when it comes to the deletion of TrpA1, one may assume an exacerbation of EAE symptoms. This is exactly what we observed. The deletion of TrpA1 worsens the EAE symptoms and animals barely improve from their peak of disease. In contrast, their littermate controls recover significantly and consistently.

In this work, we demonstrate that TrpA1 is functionally involved in CNS pathomechanisms. We could show that the channel is modulated during different inflammatory stimuli. Meseguer et al. (2014) examined the acute effects of LPS application after bacterial infection. They determined that the responses of the body observed within minutes of the exposure could be attributed largely to TrpA1 functionality. In line with this, we could show that extended exposure to LPS led to a downregulation of the channel in astrocytes. Similar effects could be observed for more EAE-specific stimuli, pointing towards a potential general feedback mechanism. All tested inflammatory stimuli led to major or minor downregulation, some of which were previously shown to initially activate the channel (Meseguer *et al.*, 2014; Kameda *et al.*, 2019; Yap *et al.*, 2020). The pattern that appears to arise is an initial activation of the channel with subsequent downregulation upon prolonged stimulation. Whether this is a pathological mechanism or meant to be protective during inflammation remains to be elucidated.

Additionally, TrpA1 was described to be involved in neurogenic inflammation and demyelination, both prototypical conditions in MS and EAE (Saghy *et al.*, 2016; Kriszta *et al.*, 2019; Shibata and Tang, 2020). We hypothesized that TrpA1 may be involved in the potential pathomechanisms of MHC class II induction on astrocytes. We could show that the absence of TrpA1 on astrocytes leads to increased levels of MHC class II compared to wild type littermates *ex vivo*. This increase is functionally relevant for the interaction with Th17 cells in a tissue-context. When blocked, the vast majority of Th17 cells form stable contacts and do not migrate or meander. This raises the questions of how and to what extent TrpA1 activity activates MHC class transcription and translation on astrocytes and which functional consequences this imposes.

Very recently, TrpA1 has also been associated with EAE (Dalenogare *et al.*, 2020). Many MS patients manifest with neuropathic pain and migraine during relapses (Truini *et al.*, 2012; Foley *et al.*, 2013). Therefore, the authors developed a relapsing-remitting EAE (RR-EAE) model that exhibits similar relapses also in B6 mice (Dalenogare *et al.*, 2020). Comparable to MS, these mice develop increasing pain perception over time. In contrast to most other EAE models and MS, these mice do not necessarily show motor deficits or disease symptoms when still showing hypersensitivity. This mechanic and cold allodynia could be largely reversed by the specific blockade of TrpA1 via antagonists. What has to be kept in mind at this point is that the analysed mice did not show any motor impairment. Rather, the model is based on the development of nociception behaviour as well the presence of inflammation and oxidative stress – a rather unconventional use of the EAE model where nociception is not routinely monitored. This puts TrpA1 in the context of MS but does not associate the channel with the disease pathology but rather only with some of its symptoms. This thesis is the first description of the standard EAE model displaying the effect of TrpA1 deletion on the course of the disease and its influence on MHC class II expression on astrocytes. Thereby, astrocytes may influence the activation status of the infiltrating proinflammatory T cells.

Overall, we could show that there is a population of Th17 cells that interacts with astrocytes in an MHC class II-dependent manner in the inflamed CNS. Indeed, we provide convincing evidence for MHC class II positive astrocytes both *ex vivo* as well as *in vivo*. The expression levels are dependent on the proinflammatory stimulus and the EAE disease state. The genetic deletion of MHC class II on astrocytes leads to an ameliorated EAE phenotype with both a lower maximum as well as an ameliorated chronic phase. Additionally, we could show that TrpA1 expression is associated with MHC class II expression levels both *ex vivo* and *in vivo*. TrpA1 expression is downregulated in conditions mimicking EAE lesions and its deletion leads to higher MHC class II levels, potentially explaining the more detrimental phenotype of the TrpA1 deletion in EAE that we could observe.

What remains to be studied are how exactly MHC class II and TrpA1 functionally interact in astrocytes. By which means does TrpA1-based signalling drive MHC class II expression and functionality in astrocytes and which other pathways may be involved in the process. Many other diseases like migraine or peripheral inflammation are linked to TrpA1-functionality. Potentially, some of these mechanisms may also be relevant to EAE disease progression.

V References

Abbott, N. J., Rönnbäck, L. and Hansson, E. (2006) 'Astrocyte-endothelial interactions at the blood-brain barrier', *Nature Reviews Neuroscience*. doi: 10.1038/nrn1824.

Aloisi, F. *et al.* (1998) 'Microglia are more efficient than astrocytes in antigen processing and in Th1 but not Th2 cell activation.', *Journal of immunology (Baltimore, Md. : 1950)*.

Amor, S. *et al.* (1994) 'Identification of epitopes of myelin oligodendrocyte glycoprotein for the induction of experimental allergic encephalomyelitis in SJL and Biozzi AB/H mice.', *Journal of immunology (Baltimore, Md. : 1950)*, 153(10), pp. 4349–56.

Anandasabapathy, N. *et al.* (2011) 'Flt3L controls the development of radiosensitive dendritic cells in the meninges and choroid plexus of the steady-state mouse brain', *Journal of Experimental Medicine*, 208(18), pp. 1695–1705. doi: 10.1084/jem.20102657.

Andriezen, W. L. (1893) 'The neuroglia elements of the brain.', *Journal of Physiology, vols. xi anid xii. 9 Internationtal Clinics, Series iii*.

Attwell, D. *et al.* (2010) 'Glial and neuronal control of brain blood flow', *Nature*. doi: 10.1038/nature09613.

Azar, G. A. *et al.* (2010) 'Subcellular dynamics of T cell immunological synapses and kinapses in lymph nodes', *Proceedings of the National Academy of Sciences*, 107(8), pp. 3675–3680. doi: 10.1073/pnas.0905901107.

Bandell, M. *et al.* (2004) 'Noxious cold ion channel TRPA1 is activated by pungent compounds and bradykinin', *Neuron*. doi: 10.1016/S0896-6273(04)00150-3.

Barres, B. A. (1991) 'New roles for Glia', *Journal of Neuroscience*, 11(12), pp. 3685–3694. doi: 10.1523/jneurosci.11-12-03685.1991.

Barres, B. A. (2008) 'The Mystery and Magic of Glia: A Perspective on Their Roles in Health and Disease', *Neuron*. Elsevier, pp. 430–440. doi: 10.1016/j.neuron.2008.10.013.

Bartholomäus, I. *et al.* (2009) 'Effector T cell interactions with meningeal vascular structures in nascent autoimmune CNS lesions', *Nature*, 462(7269), pp. 94–98. doi: 10.1038/nature08478.

Bautista, D. M. *et al.* (2005) 'Pungent products from garlic activate the sensory ion channel TRPA1', *Proceedings of the National Academy of Sciences of the United States of America*. doi: 10.1073/pnas.0505356102.

Beurel, E. *et al.* (2014) 'Astrocytes modulate the polarization of CD4+ T cells to Th1 cells', *PLoS ONE*. doi: 10.1371/journal.pone.0086257.

Birkner, K. *et al.* (2020) 'β1-Integrin– and KV1.3 channel–dependent signaling stimulates glutamate release from Th17 cells', *Journal of Clinical Investigation*. doi: 10.1172/JCI126381.

Bittner, S. *et al.* (2009) 'TASK1 modulates inflammation and neurodegeneration in autoimmune inflammation of the central nervous system', *Brain*. doi: 10.1093/brain/awp163.

Bittner, S. *et al.* (2014) 'Myelin oligodendrocyte glycoprotein (MOG35-55) induced experimental autoimmune encephalomyelitis (EAE) in C57BL/6 mice.', *Journal of visualized experiments : JoVE*, (86), p. e51275. doi: 10.3791/51275.

Bjelobaba, I. *et al.* (2018) 'Animal models of multiple sclerosis: Focus on experimental autoimmune encephalomyelitis', *Journal of Neuroscience Research*. John Wiley and Sons Inc., 96(6), pp. 1021–1042. doi: 10.1002/jnr.24224.

Bö, L. *et al.* (1994) 'Detection of MHC class II-antigens on macrophages and microglia, but not on astrocytes and endothelia in active multiple sclerosis lesions', *Journal of Neuroimmunology*, 51(2), pp. 135–146. doi: 10.1016/0165-5728(94)90075-2.

Bölcskei, K. *et al.* (2018) 'Behavioural alterations and morphological changes are attenuated by the lack of TRPA1 receptors in the cuprizone-induced demyelination model in mice', *Journal of Neuroimmunology*. Elsevier, 320, pp. 1–10. doi: 10.1016/J.JNEUROIM.2018.03.020.

Bonfanti, L. (2006) 'PSA-NCAM in mammalian structural plasticity and neurogenesis', *Progress in Neurobiology*. doi: 10.1016/j.pneurobio.2006.08.003.

Bosson, A. *et al.* (2017) 'TRPA1 channels promote astrocytic Ca2+ hyperactivity and synaptic dysfunction mediated by oligomeric forms of amyloid-β peptide', *Molecular Neurodegeneration*. Molecular Neurodegeneration, 12(1), p. 53. doi: 10.1186/s13024-017-0194-8.

Boulanger, L. M. and Shatz, C. J. (2004) 'Immune signalling in neural development, synaptic plasticity and disease', *Nature Reviews Neuroscience*. doi: 10.1038/nrn1428.

Brambilla, R. *et al.* (2009) 'Transgenic Inhibition of Astroglial NF-κB Improves Functional Outcome in Experimental Autoimmune Encephalomyelitis by Suppressing Chronic Central Nervous System Inflammation', *The Journal of Immunology*. doi: 10.4049/jimmunol.0802954.

Brambilla, R. *et al.* (2014) 'Astrocytes play a key role in EAE pathophysiology by orchestrating in the CNS the inflammatory response of resident and peripheral immune cells and by suppressing remyelination', *Glia*, 62(3), pp. 452–467. doi: 10.1002/glia.22616.

Brambilla, R. (2019) 'The contribution of astrocytes to the neuroinflammatory response in multiple sclerosis and experimental autoimmune encephalomyelitis', *Acta Neuropathologica*. Springer Verlag, pp. 757–783. doi: 10.1007/s00401-019-01980-7.

Brosnan, C. F. and Raine, C. S. (2013) 'The astrocyte in multiple sclerosis revisited', *GLIA*. doi: 10.1002/glia.22443.

Caceres, A. I. *et al.* (2009) 'A sensory neuronal ion channel essential for airway inflammation and hyperreactivity in asthma', *Proceedings of the National Academy of Sciences of the United States of America*. doi: 10.1073/pnas.0900591106.

Cahoy, J. D. *et al.* (2008) 'A Transcriptome Database for Astrocytes, Neurons, and Oligodendrocytes: A New Resource for Understanding Brain Development and Function', *Journal of Neuroscience*, 28(1), pp. 264–278. doi: 10.1523/JNEUROSCI.4178-07.2008.

Carpentier, P. A. *et al.* (2005) 'Differential activation of astrocytes by innate and adaptive immune stimuli', *Glia*, 49(3), pp. 360–374. doi: 10.1002/glia.20117.

Chen, L. and Flies, D. B. (2014) 'Molecular mechanisms of T cell co-stimulation and co-inhibition', *Nat Rev Immunol*, 13(4), pp. 227–242. doi: 10.1038/nri3405.Molecular.

Chen, Q., Zhang, X. H. F. and Massagué, J. (2011) 'Macrophage Binding to Receptor VCAM-1 Transmits Survival Signals in Breast Cancer Cells that Invade the Lungs', *Cancer Cell*. doi: 10.1016/j.ccr.2011.08.025.

Choi, J. W. *et al.* (2011) 'FTY720 (fingolimod) efficacy in an animal model of multiple sclerosis requires astrocyte sphingosine 1-phosphate receptor 1 (S1P1) modulation', *Proceedings of the National Academy of Sciences of the United States of America*. doi: 10.1073/pnas.1014154108.

Clambey, E. T. *et al.* (2014) 'Molecules in medicine mini review: The αβ T cell receptor', *Journal of Molecular Medicine*. doi: 10.1007/s00109-014-1145-2.

Coles, A. (2009) 'Multiple sclerosis', *Practical Neurology*, 9(2), pp. 118–126. doi:

10.1136/jnnp.2008.171132.

Compston, A. and Coles, A. (2008) 'Multiple sclerosis', *The Lancet*, 372(9648), pp. 1502–1517. doi: 10.1016/S0140-6736(08)61620-7.

Constantinescu, C. S. *et al.* (2005) 'Astrocytes as antigen-presenting cells: expression of IL-12/IL-23', *Journal of Neurochemistry*, 95(2), pp. 331–340. doi: 10.1111/j.1471-4159.2005.03368.x.

Cornet, A. *et al.* (2000) 'Role of astrocytes in antigen presentation and naive T-cell activation', *Journal of Neuroimmunology*, 106, pp. 69–77. doi: 10.1016/S0165-5728(99)00215-5.

Corriveau, R. A., Huh, G. S. and Shatz, C. J. (1998) 'Regulation of class I MHC gene expression in the developing and mature CNS by neural activity', *Neuron*. Cell Press, 21(3), pp. 505–520. doi: 10.1016/S0896-6273(00)80562-0.

Croft, M., Bradley, L. M. and Swain, S. L. (1994) 'Naive versus memory CD4 T cell response to antigen. Memory cells are less dependent on accessory cell costimulation and can respond to many antigen-presenting cell types including resting B cells.', *The Journal of Immunology*, 152(6).

Cross, A. H. and Ku, G. (2000) 'Astrocytes and central nervous system endothelial cells do not express B7-1 (CD80) or B7-2 (CD86) immunoreactivity during experimental autoimmune encephalomyelitis', *Journal of Neuroimmunology*. doi: 10.1016/S0165-5728(00)00327-1.

D'Amelio, F. E., Smith, M. E. and Eng, L. F. (1990) 'Sequence of tissue responses in the early stages of experimental allergic encephalomyelitis (EAE): Immunohistochemical, light microscopic, and ultrastructural observations in the spinal cord', *Glia*. doi: 10.1002/glia.440030402.

Dalenogare, D. P. *et al.* (2020) 'TRPA1 activation mediates nociception behaviors in a mouse model of relapsing-remitting experimental autoimmune encephalomyelitis', *Experimental Neurology*. Elsevier, 328(October 2019), p. 113241. doi: 10.1016/j.expneurol.2020.113241.

Daneman, R. and Prat, A. (2015) 'The blood–brain barrier', *Cold Spring Harbor Perspectives in Biology*. Cold Spring Harbor Laboratory Press, 7(1). doi: 10.1101/cshperspect.a020412.

Ding, X. *et al.* (2015) 'Silencing IFN-γ Binding/Signaling in Astrocytes versus Microglia Leads to Opposite Effects on Central Nervous System Autoimmunity', *The Journal of Immunology*. doi: 10.4049/jimmunol.1303321.

Ding, Y. Bin *et al.* (2003) 'Association of VCAM-1 overexpression with oncogenesis, tumor angiogenesis and metastasis of gastric carcinoma', *World Journal of Gastroenterology*. doi: 10.3748/wjg.v9.i7.1409.

Donato R. (2003) 'Intracellular and extracellular roles of S100 proteins', *Microscopy Research and Technique*.

Earley, S., Gonzales, A. L. and Crnich, R. (2009) 'Endothelium-Dependent Cerebral Artery Dilation Mediated by TRPA1 and Ca2+-Activated K+ Channels', *Circulation Research*. Lippincott Williams & Wilkins, 104(8), pp. 987–994. doi: 10.1161/CIRCRESAHA.108.189530.

Ellwardt, E. *et al.* (2020) 'Targeting CD52 does not affect murine neuron and microglia function', *European Journal of Pharmacology*, 871, p. 172923. doi: 10.1016/j.ejphar.2020.172923.

Ellwardt, E. and Zipp, F. (2014) 'Molecular mechanisms linking neuroinflammation and neurodegeneration in MS', *Experimental Neurology*. Academic Press Inc., 262(Part A), pp. 8–17. doi: 10.1016/j.expneurol.2014.02.006.

Emsley, J. G., Arlotta, P. and Macklis, J. D. (2004) 'Star-cross'd neurons: Astroglial effects on neural repair in the adult mammalian CNS', *Trends in Neurosciences*. doi: 10.1016/j.tins.2004.02.008.

Engel, M. A. *et al.* (2011) 'TRPA1 and substance P mediate colitis in mice', *Gastroenterology*. doi: 10.1053/j.gastro.2011.07.002.

Etzioni, A. (1996) 'Adhesion molecules - Their role in health and disease', *Pediatric Research*. doi: 10.1203/00006450-199602000-00001.

Fernandes, E. S. *et al.* (2011) 'A distinct role for transient receptor potential ankyrin 1, in addition to transient receptor potential vanilloid 1, in tumor necrosis factor α-induced inflammatory hyperalgesia and Freund's complete adjuvant-induced monarthritis', *Arthritis and Rheumatism*. doi: 10.1002/art.30150.

Fernandez-Fernandez, S., Almeida, A. and Bolaños, J. P. (2012) 'Antioxidant and bioenergetic coupling between neurons and astrocytes', *Biochemical Journal*. doi: 10.1042/BJ20111943.

Fierz, W. *et al.* (1985) 'Astrocytes as antigen-presenting cells. I. Induction of Ia antigen expression on astrocytes by T cells via immune interferon and its effect on antigen presentation.', *Journal of immunology*, 134(6), pp. 3785–3793.

Foley, P. L. *et al.* (2013) 'Prevalence and natural history of pain in adults with multiple sclerosis: Systematic review and meta-analysis', *Pain*. doi: 10.1016/j.pain.2012.12.002.

Fontana, A., Fierz, W. and Wekerle, H. (1984) 'Astrocytes present myelin basic protein to encephalitogenic T-cell lines', *Nature*, 307(5948), pp. 273–276. doi: 10.1038/307273a0.

Foo, L. C. *et al.* (2011) 'Development of a method for the purification and culture of rodent astrocytes', *Neuron*. doi: 10.1016/j.neuron.2011.07.022.

Friese, M. A. *et al.* (2007) 'Acid-sensing ion channel-1 contributes to axonal degeneration in autoimmune inflammation of the central nervous system', *Nature Medicine*, 13(12), pp. 1483–1489. doi: 10.1038/nm1668.

García-Añoveros, J. and Duggan, A. (2007) 'García-Añoveros J, Duggan A. TRPA1 in Auditory and Nociceptive Organs. Chapter 12.', in *Liedtke WB, Heller S, editors. TRP Ion Channel Function in Sensory Transduction and Cellular Signaling Cascades*.

Gerlach, J. *et al.* (2016) 'Persistent Gliosis Interferes with Neurogenesis in Organotypic Hippocampal Slice Cultures.', *Frontiers in cellular neuroscience*, 10(May), p. 131. doi: 10.3389/fncel.2016.00131.

Glatigny, S. and Bettelli, E. (2018) 'Experimental Autoimmune Encephalomyelitis (EAE) as Animal Models of Multiple Sclerosis (MS)', *Cold Spring Harbor perspectives in medicine*. NLM (Medline). doi: 10.1101/cshperspect.a028977.

Goldmann, T. *et al.* (2016) 'Origin, fate and dynamics of macrophages at central nervous system interfaces', *Nature Immunology*, 17(7), pp. 797–805. doi: 10.1038/ni.3423.

Greenwood, S. M. and Bushell, T. J. (2010) 'Astrocytic activation and an inhibition of MAP kinases are required for proteinase-activated receptor-2-mediated protection from neurotoxicity', *Journal of Neurochemistry*. John Wiley & Sons, Ltd, 113(6), p. no-no. doi: 10.1111/j.1471-4159.2010.06737.x.

Gresser, O. *et al.* (2000) 'Tumor necrosis factor alpha and interleukin-1 alpha inhibit through different pathways interferon-gamma-induced antigen presentation, processing and MHC class II surface expression on astrocytes, but not on microglia', *Cell and Tissue Research*, 300(3), pp. 373–382. doi: 10.1007/s004410000222.

Greter, M. *et al.* (2005) 'Dendritic cells permit immune invasion of the CNS in an animal model of multiple sclerosis', *Nature Medicine*, 11(3), pp. 328–334. doi: 10.1038/nm1197.

Hamilton, N. B. *et al.* (2016) 'Proton-gated Ca2+-permeable TRP channels damage myelin in conditions mimicking ischaemia', *Nature*. Nature Publishing Group, 529(7587), pp. 1–14. doi: 10.1038/nature16519.

Harrington, L. E. *et al.* (2005) 'Interleukin 17-producing CD4+ effector T cells develop via a lineage

distinct from the T helper type 1 and 2 lineages', *Nature Immunology*. doi: 10.1038/ni1254.

Hertz, L. *et al.* (1999) 'Astrocytes: Glutamate producers for neurons', *Journal of Neuroscience Research*. doi: 10.1002/(SICI)1097-4547(19990815)57:4<417::AID-JNR1>3.0.CO;2-N.

Hertz, L. and Zielke, H. R. (2004) 'Astrocytic control of glutamatergic activity: Astrocytes as stars of the show', *Trends in Neurosciences*. doi: 10.1016/j.tins.2004.10.008.

Herz, J., Zipp, F. and Siffrin, V. (2010) 'Neurodegeneration in autoimmune CNS inflammation', *Experimental Neurology*. doi: 10.1016/j.expneurol.2009.11.019.

Hickey, W. F., Hsu, B. L. and Kimura, H. (1991) 'T-lymphocyte entry into the central nervous system', *Journal of Neuroscience Research*. doi: 10.1002/jnr.490280213.

Hindinger, C. *et al.* (2012) 'IFN-γ signaling to astrocytes protects from autoimmune mediated neurological disability', *PLoS ONE*. doi: 10.1371/journal.pone.0042088.

Hölsken, A. *et al.* (2006) 'Ex vivo therapy of malignant melanomas transplanted into organotypic brain slice cultures using inhibitors of histone deacetylases.', *Acta neuropathologica*. Springer, 112(2), pp. 205–215. doi: 10.1007/s00401-006-0082-8.

Hu, X. *et al.* (2016) 'Heterogeneous astrocytes: Active players in CNS', *Brain Research Bulletin*. Elsevier Inc., 125, pp. 1–18. doi: 10.1016/j.brainresbull.2016.03.017.

Isomura, I. *et al.* (2008) 'Induction of regulatory dendritic cells by topical application of NF-κB decoy oligodeoxynucleotides', *Immunology Letters*. Immunol Lett, 119(1–2), pp. 49–56. doi: 10.1016/j.imlet.2008.04.002.

Jain, A. *et al.* (2011) 'TRP-channel-specific cutaneous eicosanoid release patterns', *Pain*. doi: 10.1016/j.pain.2011.08.025.

Jang, I. K. *et al.* (2014) 'B7-H1 inhibits T cell proliferation through MHC class II in human mesenchymal stem cells', *Transplantation Proceedings*. Elsevier USA, 46(5), pp. 1638–1641. doi: 10.1016/j.transproceed.2013.12.059.

Jaquemar, D., Schenker, T. and Trueb, B. (1999) 'An ankyrin-like protein with transmembrane domains is specifically lost after oncogenic transformation of human fibroblasts', *Journal of Biological Chemistry*. doi: 10.1074/jbc.274.11.7325.

Jiang, H. R. *et al.* (2012) 'IL-33 attenuates EAE by suppressing IL-17 and IFN-γ production and inducing alternatively activated macrophages', *European Journal of Immunology*. doi: 10.1002/eji.201141947.

Joly, E., Mucke, L. and Oldstone, M. B. A. (1991) 'Viral persistence in neurons explained by lack of major histocompatibility class I expression', *Science*. American Association for the Advancement of Science, 253(5025), pp. 1283–1285. doi: 10.1126/science.1891717.

Kádková, A. *et al.* (2017) 'Molecular Basis of TRPA1 Regulation in Nociceptive Neurons. A Review', *Physiological Research*, 66(3), pp. 425–439.

Kambayashi, T. and Laufer, T. M. (2014) 'Atypical MHC class II-expressing antigen-presenting cells: Can anything replace a dendritic cell?', *Nature Reviews Immunology*, 14(11), pp. 719–730. doi: 10.1038/nri3754.

Kameda, T. *et al.* (2019) 'Expression and activity of TRPA1 and TRPV1 in the intervertebral disc: Association with inflammation and matrix remodeling', *International Journal of Molecular Sciences*. MDPI AG, 20(7). doi: 10.3390/ijms20071767.

Kang, Z. *et al.* (2010) 'Astrocyte-Restricted Ablation of Interleukin-17-Induced Act1-Mediated Signaling Ameliorates Autoimmune Encephalomyelitis', *Immunity*. doi: 10.1016/j.immuni.2010.03.004.

Kettenmann, H. and Verkhratsky, A. (2008) 'Historical Perspective Neuroglia: the 150 years after', *Trends in Neurosciences*. doi: 10.1016/j.tins.2008.09.003.

Khrameeva, E. *et al.* (2020) 'Single-cell-resolution transcriptome map of human, chimpanzee, bonobo, and macaque brains', *Genome Research*. Cold Spring Harbor Laboratory Press, 30(5), pp. 776–789. doi: 10.1101/gr.256958.119.

Kim, R. Y. *et al.* (2014) 'Astrocyte CCL2 sustains immune cell infiltration in chronic experimental autoimmune encephalomyelitis', *Journal of Neuroimmunology*. Elsevier B.V., 274(1–2), pp. 53–61. doi: 10.1016/j.jneuroim.2014.06.009.

Kimelberg, H. K. (2010) 'Functions of Mature Mammalian Astrocytes: A Current View', *The Neuroscientist*, 16(1), pp. 79–106. doi: 10.1177/1073858409342593.

Kiss, J. Z. and Muller, D. (2001) 'Contribution of the neural cell adhesion molecule to neuronal and synaptic plasticity', *Reviews in the Neurosciences*. doi: 10.1515/REVNEURO.2001.12.4.297.

Kornek, B. *et al.* (2000) 'Multiple sclerosis and chronic autoimmune encephalomyelitis: A comparative quantitative study of axonal injury in active, inactive, and remyelinated lesions', *American Journal of Pathology*.

Kriegstein, A. R. and Götz, M. (2003) 'Radial glia diversity: A matter of cell fate', *GLIA*. doi: 10.1002/glia.10250.

Krishnamoorthy, G. *et al.* (2009) 'Myelin-specific T cells also recognize neuronal autoantigen in a transgenic mouse model of multiple sclerosis', *Nature Medicine*. Nature Publishing Group, 15(6), pp. 626–632. doi: 10.1038/nm.1975.

Krishnamoorthy, G. and Wekerle, H. (2009) 'EAE: An immunologist's magic eye', *European Journal of Immunology*, 39(8), pp. 2031–2035. doi: 10.1002/eji.200939568.

Kriszta, G. *et al.* (2019) 'Investigation of Cuprizone-Induced Demyelination in mGFAP-Driven Conditional Transient Receptor Potential Ankyrin 1 (TRPA1) Receptor Knockout Mice', *Cells*. MDPI AG, 9(1), p. 81. doi: 10.3390/cells9010081.

Kuchroo, V. K. *et al.* (1995) 'B7-1 and B7-2 costimulatory molecules differentially activate the TH1/TH2 developmental pathways: application to autoimmune disease therapy', *Cell*, 80, pp. 707–718.

Kwan KY *et al.* (2006) 'TRPA1 Contributes to Cold, Mechanical, and Chemical Nociception but Is Not Essential for Hair-Cell Transduction', *Neuron*, 50(2), pp. 277–289. doi: 10.1016/j.neuron.2006.03.042.

Larochelle, C. *et al.* (2016) 'Secondary Progression in Multiple Sclerosis: Neuronal Exhaustion or Distinct Pathology?', *Trends in Neurosciences*. Elsevier Ltd, 39(5), pp. 325–339. doi: 10.1016/j.tins.2016.02.001.

Lee, K.-I. *et al.* (2016) 'Role of transient receptor potential ankyrin 1 channels in Alzheimer's disease.', *Journal of neuroinflammation*. Journal of Neuroinflammation, 13(1), p. 92. doi: 10.1186/s12974-016-0557-z.

Lee, S. M. *et al.* (2012) 'An ultrastructural evidence for the expression of transient receptor potential ankyrin 1 (TRPA1) in astrocytes in the rat trigeminal caudal nucleus', *Journal of Chemical Neuroanatomy*. doi: 10.1016/j.jchemneu.2012.07.003.

Liddelow, S. and Hoyer, D. (2016) 'Astrocytes: Adhesion Molecules and Immunomodulation', *Current Drug Targets*. Bentham Science Publishers Ltd., 17(16), pp. 1871–1881. doi: 10.2174/1389450117666160101120703.

Liesi, P., Dahl, D. and Vaheri, A. (1983) 'Laminin is produced by early rat astrocytes in primary culture', *Journal of Cell Biology*. doi: 10.1083/jcb.96.3.920.

Liesi, P., Kirkwood, T. and Vaheri, A. (1986) 'Fibronectin is expressed by astrocytes cultured from embryonic and early postnatal rat brain', *Experimental Cell Research*. doi: 10.1016/0014-4827(86)90570-7.

Liesi, P. and Silver, J. (1988) 'Is astrocyte laminin involved in axon guidance in the mammalian CNS?', *Developmental Biology*. doi: 10.1016/0012-1606(88)90366-1.

Lin, R. C. S. and Matesic, D. F. (1994) 'Immunohistochemical demonstration of neuron-specific enolase and microtubule-associated protein 2 in reactive astrocytes after injury in the adult forebrain', *Neuroscience*, 60(1), pp. 11–16. doi: 10.1016/0306-4522(94)90199-6.

Linker, R. A. *et al.* (2010) 'Functional role of brain-derived neurotrophic factor in neuroprotective autoimmunity: Therapeutic implications in a model of multiple sclerosis', *Brain*. doi: 10.1093/brain/awq179.

Linsley, P. S. and Ledbetter, J. A. (1993) 'The role of the CD28 receptor during T cell responses to antigen', *Annual Review of Immunology*. Annu Rev Immunol, pp. 191–212. doi: 10.1146/annurev.iy.11.040193.001203.

Liu, X. *et al.* (2014) 'Interleukin-17 (IL-17)-induced MicroRNA 873 (miR-873) Contributes to the Pathogenesis of Experimental Autoimmune Encephalomyelitis by Targeting A20 Ubiquitin-editing Enzyme', *Journal of Biological Chemistry*. American Society for Biochemistry and Molecular Biology Inc., 289(42), pp. 28971–28986. doi: 10.1074/jbc.M114.577429.

Loos, J. *et al.* (2020) 'Functional characteristics of Th1, Th17, and ex-Th17 cells in EAE revealed by intravital two-photon microscopy', *Journal of Neuroinflammation*. BioMed Central Ltd, 17(1). doi: 10.1186/s12974-020-02021-x.

Loria, F. *et al.* (2017) 'α-Synuclein transfer between neurons and astrocytes indicates that astrocytes play a role in degradation rather than in spreading', *Acta Neuropathologica*. Springer Verlag, 134(5), pp. 789–808. doi: 10.1007/s00401-017-1746-2.

Louveau, A. *et al.* (2015) 'Structural and functional features of central nervous system lymphatic vessels', *Nature*. Nature Publishing Group, 523(7560), pp. 337–341. doi: 10.1038/nature14432.

Louveau, A. *et al.* (2018) 'CNS lymphatic drainage and neuroinflammation are regulated by meningeal lymphatic vasculature', *Nature Neuroscience*. Nature Publishing Group, 21(10), pp. 1380–1391. doi: 10.1038/s41593-018-0227-9.

Lublin, F. D. and Reingold, S. C. (1996) 'Defining the clinical course of multiple sclerosis: Results of an international survey', *Neurology*. Lippincott Williams and Wilkins, pp. 907–911. doi: 10.1212/WNL.46.4.907.

Luckheeram, R. V. *et al.* (2012) 'CD4 +T cells: Differentiation and functions', *Clinical and Developmental Immunology*. doi: 10.1155/2012/925135.

Ludwin, S. K. *et al.* (2016) 'Astrocytes in multiple sclerosis.', *Multiple sclerosis journal*, 22(9), pp. 1–11. doi: 10.1177/1352458516643396.

Luessi, F. *et al.* (2015) 'FTY720 (fingolimod) treatment tips the balance towards less immunogenic antigen-presenting cells in patients with multiple sclerosis', *Multiple Sclerosis*. doi: 10.1177/1352458515574895.

Luessi, F., Siffrin, V. and Zipp, F. (2012) 'Neurodegeneration in multiple sclerosis: novel treatment strategies', *Expert Review of Neurotherapeutics*. Taylor & Francis, 12(9), pp. 1061–1077. doi: 10.1586/ern.12.59.

Luo, J. *et al.* (2008) 'Bioluminescence in vivo imaging of autoimmune encephalomyelitis predicts disease', *Journal of Neuroinflammation*, 5(6), pp. 1–6. doi: 10.1186/1742-2094-5-6.

Magistretti, P. J. (2011) 'Neuron-glia metabolic coupling and plasticity', in *Experimental Physiology*. doi: 10.1113/expphysiol.2010.053157.

Mascanfroni, I. D. *et al.* (2013) 'IL-27 acts on DCs to suppress the T cell response and autoimmunity by inducing expression of the immunoregulatory molecule CD39', *Nature Immunology*. doi: 10.1038/ni.2695.

Mascanfroni, I. D. *et al.* (2015) 'Metabolic control of type 1 regulatory T cell differentiation by AHR and HIF1-α', *Nature Medicine*. doi: 10.1038/nm.3868.

Matsumoto, Y., Ohmori, K. and Fujiwara, M. (1992) 'Immune regulation by brain cells in the central nervous system: Microglia but not astrocytes present myelin basic protein to encephalitogenic T cells under in vivo-mimicking conditions', *Immunology*.

Matthiessen, H. P., Schmalenbach, C. and Müller, H. W. (1989) 'Astroglia-released neurite growth-inducing activity for embryonic hippocampal neurons is associated with laminin bound in a sulfated complex and free fibronectin', *Glia*. doi: 10.1002/glia.440020307.

Mayo, L., Trauger, Sunia A, *et al.* (2014) 'B4GALT6 regulates astrocyte activation during CNS inflammation', *Nature Medicine*. NIH Public Access, 20(10), pp. 1147–56. doi: 10.1038/nm.3681.

Mayo, L., Trauger, Sunia A., *et al.* (2014) 'Regulation of astrocyte activation by glycolipids drives chronic CNS inflammation', *Nature Medicine*, 20(10), pp. 1147–1156. doi: 10.1038/nm.3681.

McCaslin, A. F. H. *et al.* (2011) 'In vivo 3D morphology of astrocyte-vasculature interactions in the somatosensory cortex: Implications for neurovascular coupling', *Journal of Cerebral Blood Flow and Metabolism*. doi: 10.1038/jcbfm.2010.204.

Meares, G. P. *et al.* (2012) 'Regulation of CCL20 expression in astrocytes by IL-6 and IL-17', *GLIA*. doi: 10.1002/glia.22307.

Meseguer, V. *et al.* (2014) 'TRPA1 channels mediate acute neurogenic inflammation and pain produced by bacterial endotoxins', *Nature Communications*, 5(3125). doi: 10.1038/ncomms4125.

Montell, C. (2005) 'The TRP superfamily of cation channels.', *Science's STKE : signal transduction knowledge environment*. American Association for the Advancement of Science, 2005(272), p. re3. doi: 10.1126/stke.2722005re3.

Moreno, M. *et al.* (2013) 'Origins and significance of astrogliosis in the multiple sclerosis model, MOG peptide EAE', *Journal of neurological science*, 333(0), pp. 55–59. doi: 10.1038/jid.2014.371.

Muhlethaler-Mottet, A. *et al.* (1998) 'Activation of the MHC class II transactivator CIITA by interferon-γ requires cooperative interaction between Stat1 and USF-1', *Immunity*. doi: 10.1016/S1074-7613(00)80468-9.

Mukhopadhyay, I. *et al.* (2011) 'Expression of functional TRPA1 receptor on human lung fibroblast and epithelial cells', *Journal of Receptors and Signal Transduction*. doi: 10.3109/10799893.2011.602413.

Nagata, K. *et al.* (2005) 'Nociceptor and hair cell transducer properties of TRPA1, a channel for pain and hearing', *Journal of Neuroscience*. doi: 10.1523/JNEUROSCI.0013-05.2005.

Nassini, R. *et al.* (2012) 'Transient receptor potential ankyrin 1 channel localized to non-neuronal airway cells promotes non-neurogenic inflammation', *PLoS ONE*. doi: 10.1371/journal.pone.0042454.

Nemoto, E. M. and Frinak, S. (1981) 'Brain Tissue pH after global brain ischemia and barbiturate loading in rats', *Stroke*, 12(1), pp. 77–82. doi: 10.1161/01.STR.12.1.77.

Nikcevich, K. M. *et al.* (1997) 'IFN-γ-Activated Primary Murine Astrocytes Express B7 Costimulatory Molecules and Prime Naive Antigen-Specific T Cells', *Journal of Immunology*, 158(2), pp. 614–621.

Nikić, I. *et al.* (2011) 'A reversible form of axon damage in experimental autoimmune encephalomyelitis and multiple sclerosis', *Nature Medicine*, 17(4), pp. 495–499. doi: 10.1038/nm.2324.

Nilius, B., Appendino, G. and Owsianik, G. (2012) 'The transient receptor potential channel TRPA1: From gene to pathophysiology', *Pflugers Archiv European Journal of Physiology*. doi: 10.1007/s00424-012-1158-z.

Nilius, B. and Owsianik, G. (2011) 'The transient receptor potential family of ion channels', *Genome Biology*, 12(3), p. 218. doi: 10.1186/gb-2011-12-3-218.

Ojeda, S. R. *et al.* (2003) 'Glia-to-neuron signaling and the neuroendocrine control of female puberty', *Annals of Medicine*. doi: 10.1080/07853890310005164.

Oliveira, A. L. R. *et al.* (2004) 'A role for MHC class I molecules in synaptic plasticity and regeneration of neurons after axotomy', *Proceedings of the National Academy of Sciences of the United States of America*. National Academy of Sciences, 101(51), pp. 17843–17848. doi: 10.1073/pnas.0408154101.

Pires, P. W. and Earley, S. (2018) 'Neuroprotective effects of Trpa1 channels in the cerebral endothelium following ischemic stroke', *eLife*. eLife Sciences Publications Ltd, 7, pp. 1–29. doi: 10.7554/eLife.35316.

Praet, J. *et al.* (2014) 'Cellular and molecular neuropathology of the cuprizone mouse model: Clinical relevance for multiple sclerosis', *Neuroscience and Biobehavioral Reviews*. Elsevier Ltd, 47, pp. 485–505. doi: 10.1016/j.neubiorev.2014.10.004.

Prajeeth, C. K. *et al.* (2017) 'Effectors of Th1 and Th17 cells act on astrocytes and augment their neuroinflammatory properties', *Journal of Neuroinflammation*. BioMed Central Ltd., 14(1), p. 204. doi: 10.1186/s12974-017-0978-3.

Quintana, F. J. (2017) 'Astrocytes to the rescue! Glia limitans astrocytic endfeet control CNS inflammation', *The Journal of Clinical Investigation*. American Society for Clinical Investigation, 127(8), pp. 2897–2899. doi: 10.1172/JCI95769.

Racke, M. K. *et al.* (1995) 'Distinct roles for B7-1 (CD-80) and B7-2 (CD-86) in the initiation of experimental allergic encephalomyelitis', *Journal of Clinical Investigation*. doi: 10.1172/JCI118274.

Radjavi, A., Smirnov, I. and Kipnis, J. (2014) 'Brain antigen-reactive CD4+ T cells are sufficient to support learning behavior in mice with limited T cell repertoire', *Brain, Behavior, and Immunity*, 35, pp. 58–63. doi: 10.1016/j.bbi.2013.08.013.

Ransohoff, R. M. M. and Engelhardt, B. (2012) 'The anatomical and cellular basis of immune surveillance in the central nervous system', *Nature Reviews Immunology*. Nature Publishing Group, 12(9), pp. 623–635. doi: 10.1038/nri3265.

Rock, K. L., Reits, E. and Neefjes, J. (2016) 'Present Yourself! By MHC Class I and MHC Class II Molecules', *Trends in Immunology*, 37(11), pp. 724–737. doi: 10.1016/j.it.2016.08.010.

Rostami, J. *et al.* (2020) 'Astrocytes have the capacity to act as antigen-presenting cells in the Parkinson's disease brain', *Journal of Neuroinflammation*. Journal of Neuroinflammation, 17(1), pp. 1–18. doi: 10.1186/s12974-020-01776-7.

Rothhammer, V. *et al.* (2017) 'Sphingosine 1-phosphate receptor modulation suppresses pathogenic astrocyte activation and chronic progressive CNS inflammation.', *Proceedings of the National Academy of Sciences of the United States of America*. National Academy of Sciences, 114(8), pp. 2012–2017. doi: 10.1073/pnas.1615413114.

Rothhammer, V. and Quintana, F. J. (2015) 'Control of autoimmune CNS inflammation by astrocytes', *Seminars in Immunopathology*, 37(6), pp. 625–638. doi: 10.1007/s00281-015-0515-3.

Ruco, L. P. *et al.* (1996) 'Expression of ICAM-1 and VCAM-1 in human malignant mesothelioma', *Journal of Pathology*. doi: 10.1002/(SICI)1096-9896(199607)179:3<266::AID-PATH592>3.0.CO;2-Y.

Rudge, J. S. *et al.* (1992) 'Expression of Ciliary Neurotrophic Factor and the Neurotrophins – Nerve Growth Factor, Brain-Derived Neurotrophic Factor and Neurotrophin 3—in Cultured Rat Hippocampal Astrocytes', *European Journal of Neuroscience*. doi: 10.1111/j.1460-9568.1992.tb00896.x.

Saghy, E. *et al.* (2016) 'TRPA1 deficiency is protective in cuprizone-induced demyelination-A new target against oligodendrocyte apoptosis', *Glia*. John Wiley and Sons Inc., 64(12), pp. 1–15. doi: 10.1002/glia.23051.

Saijo, K. and Glass, C. K. (2011) 'Microglial cell origin and phenotypes in health and disease', *Nature Reviews Immunology*. doi: 10.1038/nri3086.

Satoh, J. ichi, Lee, Y. B. and Kim, S. U. (1995) 'T-cell costimulatory molecules B7-1 (CD80) and B7-2 (CD86) are expressed in human microglia but not in astrocytes in culture', *Brain Research*, 704(1), pp. 92–96. doi: 10.1016/0006-8993(95)01177-3.

Schattling, B. *et al.* (2012) 'TRPM4 cation channel mediates axonal and neuronal degeneration in experimental autoimmune encephalomyelitis and multiple sclerosis', *Nature Medicine*. doi: 10.1038/nm.3015.

Schmitt, K. *et al.* (2017) 'Asc1p/RACK1 Connects Ribosomes to Eukaryotic Phosphosignaling', *Molecular and Cellular Biology*, 37(3), p. MCB.00279-16. doi: 10.1128/MCB.00279-16.

Shatz, C. J. (2009) 'MHC Class I: An Unexpected Role in Neuronal Plasticity', *Neuron*. NIH Public Access, pp. 40–45. doi: 10.1016/j.neuron.2009.09.044.

Shibata, M. and Tang, C. (2020) 'Implications of Transient Receptor Potential Cation Channels in Migraine Pathophysiology', *Neuroscience Bulletin*. Springer Singapore. doi: 10.1007/s12264-020-00569-5.

Shigetomi, E. *et al.* (2011) 'TRPA1 channels regulate astrocyte resting calcium and inhibitory synapse efficacy through GAT-3', *Nature Neuroscience*. Nature Publishing Group, 15(1), pp. 70–80. doi: 10.1038/nn.3000.

Shigetomi, E. *et al.* (2013) 'TRPA1 Channels Are Regulators of Astrocyte Basal Calcium Levels and Long-Term Potentiation via Constitutive D-Serine Release', *Journal of Neuroscience*, 33(24), pp. 10143–10153. doi: 10.1523/JNEUROSCI.5779-12.2013.

Shrikant, P. and Benveniste, E. N. (1996) 'The central nervous system as an immunocompetent organ: role of glial cells in antigen presentation.', *Journal of immunology (Baltimore, Md. : 1950)*.

Snow, D. M. *et al.* (1990) 'Sulfated proteoglycans in astroglial barriers inhibit neurite outgrowth in vitro', *Experimental Neurology*. doi: 10.1016/S0014-4886(05)80013-5.

Sofroniew, M. V. and Vinters, H. V. (2010) 'Astrocytes: Biology and pathology', *Acta Neuropathologica*. Springer, 119(1), pp. 7–35. doi: 10.1007/s00401-009-0619-8.

Sofroniew, M. V (2015) 'Astrocyte barriers to neurotoxic inflammation.', *Nature reviews. Neuroscience*. NIH Public Access, 16(5), pp. 249–63. doi: 10.1038/nrn3898.

Somjen, G. G. (1988) 'Nervenkitt: Notes on the history of the concept of neuroglia', *Glia*. doi: 10.1002/glia.440010103.

Soos, J. M. *et al.* (1999) 'Differential expression of B7 co-stimulatory molecules by astrocytes correlates with T cell activation and cytokine production', *International Immunology*, 11(7), pp. 1169–1179. doi: 10.1093/intimm/11.7.1169.

Stork, O. *et al.* (2000) 'Recovery of emotional behaviour in neural cell adhesion molecule (NCAM) null

mutant mice through transgenic expression of NCAM180', *European Journal of Neuroscience*. doi: 10.1046/j.1460-9568.2000.00197.x.

Straub, R. H. (2014) 'TRPV1, TRPA1, and TRPM8 channels in inflammation, energy redirection, and water retention: Role in chronic inflammatory diseases with an evolutionary perspective', *Journal of Molecular Medicine*, 92(9), pp. 925–937. doi: 10.1007/s00109-014-1175-9.

Stromnes, I. M. and Goverman, J. M. (2006) 'Active induction of experimental allergic encephalomyelitis', *Nature Protocols*. Nature Publishing Group, 1(4), pp. 1810–1819. doi: 10.1038/nprot.2006.285.

Stucky, C. L. *et al.* (2009) 'Roles of transient receptor potential channels in pain', *Brain Research Reviews*, 60(1), pp. 2–23.

Sun, D. and Wekerle, H. (1986) 'Ia-restricted encephalitogenic T lymphocytes mediating EAE lyse autoantigen-presenting astrocytes', *Nature*, 320(6057), pp. 70–72. doi: 10.1038/320070a0.

Trapp, B. D. *et al.* (1998) 'Axonal transection in the lesions of multiple sclerosis [see comments]', *N Engl J Med*.

Truini, A. *et al.* (2012) 'Mechanisms of pain in multiple sclerosis: A combined clinical and neurophysiological study', *Pain*. doi: 10.1016/j.pain.2012.05.024.

Tsai, H.-H. *et al.* (2012) 'Regional astrocyte allocation regulates CNS synaptogenesis and repair.', *Science (New York, N.Y.)*, 337(6092), pp. 358–62. doi: 10.1126/science.1222381.

Tsuji, F. *et al.* (2010) 'Transient receptor potential vanilloid 1 agonists as candidates for anti-inflammatory and immunomodulatory agents', *European Journal of Pharmacology*. Elsevier B.V., 627(1–3), pp. 332–339. doi: 10.1016/j.ejphar.2009.10.044.

Vaca, K. and Wendt, E. (1992) 'Divergent effects of astroglial and microglial secretions on neuron growth and survival', *Experimental Neurology*. doi: 10.1016/0014-4886(92)90023-J.

Vass, K. and Lassmann, H. (1990) 'Intrathecal application of interferon gamma. Progressive appearance of MHC antigens within the rat nervous system', *American Journal of Pathology*.

Vennekens, R., Menigoz, A. and Nilius, B. (2012) 'TRPs in the Brain.', *Reviews of physiology, biochemistry and pharmacology*, 163, pp. 27–64. doi: 10.1007/112_2012_8.

Vergo, S. *et al.* (2011) 'Acid-sensing ion channel 1 is involved in both axonal injury and demyelination in multiple sclerosis and its animal model', *Brain*. doi: 10.1093/brain/awq337.

Verkhratsky, A. (2010) 'Physiology of neuronal-glial networking', *Neurochemistry International*. doi: 10.1016/j.neuint.2010.02.002.

Verkhratsky, A. and Nedergaard, M. (2016) 'The homeostatic astroglia emerges from evolutionary specialization of neural cells', *Philosophical Transactions of the Royal Society B: Biological Sciences*, 371(1700), p. 20150428. doi: 10.1098/rstb.2015.0428.

Verkhratsky, A., Reyes, R. C. and Parpura, V. (2013) 'TRP channels coordinate ion signalling in astroglia', *Review in physiological Biochemistry Pharmacology*, 112, pp. 1–22. doi: 10.1007/112.

Vogt, J. *et al.* (2009) 'Lower motor neuron loss in multiple sclerosis and experimental autoimmune encephalomyelitis', *Annals of Neurology*, 66(3), pp. 310–322. doi: 10.1002/ana.21719.

Volterra, A. and Meldolesi, J. (2005) 'Astrocytes, from brain glue to communication elements: The revolution continues', *Nature Reviews Neuroscience*. doi: 10.1038/nrn1722.

Wang, D. D. and Bordey, A. (2009) *The Astrocyte Odyssey*, *Progress in Neurobiology*. doi: 10.1016/j.pneurobio.2008.09.015.The.

Wekerle, H. *et al.* (1986) 'Cellular immune reactivity within the CNS', *Trends in Neurosciences*. doi: 10.1016/0166-2236(86)90077-9.

Williams, J. L. *et al.* (2020) 'Astrocyte-T cell crosstalk regulates region-specific neuroinflammation', *Glia*. John Wiley and Sons Inc., pp. 1–14. doi: 10.1002/glia.23783.

Windhagen, A. *et al.* (1995) 'Expression of costimulatory molecules B7-1 (CD80), B7-2 (CD86), and interleukin 12 cytokine in multiple sclerosis lesions', *Journal of Experimental Medicine*. doi: 10.1084/jem.182.6.1985.

Wolf, Y. *et al.* (2018) 'Microglial MHC class II is dispensable for experimental autoimmune encephalomyelitis and cuprizone-induced demyelination', *European Journal of Immunology*, 48(8), pp. 1308–1318. doi: 10.1002/eji.201847540.

Wu, G. F. *et al.* (2011) 'Limited Sufficiency of Antigen Presentation by Dendritic Cells in Models of Central Nervous System Autoimmunity', *Journal of autoimmunology*, 36(1), pp. 56–64. doi: 10.1016/j.jaut.2010.10.006.

Xie, L. *et al.* (2015) 'Cerebral regulatory T cells restrain microglia/macrophage-mediated inflammatory responses via IL-10', *European Journal of Immunology*. doi: 10.1002/eji.201444823.

Xie, L. and Yang, S.-H. (2015) 'Interaction of astrocytes and T cells in physiological and pathological conditions', *Brain Research*. Elsevier, 1623, pp. 63–73. doi: 10.1016/j.brainres.2015.03.026.

Yang, J. F. *et al.* (2012) 'Characterization of the interaction between astrocytes and encephalitogenic lymphocytes during the development of experimental autoimmune encephalitomyelitis (EAE) in mice.', *Clinical and experimental immunology*. Wiley-Blackwell, 170(3), pp. 254–65. doi: 10.1111/j.1365-2249.2012.04661.x.

Yang, T., Guo, R. and Zhang, F. (2019) 'Brain perivascular macrophages: Recent advances and implications in health and diseases', *CNS Neuroscience & Therapeutics*. Blackwell Publishing Ltd, 25(12), pp. 1318–1328. doi: 10.1111/cns.13263.

Yap, J. M. G. *et al.* (2020) 'An inflammatory stimulus sensitizes TRPA1 channel to increase cytokine release in human lung fibroblasts', *Cytokine*. Academic Press, 129. doi: 10.1016/j.cyto.2020.155027.

Yogev, N. *et al.* (2012) 'Dendritic cells ameliorate autoimmunity in the cns by controlling the homeostasis of PD-1 receptor+ regulatory T cells', *Immunity*, 37(2), pp. 264–275. doi: 10.1016/j.immuni.2012.05.025.

Yosef, N., Xi, Y. and McCarty, J. H. (2020) 'Isolation and transcriptional characterization of mouse perivascular astrocytes', *PLoS ONE*. Public Library of Science, 15(10 October). doi: 10.1371/journal.pone.0240035.

Yoshikawa, M. *et al.* (1998) 'Neurotoxicity evoked by N-methyl-D-aspartate in the organotypic static slice cultures of rat cerebral cortices: Effect of GABAA receptor activation', *Acta Neuropathologica*. Springer Verlag, 95(6), pp. 592–596. doi: 10.1007/s004010050845.

Zamanian, J. L. J. *et al.* (2012) 'Genomic analysis of reactive astrogliosis', *The Journal of Neuroscience*, 32(18), pp. 6391–6410. doi: 10.1523/JNEUROSCI.6221-11.2012.

Zeinstra, E., Wilczak, N. and De Keyser, J. (2003) 'Reactive astrocytes in chronic active lesions of multiple sclerosis express co-stimulatory molecules B7-1 and B7-2', *Journal of Neuroimmunology*. doi: 10.1016/S0165-5728(02)00462-9.

Zhang, Y. *et al.* (2014) 'An RNA-sequencing transcriptome and splicing database of glia, neurons, and vascular cells of the cerebral cortex', *Journal of Neuroscience*. doi: 10.1523/JNEUROSCI.1860-14.2014.

Zhang, Y. and Barres, B. A. (2010) 'Astrocyte heterogeneity: An underappreciated topic in

neurobiology', *Current Opinion in Neurobiology*. Elsevier Ltd, 20(5), pp. 588–594. doi: 10.1016/j.conb.2010.06.005.

Zhou, Y. *et al.* (2011) 'IL-9 Promotes Th17 Cell Migration into the Central Nervous System via CC Chemokine Ligand-20 Produced by Astrocytes', *The Journal of Immunology*. doi: 10.4049/jimmunol.1003307.

Zlokovic, B. V. (2008) 'The Blood-Brain Barrier in Health and Chronic Neurodegenerative Disorders', *Neuron*. doi: 10.1016/j.neuron.2008.01.003.

Appendix

List of Figures

List of tables

List of abbreviations

Table 17: List of abbreviations

abbreviation	name
2d2	MOG-specific TCR transgenic mice on a C57BL/6 background
Aldh1l1	Aldehyde Dehydrogenase 1 Family Member L1
APC	Antigen presenting cell
AQP-4	Aquaporin 4
ASIC	Acid-sensing ion channel
B6	C57BL/6
BAFF	B cell activating factor
BBB	Blood brain barrier
BDNF	Brain-derived neurotrophic factor
C. elegans	Caenorhabditis elegans
Ca	Calcium
CCL	CC-chemokine ligand
CFA	Complete Freund adjuvant
CNS	Central nervous system
DAPI	4',6-diamidino-2-phenylindole, nuclear stain
e.g.	For example
EAE	Experimental autoimmune encephalomyelitis
eGFP	Enhanced green fluorescent protein
FGF	Fibroblast Growth Factor
FTY720	Fingolimod
GABA	gamma-Aminobutyric acid
GFAP	Glial fibrillary acidic protein
H+	Hydrogen
I-CAM	Intercellular adhesion molecule
IFNγ	Interferon γ
IL	interleukin
iNOS	Inducible nitric oxide synthase
Ko	Knockout
LFA1	Lymphocyte function-associated antigen 1
LPS	lipopolysaccharide
Mac1	Macrophage-1 antigen
MBP	Myelin basic protein
MHC	Major histocompatibility complex
MM	Mouse medium
MOG	Myelin oligodendrocyte glycoprotein
mRNA	Mitochondrial RNA
MS	Multiple sclerosis
Na	Sodium
N-CAM	Neural cell adhesion molecule
NF-κB	Nuclear factor 'kappa-light-chain-enhancer' of activated B-cells
NMO	Neuromyelitis optica
OHSC	Organotypic hippocampal slice culture
OT2	Chicken ovalbumin-specific TCR transgenic mice on a C57BL/6 background
PFA	Paraformaldehyde
PLC	Phospholipase C
PLP	Proteolipid protein
PPMS	Primary progressive multiple sclerosis
PSA	Polysialic acid

PTX	Pertussis toxin
RFP	Red fluorescent protein
RNS	Reactive nitrogen species
ROS	Reactive oxygen species
Rps	Ribosomal protein small subunit
RR-EAE	Relapsing remitting EAE
RRMS	Relapsing-remitting multiple sclerosis
S1P-R	Sphingosine 1-phosphate receptor
SPMS	Secondary progressive multiple sclerosis
SR101	Sulforhodamine 101
TASK-1	Potassium channel subfamily K member 3
Tbet	T-box transcription factor TBX21
Tfh	T Follicular helper cell
TGF-β	Transforming growth factor beta
Th	T helper
TMEV	Theiler's murine encephalomyelitis virus
TNFα	Tumour necrosis factor
Tr1	Type 1 regulatory T cell
Treg	Regulatory T cell
TRP	Transient receptor potential
TrpA	Transient receptor potential Ankyrin
TrpM	Transient receptor potential melastatin
TrpV	Transient receptor potential vanilloid
TWEAK	TNF-related weak inducer of apoptosis
V-CAM	Vascular cell adhesion molecule
VLA4	Very late antigen 4
WM	Wash medium
Wt	Wildtype

Curriculum Vitae

Personal data:

Name:	Samantha Schmaul
Date and place of birth:	27th May 1992 (Marburg)
Nationality:	German
Address:	Rathausstraße 14 55128 Mainz
Phone:	0179 / 3627055
Email:	sschmaul@googlemail.com

Academic career:

Since 10/2016	PhD at the department of Neurology of the university medicine Mainz in the lab of Prof Stefan Bittner on 'TrpA1 activation dampens neuroinflammation via MHC class II modulation on astrocytes' Main methods: diverse primary murine cell cultures, two-photon and confocal imaging, histology qPCR
2016	Master degree in neurosciences (grade 1.5) on 'Regulation and function of Spir proteins in vesicle transport processes' Main methods: mass spectrometry, mammalian cell culture
09/2014 – 08/2016	Beginning of elite master degree in 'experimental and clinical neurosciences' at the Regensburg University
2014	Bachelor degree in biochemistry (grade 1.8) on 'quantitative proteome analysis for Asc1p isoforms mimicking different T143 phosphorylation states in *Saccharomyces cerevisiae*' Main methods: mass spectrometry, introduction of point mutations into plasmids, strep-tagged protein purification
10/2011 - 07/2014	bachelor studies at the Georg-August-University Göttingen in biochemistry

Congress participations:

09/2019	ASNI 2019, Montreal Canada 'Proinflammatory T Cells Drive Distinct Inflammatory Astrocyte Profiles'
07/2019	Glia 2019, Porto Portugal 'Astrocyte – T-lymphocyte communication under neuroinflammatory conditions'
03/2019	NWG 2019, Göttingen Germany 'Astrocyte – T-lymphocyte communication under neuroinflammatory conditions'
10/2018	ECTRIMS 2018, Berlin Germany
08/2018	ISNI 2018, Brisbane Australia 'A novel β1-integrin/Kv1.3-mediated vesicular glutamate release pathway in Th17 cells'
06/2018	Oberwesel 2018, Oberwesel Germany 'Two-photon live imaging of astrocyte - T-cell interactions in autoimmune neuroinflammation'